Fall 2010

Optimal excitation controllers, and location and sizing of energy storage for all-electric ship power system

Chuan Yan

Department: Electrical and Computer Engineering

OPTIMAL EXCITATION CONTROLLERS, AND LOCATION AND SIZING OF ENERGY STORAGE FOR ALL-ELECTRIC SHIP POWER SYSTEM

by

CHUAN YAN

A DISSERTATION

Presented to the Faculty of the Graduate School of the

MISSOURI UNIVERSITY OF SCIENCE AND TECHNOLOGY

In Partial Fulfillment of the Requirements for the Degree

DOCTOR OF PHILOSOPHY

in

ELECTRICAL ENGINEERING

2010

Approved by

Ganesh Kumar Venayagamoorthy, Co-Advisor
Keith A. Corzine, Co-Advisor
Mehdi Ferdowsi
Jonathan W. Kimball
Cihan H. Dagli

PUBLICATION DISSERTATION OPTION

This dissertation consists of the following four articles that have been submitted for publication as follows:

Pages 11-39 are accepted for publication in IEEE TRANSACTION ON INDUSTRY APPLICATION.

Pages 40-78 are submitted to ELSEVIER JOURNAL OF ENERGY CONVERSION AND MANAGEMENT.

Pages 79-107 are submitted to IEEE TRANSACTION ON INDUSTRIAL ELECTRONICS.

Pages 108-143 are to be submitted to IEEE TRANSACTION ON POWER DELIVERY.

ABSTRACT

The Navy's future all-electric ship power system is based on the integrated power system (IPS) architecture consisting of power generation, propulsion systems, hydrodynamics, and DC zonal electric distribution system (DC-ZEDS). To improve the power quality, optimal excitation systems, and optimal location and sizing of energy storage modules (ESMs) are studied.

In this dissertation, clonal selection algorithm (CSA) based controller design is firstly introduced. CSA based controller design shows better exploitation ability with relatively long search time when compared to a particle swarm optimization (PSO) based design. Furthermore, 'optimal' small population PSO (SPPSO) based excitation controller is introduced. Parameter sensitivity analysis shows that the parameters of SPPSO for regeneration can be fined tuned to achieve fast optimal controller design, and thus exploiting SPPSO features for problem of particles get trapped in local minima and long search time. Furthermore, artificial immune system based concepts are used to develop adaptive and coordinated excitation controllers for generators on ship IPS. The computational approaches for excitation controller designs have been implemented on digital signal processors interfaced to an actual laboratory synchronous machine, and to multimachine electric ship power systems simulated on a real-time digital simulator.

Finally, an approach to evaluate ESM location and sizing is proposed using three metrics: quality of service, survivability and cost. Multiple objective particle swarm optimization (MOPSO) is used to optimize these metrics and provide Pareto fronts for optimal ESM location and sizing.

ACKNOWLEDGMENTS

I would like to acknowledge my advisors, Dr. Ganesh Kumar Venayagamoorthy and Dr. Keith A. Corzine, for their continued support, suggestion and guidance throughout my research and also in my coursework.

I would also like to acknowledge the Real-Time Power and Intelligent Systems (RTPIS) Laboratory and the US Office of Naval Research (ONR) for the financial support throughout my study and research, under the grant N00014-07-1-0806.

I would like to acknowledge Dr. Mehdi Ferdowsi, Dr. Jonathan W. Kimball and Dr. Cihan H. Dagli, for serving as my committee members, and for their input, guidance, help, and interest in this research towards my dissertation.

Finally, I would like to acknowledge my friends, fellow lab scholars, and family for their continuous support.

TABLE OF CONTENTS

LIST OF ILLUSTRATIONS

LIST OF TABLES

1. INTRODUCTION

1.1. OVERVIEW

Nowadays, most military vessels use mechanical drive. These systems convert the engine's high-speed revolutions per minute (RPMs) to low speed RPMs using a set of gears. Ships with mechanical drive systems actually have two sets of engines. One set is used for ship propulsion. A second and separate set, connected to generators, is used to create electricity for all of the electrically powered equipment on the ship, all of which are shown in Figure 1.1.

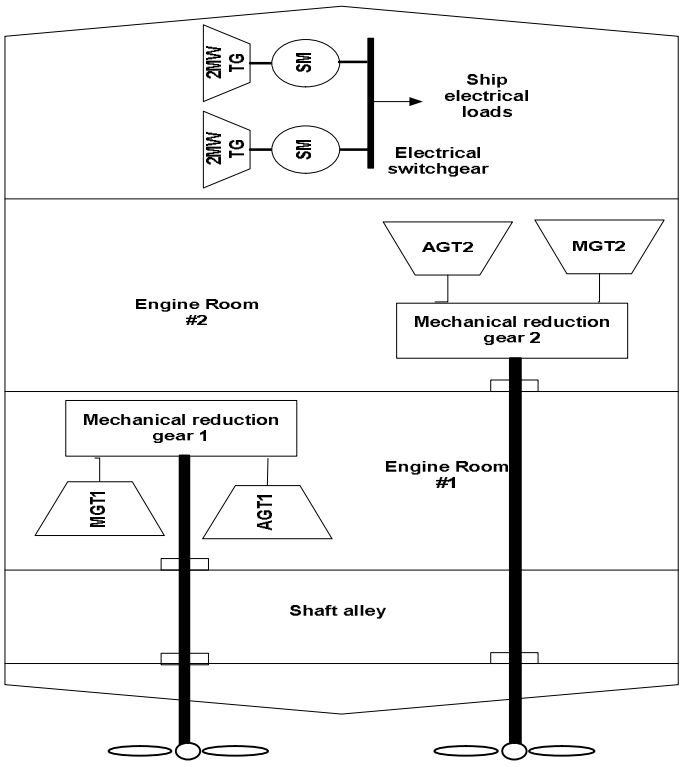

Figure 1.1. Typical Mechanical-drive layout. (SM: Synchronous Machine; MGT: Main Gas Turbine; AGT: Auxiliary Gas Turbine; TG: Turbine Generator)

However, this cannot meet the future navy demand. In an Electric ship, a generator converts the engine's high speed RPMs into electricity firstly. Ships with such a system can be designed so that a single set of engines produces a common pool of electricity for use by the ship's propulsion and non-propulsion systems. And the ship

contains a number of pulsed power loads for high-energy applications such as radar, railguns, electrical launcher and advanced weapons, which is shown in Figure 1.2.

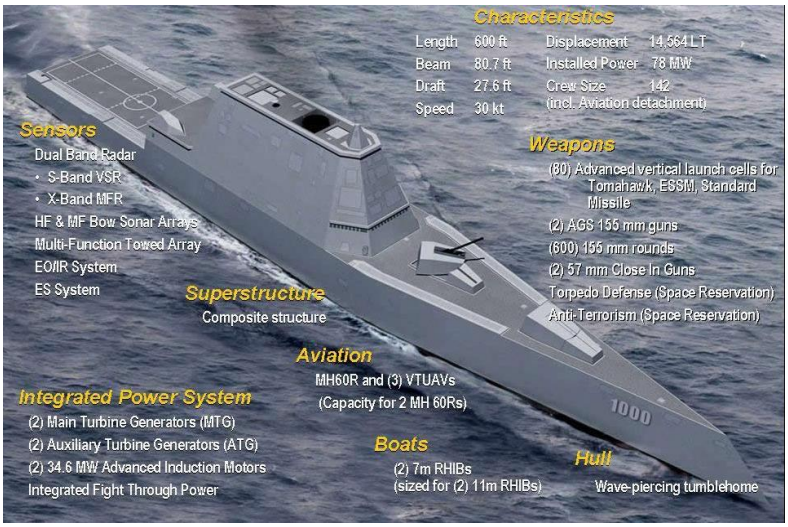

Figure 1.2. Navy's DDG-1000 All Electric Ship [19].

And it has the following advantages [1, 2]:

Arrangement. Some mechanical devices can be removed such shaft, gear so that frees up large ship space. And the arrangement of generators and propulsion motors can be more flexible.

Capability for high energy loads. The operation of high energy loads such as railgun, EM launcher and laser system will consume huge amounts of energy, which is not capable for mechanical drive ship.

Survivability. The electric ship can have reconfigurability so that even one part is damaged, the ship can reconfigure its power system to make sure the important load can work properly.

Maintainability.

1.2. INTEGRATED POWER SYSTEM

Navy's future electric ships power system is based on the integrated power system (IPS) architecture consisting of power generation, propulsion systems, hydrodynamics, and DC zonal electric distribution system (DC-ZEDS) [3]. The ship contains a number of pulsed power loads for high-energy applications such as radar, railguns, electrical launcher and advanced weapons. This pulse energy demand has to be provided by the ship energy sources, while not impacting the operation of the rest of the system. It is clear from studies carried out earlier that disturbances are created at the generator ac bus. Therefore, energy storage modules (ESM) are introduced. The ship power system first charge the energy storage devices gradually, then these devices discharge and supply power for the pulsed loads during a short time. However, this leads to two main problems. The first one is that the energy storage devices take too much space on the electric ship; the second one is that the energy storage devices increase the cost for ship. Now, Navy's DDG-1000 electric ship costs $3.3 billion dollars [20], which is over the budget greatly. Thus, it is necessary to explore the possibility of reduced energy storage system capacity without lower ship power quality. What is more, the ship IPS has no slack bus, which can give constant voltage and infinite reactive power. Therefore, the excitation system plays a more important role in Ship's IPS to improve its performance [4].

In addition to generator sets, ESMs are used to supply power for ship equipments including high energy loads and critical loads. ESMs prevent critical equipments from both potentially damages by a threat and normal system transient so that increase ship's survivability and quality of service (QOS). Furthermore, ESM can also be used to supply power peaks and to level the power demanded from main generators, leading not only to functional benefits, but also to operational benefits in terms of power quality and fuel economy [21]. Therefore, it is necessary to study ESMs for ship power system.

1.3. COMPUTATIONAL INTELLIGENCE BASED OPTIMIZATION FOR EXCITATION CONTROLLER DESIGN FOR ELECTRIC SHIP

To some extent, the generator field excitation control can be used along with energy storage devices to maintain the system voltage. The excitation control is one of

the most effective and economical techniques to stabilizing the terminal voltage of synchronous generators. Excitation control elements mainly include an automatic voltage regulator (AVR) which senses and maintains the terminal voltage of the generator and a power system stabilizer (PSS) which provides the required auxiliary control signal to improve the dynamic performance. An optimally tuned excitation system offers benefits in overall operating performance during transient conditions caused by system faults, disturbance, or motor starting [5]. In order to optimize them, many algorithms are extended to the design of the optimal excitation controller for the synchronous generators. Two methods are predominantly used, one being the pole-placement method and the other being the cancellation approach [5, 6]. However, transfer function and parameters of machines are needed. And they are not optimal oriented. In [7], Lyapunov's direct method has been used to optimize excitation controller. But again, machine parameters are needed.

Recently, computational intelligence (CI) methods are widely used in optimizing excitation controllers such as fuzzy set theory [8], particle swarm optimization (PSO) theory [9, 10], and online trained neurocontroller [11, 12] all of which have good performance at maintaining the terminal voltage. In [10], a comparison of a PSO based AVR and a genetic algorithm (GA) based AVR is made. And it is clearly shown from results that the PSO based AVR has more robust stability and efficiency, and can solve the searching and tuning problems of excitation system more easily and quickly than the GA method. In [13], a comparison of differential evolution based particle swarm optimization (DEPSO), Clonal selection algorithm (CSA), small population based particle swarm optimization (SPPSO) and population based incremental learning (PBIL) for power system stabilizer design is made. The results show that CSA consistently performs better than the other three algorithms. Furthermore, in [10] and [13], all comparison results were obtained by Matlab simulation. Therefore, it is necessary to study the performance of these CI based excitation system and hardware implementation comparison.

CI based controller designs use fitness functions mainly based on rise time, settling time and overshoot. Reactive power control in a multimachine power system is essential for improved system performance and minimization of power losses. Besides,

an optimal excitation controller developed using CI techniques can only provide optimal performance for the range of operation conditions considered in the design, however, its performances degrades when the operation condition changes. Therefore, adaptive excitation controllers are used [14, 15]. Furthermore, the design of multiple excitation controllers to provide optimal performance with changing operating conditions is a challenging task, and critical for Navy applications. This requires coordinated development of the excitation controllers and adaptive online-operation. In Figure 1.3, a schematic of intelligent optimal excitation controllers for IPS is shown.

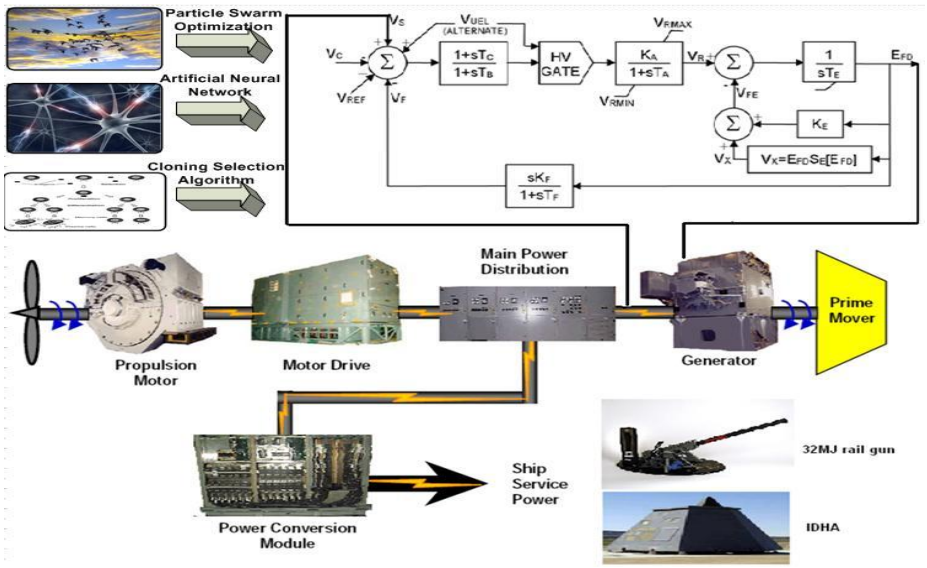

Figure 1.3. Schematic of intelligent optimal excitation controllers for IPS.

1.4. COMPUTATIONAL INTELLIGENCE BASED MULTIOBJECTIVE OPTIMIZATION FOR ELECTRIC SHIP

There are mainly three aspects for ESM design for shipboard power system: 1) type; 2) management and controls for ESM and auxiliary devices; 3) size and location. Lots of studies were carried out in the literature [22-32].

The type of ESS depends on many factors such as reliability, efficiency, cost and rate of discharge, etc [25]. Lots of studies have been carried out in this aspect [22, 25].

Four types of ESM using different physical principles for energy storage that could apply to the Navy's future needs are considered as follows: advanced capacitors (electrostatic); batteries (chemical), flywheels (kinetic) and superconducting magnetic energy storage (SMES) (magnetic) [22 - 28]. Supercapacitors have extremely high power capability and much longer lifetime. However, main drawbacks are at the cost of low energy density, high self discharge, and insufficient discharge time [22]. Batteries are one of the most cost-effective and matured energy storage technologies available. The U.S. Army has been a leader in the development of high-density, high-power, 6- to 12-V battery power systems for vehicles, pulsed-power weapons, remote power backup, and missile systems [27]. Flywheel has advantages such as fast acting and great power delivery profile. However, its main drawbacks are energy density issue and safety issue [22, 27]. As for SMES, it has similar advantages as supercapacitors. However, its main disadvantages are relative high cost and significant auxiliary equipment [22, 27].

As for management and control, studies are carried out at the power system level [21, 30]. In [21], a comprehensive approach is introduced to study the energy management for all electric ship. It describes some control challenges and ESS stability analysis. In [30], optimal generation scheduling with ESS is studied. Some studies are carried out at the power electronics level [31, 32].

However, few studies are carried out about location and size studies. According to [26, 29], neither of Navy's current two softwares, Advanced Surface Ship and Submarine Evaluation Tool (ASSET) and the Electric Plant Load Analysis (EPLA), are capable of developing optimized ESS location design, and location study is still an open issue. Therefore, it is necessary to study the optimal ESS location evaluation and design.

In order to evaluate ESM location and size design, three main factors can be considered: survivability, QOS and cost. Therefore, the design involves multiple objective optimization problems. Multiple objective particle swarm optimization (MOPSO) is widely used for multiobjective optimization in the last few years [33-35]. According to [33], MOPSO has a better average performance with respect to some of the best multiobjective evolutionary algorithms known to date. Therefore, MOPSO is used to optimize the ESM design.

1.5. OBJECTIVES OF THIS RESEARCH

The objectives are mainly two-fold:

- Development of an excitation controller for the synchronous generators to improve the power quality for an electric ship power system under pulsed loads. The excitation controller on a generator has to provide
  - Optimal performance for pulsed loads of known different magnitudes and durations.
  - Adaptive performance for pulsed loads of unknown magnitudes and durations.
  - Reactive power compensation in a coordinated manner with rest of excitation controllers on the electric ship.
- Determine an optimal location and size of energy storage modules. This has to determined to satisfy the following objectives:
  - Maximize quality of supply
  - Maximize survivability
  - Minimize cost of energy storage modules
  - Provide a set of optimal solutions.

1.6. CONTRIBUTIONS

- CSA based optimal excitation controller has been implemented and verified under a scaled down IPS with lab hardware setup. A comparison of CSA and PSO based controllers has been made [16].
- Developed and hardware implementation of a small particle swarm optimization (SPPSO) based optimal excitation controller for electric ship [17].
- AIS-based coordinated and adaptive excitation control has been applied for electric ship power system. A full scaled IPS has been built using RTDS and DSP in order to verify the proposed controller [18].
- An approach to evaluate ESM location and size is proposed based on QOS, survivability and cost. MOPSO is used to optimize the proposed multiple objectives.

1.7. REFERENCE

[1] R. Hepburn, "Why a naval architect likes an electric ship," *IEEE Symposium on Power Electronics, Electrical Drives, Automation and Motion,* 2008, pp. 580-585.

[2] L. J. Petersen, "Next Generation Integrated Power System: The backbone of the electric warship(Hybrid Electric Drive: A near term opportunity)," *IEEE International Conference on Electric Machines and Drives*, 2009, pp. xiv – xv.

[3] L. N. Domaschk, A. Ouroua, R. E. Hebner, "Coordination of Large Pulsed Loads on Future Electric Ships," *IEEE Transaction on Magnetics*, vol. 43, no.1, January 2007.

[4] V. Arcidiacono, R. Menis and G. Sulligoi, "Improving Power Quality in All Electric Ships Using a Voltage and VAR Integrated Regulator," *IEEE Electric Ship Technologies Symposium,* May, 2007, pp. 322-327.

[5] K. Kim, R. C. Schaefer, "Tuning a PID Controller for a Digital Excitation Control System," *IEEE Transactions on Industry Application*, no.2, vol.41, pp.485-492, March/April 2005.

[6] K. Kim, A. Godhwani, M. J. Basler and T. W. Eberly, "Commissioning experience with a modern digital excitation system," *IEEE Transaction on Energy Conversion*, vol.13, no.2, pp.183-187, June 1998.

[7] J. Machowski, S. Robak, J. W. Bialek, J. R. Bumby, N. AbiSamra, "Decentralized Stability-Enhancing Control of Synchronous Generator," *IEEE Transactions on Power Systems*, no.4, vol.15, November 2000.

[8] Feng Zheng, Qingguo Wang, Tong H. Lee, Xiaogang Huang, "Robust PI Controller Design for Nonlinear Systems via Fuzzy Modeling Approach," *IEEE Transactions on Systems, Man, and Cybernetics*, no.6, vol.31, November 2001.

[9] Ali Karimi, Ali Feliachi, "PSO-tuned Adaptive Backstepping Control of Power Systems," *IEEE Power Systems Conference and Exposition*, Page(s):1315-1320, October 2006.

[10] Zwe-Lee Gaing, "A particle swarm optimization approach for optimum design of PID controller in AVR system," *IEEE Transaction on Energy Conversion,* vol.19, pp.384-391, June 2004.

[11] G. K. Venayagamoorthy, R. G. Harley, "A Continually Online Trained Neurocontroller for Excitation and Turbine Control of a Turbogenerator," *IEEE Transactions on Energy Conversion*, no.3, vol.16, pp.261-269, September 2001.

[12] G. K. Venayagamoorthy, R. G. Harley, "Two Separate Continually Online-Trained Neurocontrollers for Excitation and Turbine Control of a Turbogenerator," *IEEE Transactions on Industry Applications*, no.3, vol.38, pp.887-893, May/June 2002.

[13] P. Mitra, C. Yan, L. Grant, G. K. Venayagamoorthy and K. Folly, "Comparative Study of Population Based Techniques for Power System Stabilizer Design," *International Conference on Intelligent System Applications to Power Systems*, pp.1-6, 2009

[14] K. Wang, H. Xin and D. Gan, "Robust adaptive excitation control based on a new backstepping approach," *IEEE Power & Energy Society General Meeting*, pp.1-5, 2009.

[15] O.P. Malik and G.S. Hope, "An Adaptive Generator Excitation Controller Based on Linear Optimal Control," *IEEE Transactions on Energy Conversion*, volume 5, number 4, December 1990.

[16] C. Yan, G. K. Venayagamoorthy, and K. A. Corzine, "Hardware implementation of an AIS-based optimal excitation controller for an electric ship," *first revision to IEEE Transaction on Industry Application.*

[17] C. Yan; G. K. Venayagamoorthy, Corzine, K.A, "Implementation of a SPPSO based online design of an optimal excitation controller," *to be submitted to IEEE Transaction on Engineering Applications of Computational Intelligence.*

[18] C. Yan, G. K. Venayagamoorthy, and K. A. Corzine, "AIS-based Coordinated and Adaptive Control of Generator Excitation Systems for an Electric Ship," *submitted to IEEE Transaction on Industry Electronics.*

[19] *http://www.defenseindustrydaily.com/images/SHIP_DDG-1000_Features_lg.jpg*, DDG-1000, August, 2010.

[20] http://www.defensenews.com/story.php?i=3639737, DDG-1000 Cost, August, 2010.

[21] A. Monti, S. D'Arco, L. Gao and R. A. Dougal, "Energy storage management as key issue in control of power systems in future all electric ships," *International Symposium on Power Electronics, Electrical Drives, Automation and Motion*, pp.580-585, 2008.

[22] Holsonback, C., T. Webb, T. Kiehne and C. C. Seepersad, "System-Level Modeling and Optimal Design of an All-Electric Ship Energy Storage Module," *Electric Machines Technology Symposium*, Philadelphia, PA. May, 2006.

[23] W. Du, H.F. Wang, R. Duun, "Power System Oscillation stability and control by FACTS and ESS - A survey," *International conference on Sustainable Power Generation and Supply*, pp.1-13, 2009.

[24] F. C. Beach and I.R. McNab, "Present and Future Naval Applications for Pulsed Power," *IEEE Pulsed Power*, pp.1-7, 2005.

[25] J.V. Amy, "Considerations in the Design of Naval Electric Power Systems," *IEEE Proceedings of Power Engineering Society Summer Meeting*, pp.331-335, 2002.

[26] N. Doerry, "Next Generation Integrated Power Systems (NGIPS) for the Future Fleet," *Electric Ship Technologies Symposium*, 2009.

[27] "National academy press. Technology for the United States Navy and Marine Corps 2000-2035 Becoming a 21st-Century Force," Vol.2: Technology, Chapter 8, 1997.

[28] S. Young, J. Newell and G. Little, "Beyond Electric Ship," *Naval Engineers Journal*, vol.113, no.4, pp.79-92, 2001.

[29] N. Doerry, "Institutionalizing the Electric Warship," *Naval Engineers Journal*, vol.118, no.4, pp.57-64, 2008.

[30] W. Wu, D. Wang, A. Arapostathis and K. Davey, "Optimal Power Generation Scheduling of a Shipboard Power System," *Electric Ship Technologies Symposium*, pp.519-522, 2007.

[31] L Liu, H. Li and J.M. Kim, "An Ultracapacitor-based Energy Storage System Design for High Power Motor Drive with Dynamic Real Power Compensation and harmonic Cancellation," *IEEE Energy Conversion Congress and Exposition (ECCE'01)*, pp.1745-1752, 2009.

[32] L Liu, Z W and H. Li, "A Single-stage Grid-connected Inverter with Wide Range Reactive Power Compensation using Energy Storage System (ESS)," *IEEE Applied Power Electronics Conference and Exposition, (APEC'10)*, Feb, 2010.

[33] C.A.C. Coello, G.T. Pulido and M.S. Lechuga, "Handling Multiple Objectives with Particle Swarm Optimization," *IEEE Transactions on Evolutionary Computation*, vol.8, no.3, pp.256-279, 2004.

[34] L.D.S. Coelho, L.Z. Barbosa and L. Lebensztajn, "Multiobjective Particle Swarm Approach for the design of a Brushless DC wheel Motor," *IEEE Transactions on Magnetics*, vol.46, no.8, pp.2994-2997, 2010.

[35] J.S. Heo, K.Y. Lee and R. Garduno-Ramirez, "Multiobjective Control of Power Plants using Particle Swarm Optimization Techniques," *IEEE Transactions on Energy Conversion*, vol.21, no.2, pp.552-561, 2006.

PAPER

1. HARDWARE IMPLEMENTATION OF AN AIS-BASED OPTIMAL EXCITATION CONTROLLER FOR AN ELECTRIC SHIP

Chuan Yan, Ganesh K. Venayagamoorthy, *Senior Member, IEEE*, Keith Corzine, *Senior Member, IEEE*

Abstract - The operation of high energy loads on Navy's future electric ships, such as directed energy weapons, will cause disturbances in the main bus voltage and impact the operation of the rest of the power system when the pulsed loads are directly powered from the main dc bus. This paper describes an online design and laboratory hardware implementation of an optimal excitation controller using an artificial immune system (AIS) based algorithm. The AIS algorithm, a clonal selection algorithm (CSA), is used to minimize the effects of pulsed loads by improved excitation control and thus, reduce the requirement on energy storage device capacity. The CSA is implemented on the MSK2812 DSP hardware platform. A comparison of CSA and the particle swarm optimization (PSO) algorithm is presented. Both simulation and hardware measurement results show that the CSA optimized excitation controller provides effective control of a generator's terminal voltage during pulsed loads, restoring and stabilizing it quickly.

Index Terms - Clonal selection algorithm (CSA), Electric ship, optimal excitation controller, particle swarm optimization (PSO), pulsed loads.

I. INTRODUCTION

The Navy's future electric ship power system is based on the integrated power system 1 (IPS) architecture consisting of power generation, propulsion systems,

---

Part of this paper was presented at the IEEE IAS 2008 annual meeting. The financial support for this research from the US Office of Naval Research 2007 Young Investigator Award to Dr. Venayagamoorthy (The Intelligent All Electric Ship Power System) is gratefully acknowledged (contracting number – N00014-07-1-0806).

hydrodynamics, and DC zonal electric distribution system (DC-ZEDS) [1]. In order to maintain power quality in IPS, immediate energy storage devices with their corresponding charging systems are proposed to make the pulsed power required compatible with the supply system [16]. However, this will increase the system weight and volume. To some extent, the generator field excitation control can be used along with energy storage to maintain the system voltage. The excitation control is one of the most effective and economical techniques for stabilizing the terminal voltage of the synchronous generators. An optimally tuned excitation system offers benefits in overall operating performance during transient conditions caused by system faults, disturbance, or motor starting [2]. In order to optimize them, many algorithms are extended to the design of the optimal excitation controller for the synchronous generators. Two methods are predominantly used, one being the pole-placement method and the other being the cancellation approach [2, 3]. However, transfer function and parameters of machines are needed. And they are not optimal oriented. In [4], Lyapunov's direct method has been used to optimize excitation controller. But again, machine parameters are needed.

Recently, computational intelligence methods are widely used in optimizing excitation controllers such as fuzzy set theory [5], particle swarm optimization (PSO) theory [6, 7], and online trained neurocontroller [8, 9] all of which have good performance at maintaining the terminal voltage. In [7], a comparison of a PSO based AVR and a genetic algorithm (GA) based AVR is made. And it is clearly shown from results that the PSO based AVR has more robust stability and efficiency, and can solve the searching and tuning problems of excitation system more easily and quickly than the GA method. In [10], a comparison of differential evolution based particle swarm optimization (DEPSO), Clonal selection algorithm (CSA), small population based particle swarm optimization (SPPSO) and population based incremental learning (PBIL) for power system stabilizer design is made. And the results show that CSA consistently performs better than the other three algorithms. Furthermore, in [7] and [10], all comparison results were obtained by Matlab simulation. Therefore, it is necessary to study the performance of CSA based excitation system and hardware implementation comparison.

Artificial immune system (AIS) can be defined as computational systems that are inspired by theoretical immunology. CSA is a member of the family of AIS techniques. In the past few years, CSA has been gradually used to solve the optimal control problems [14-19]. In this paper, an online CSA-based optimal excitation controller for the electric ship is implemented on the MSK2812 DSP hardware platform to minimize the voltage deviations when high power pulsed loads are directly powered from the dc side; exploring the possibility of reduced energy storage. The hardware results show that the on-line CSA-based controller improves the dynamic performance of the synchronous generator with stability. In addition, PSO [11] has been implemented and comparison with CSA in terms of performance and computational complexity for real-time tuning is discussed in the paper

. This paper is organized as follows: A description of a laboratory power system model for an electric ship and its hardware setup is provided in Section 1.2. Section 1.3 provides a detailed description of the DSP based hardware implementation of a real-time CSA algorithm for optimal excitation controller design. Section 1.4 and 1.5 presents the experimental results and some discussions on the CSA algorithm in comparison to PSO. Finally, the conclusion is given in Section 1.6.

II. POWER SYSTEM MODEL FOR THE ELECTRIC SHIP AND ITS HARDWARE IMPLEMENTATION

A. Electric Ship Integrated Power System

The power system of the all-electric ship system mainly consists of four parts: prime movers, advanced propulsion induction motors, dc zonal distribution loads, and other auxiliary loads which are shown in Fig. 1. All prime mover power is first converted into electric power, and then it is distributed and allocated between propulsion, pulsed power weapons, ship service power and other electrical loads as required. In the laboratory setup, these four parts are separately implemented. More details are given below on the individual modules in the hardware setup below.

B. Power Generation

The DDG-1000 proposed electric ship power system architecture consists of four gas turbine-generator sets. Two main 36MW and two auxiliary 4MW generator sets, generate a total of 80MW of electric power [12]. The IPS is a symmetrical system and

modeling of one of the pairs is sufficiently enough to study the excitation control. In the laboratory setup (Fig. 1), a small-scale power generation system is used to emulate the gas turbine-generator sets of the electric ship. This small-scale system consists of a three-phase 60Hz 3.7kVA synchronous generator and a 15kW dc motor to supply mechanical torque for the synchronous generator. The rated line-to-line voltage and speed of the generator is 230V and 1800 RPM respectively. Parameter of the synchronous generator is shown in the Table 1. For the scaled down laboratory model, the propulsion load and pulsed loads of the IPS in the electric ship are reduced in magnitude.

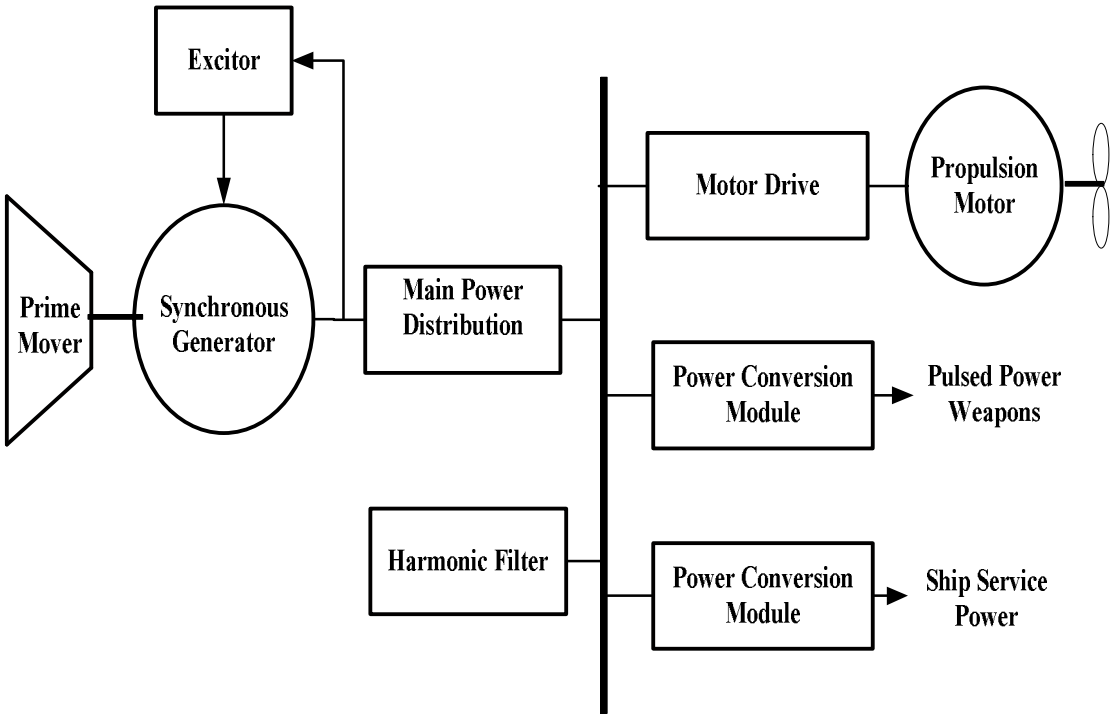

(a)

Fig. 1. Laboratory implementation with (a) simplified IPS of an electric ship and (b) laboratory hardware implementation

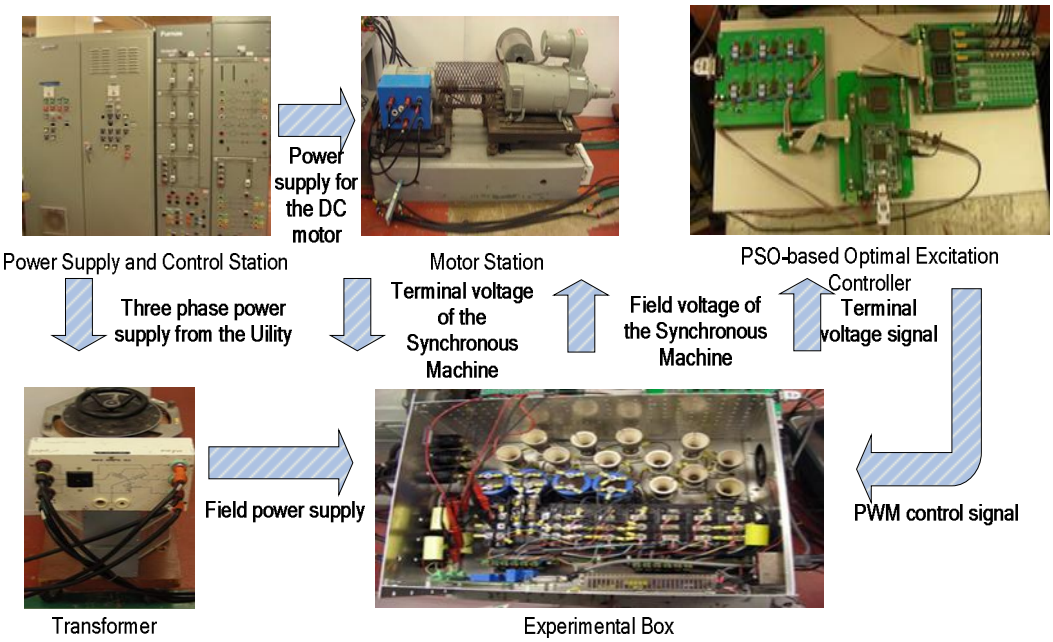

(b)

Fig. 1. (Continued) Laboratory implementation with (a) simplified IPS of an electric ship and (b) laboratory hardware implementation.

Table 1. Synchronous Machine Ratings and Parameters.

Power 3.7 kVA		field voltage 150 VMAX	
voltage 230 V		field current 1.05 A	
rated current 6.28 A		speed 1800 RPM	
frequency 60 Hz		$N_s/N_{fd} = 0.0271$	
$r_s = 0.38\,\Omega$	$L_{ls} = 1.12$ mH	$L_{mq} = 29.4$ mH	$L_{md} = 39.3$ mH
$r'_{fd} = 0.11\,\Omega$	$L'_{lfd} = 1.5$ mH	$r'_{kd1} = 128\,\Omega$	$L'_{lkd1} = 7.90$ mH
$r'_{kd2} = 1.77$ mΩ	$L'_{lkd2} = 4.83$ mH	$r'_{kq1} = 5.07\,\Omega$	$L'_{lkq1} = 4.21$ mH
$r'_{kq2} = 1.06\,\Omega$	$L'_{lkq2} = 3.50$ mH	$r'_{kq3} = 0.447\,\Omega$	$L'_{lkq3} = 26.2$ mH

C. Excitation System

The synchronous generator excitation system includes a terminal voltage transducer and load compensator, excitation control elements and an exciter [13]. Since the proposed excitation system is simplified, some parts such as power system stabilizer

and under-excitation limiter are not considered. A simple functional block diagram for excitation controller is shown in Fig. 2.

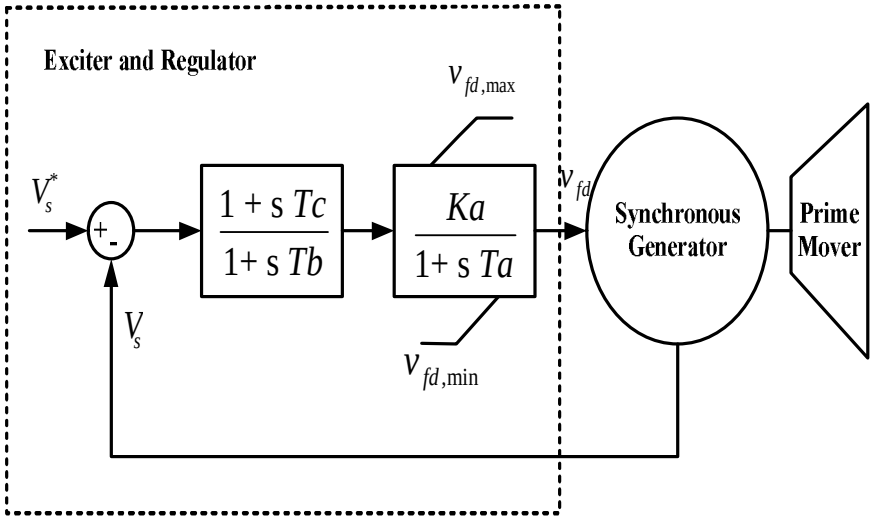

Fig. 2. Simple functional block diagram for synchronous machine excitation control system.

In this case, the key element in the design of the optimal excitation controller is finding the optimal controller parameters (K_a, T_a, T_b and T_c) to provide optimal performance during the pulsed loads. As is shown in Fig. 2, V_s^* is the rms terminal voltage reference of the synchronous generator and V_s is the measured value. The rms line-to-neutral terminal voltage is calculated in terms of instantaneous quantities using

$$V_s = \frac{\sqrt{v_{as}^{\,2} + v_{bs}^{\,2} + v_{cs}^{\,2}}}{\sqrt{3}} \qquad (1)$$

In the laboratory setup, the excitation controller consists of a sensor board, an A/D conversion board, a MSK2812 DSP board consisting of the TMS320F2812 processor, and a D/A conversion board. The A/D conversion board receives the terminal voltage signal form the sensor board and outputs a digital signal to the central controller. The D/A conversion board receives PWM signals from the central controller and send signals to the IGBTs. The field of the synchronous generator is connected with a four-quadrant PWM dc drive supplied by 200V dc.

III. CSA BASED OPTIMAL EXCITATION CONTROLLER ONLINE DESIGN

The clonal selection algorithm is a biologically motivated computational intelligence algorithm developed by Castro and Zuben in 2001 [14]. Clonal selection principle based immune response is generated when a non-self antigenic pattern is recognized by the B cells (antibodies) and this is explained in [14]. Just like many other heuristic optimization algorithms, CSA is known as an evolutionary strategy capable of solving complex machine learning and pattern recognition tasks by adopting the clonal operator. CSA can handle complex optimization problems, finding global solutions with fast convergence speeds, especially for functions of multimodal and highly combinatorial nature [15-19]. The detailed operation of CSA is illustrated in the flowchart depicted in Fig. 3 and the main steps are briefly explained below. In this paper, by online, it means the parameters of excitation controller are determined via several runs / iterations of CSA algorithm using the actual hardware in Fig. 3 (b).

Initialization: A population N of antibodies (A_b) is randomly initialized. Since there is no explicit antigen population (A_g) to be recognized like in a biological system, the objective function serves as the Ag and needs to be minimized or kept zero. In order to keep the hardware overhead within real time constraints, N is selected to be 20. The initialization range for parameters is obtained by trial and error which can make system stable. K_a is from 100 to 7000; T_a ranges from 0 to 5; T_b and T_c range from 0 to 10.

Evaluation: In the excitation control loop of Fig. 2, the proportional gain K_a and time constants $T_{a,}$ T_b and T_c have to be carefully selected to provide satisfactory performance under normal and pulsed load conditions. The objective of the CSA algorithm is to find these parameters in order to restore and stabilize the terminal voltage quickly; especially after pulsed loads of different magnitudes and durations are experienced by the IPS.

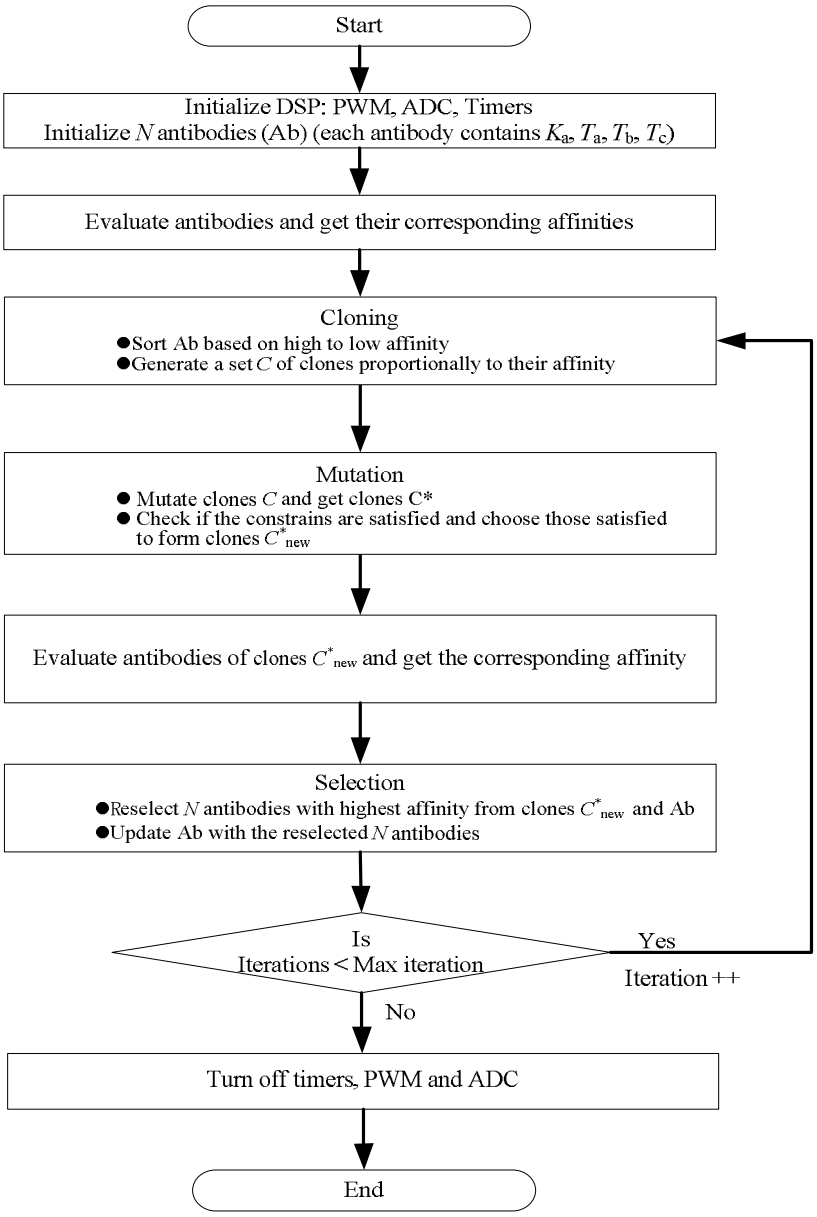

(a)

Fig. 3. Flowcharts of the (a) CSA-based optimal excitation controller design with and (b) evaluation operation

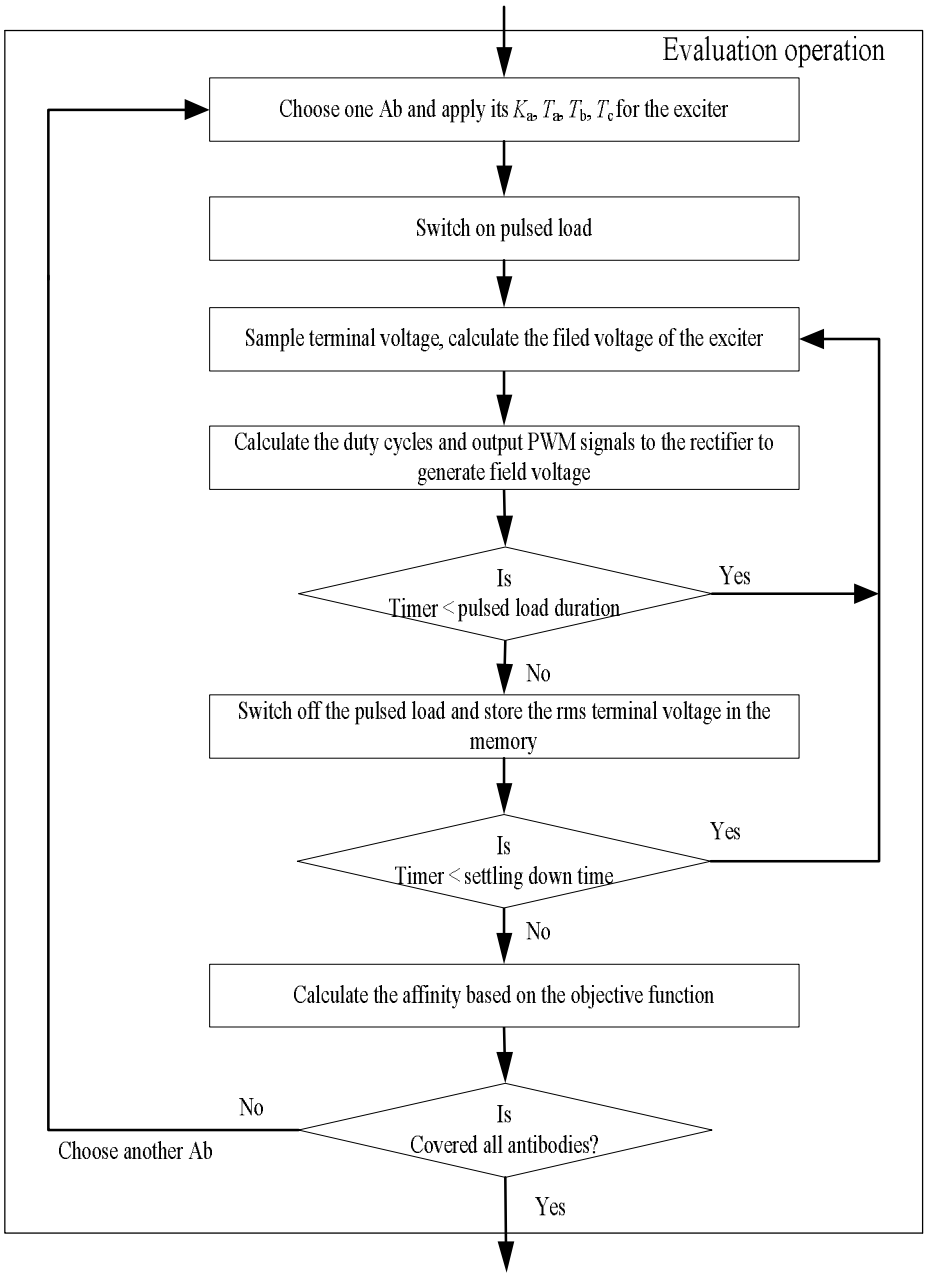

(b)

Fig. 3. (Continued) Flowcharts of the (a) CSA-based optimal excitation controller design with and (b) evaluation operation

Most objective functions used for excitation controllers design in literature involve settling time, rise time and overshoot. In this paper, the objective function associated with the AVR performance is obtained by calculating the transient response

area (2) [20, 21]. This can be used as a fitness function to guide the PSO design process to minimize the time response characteristics such as rising time, overshoot and settling time.

$$Fitness = \frac{1}{2}\sum_{k=1}^{n}\{\sqrt{[V_s^* - V_s(k)]^2 + [V_s^* - V_s(k+1)]^2}\}\Delta t \qquad (2)$$

where

V^*_s	reference terminal voltage value;
k	sampling instant;
Δt	sampling interval;
V_s	measured terminal voltage;

Due to the high computational overhead involved in computing the square root function on a DSP, (2) is modified to (3) for controller design. The term ($k\Delta t$) is a weighting factor that puts an increasing penalty as oscillations persist for a longer time; thus guiding the CSA design approach to minimize the settling time of the system oscillations in addition to the maximum overshoot after a disturbance.

$$Fitness = \frac{1}{2}\sum_{k=1}^{n}\left\{\left[V_s^* - V_s(k)\right]^2 + \left[V_s^* - V_s(k+1)\right]^2\right\}(k\cdot\Delta t)\Delta t \qquad (3)$$

where i = the number of A_b with the range of 1~20

$Fitness_i$ = the fitness of the i^{th} antibody

Since the fitness value is always positive, range of affinity value is normalized over the interval [0, 1].

In the laboratory setup, the sampling window is 1s, starting from the time the pulsed load is removed. The sampling period is 2ms and a total of n = 500 samples points are collected in the data sampling window.

Cloning: All antibodies are ranked based affinity from high to low. A set C of clones are generated proportionally to the affinities of the Abs in the population given (5)

$$N_c = \sum_{\#=1}^{r}\text{round}\left(\frac{\beta\times N}{r_\#}\right) \qquad (5)$$

where N_c = number of clones in each set

β = multiplying factor

r = number of selected ranks
$r_{\#}$ = 1 for highest affinity, 2 for second highest affinity and so on.

In [14, 16], it is clear that a high *beta* can give a better convergence. However, the number of function evaluation will also increase corresponding. In this study, *beta* and *r* are set to be 0.5 and 5 respectively, which can give a good convergence. In this case, the population of matured clones is 23, which is close to N_c. Therefore, the number of function evaluation for CSA is close to the one for PSO, which gives a fair comparison.

Mutation: The mutation rate is selected to be proportional to the individuals' affinities as given in (6)

$$\alpha = \exp(-\rho \times f) \tag{6}$$

where α = mutation rate
ρ = decay factor of the mutation rate
f = antigenic (A_g) affinity

The tradeoff between the mutation rate α and the antigenic affinity f is shown in [14]. A small decay factor gives large mutation and vice-versa. A large mutation rate means more exploration while a small mutation rate results in exploitation and vice-versa. In this study, decay factor is set to be 1. The antigenic affinity and mutation rate are both normalized over the interval [0, 1]. The process of mutation is given by (7) developed in [17].

$$C^* = C + \alpha \times randn \times C + \alpha \times randn \times (C - Ab_{best}) \tag{7}$$

where C^* = mutated clones
Ab_{best} = antibody with highest affinity

In the laboratory setup, the excitation controller parameters K_a, T_a, T_b, and T_c to be used for fitness evaluation have to be within a range of values. This is necessary to ensure that the electrical machine remains stable. Antibodies that satisfy this constraint which is the same with initialization range are referred to as feasible antibodies in the set C^* (obtained from operation using (7)) and form a new set C^*_{new}.

Selection: reselect N antibodies with highest affinity from clones C^* and C^*_{new} and update A_b.

The CSA algorithm parameters setting are shown in Table 2.

Table 2. Speciation for CSA and PSO Algorithms Parameters

Decay factor of mutation rate ρ	1
Multiplying factor β	0.5
Total number of antibodies	20
Number of selected highest Ab	5
Ab constrains for Ka, Ta , Tb , Tc	(0, +∞)

The pulsed load magnitudes and duration used in controller development and testing are shown in Table 2. Two pulsed loads, which are labeled "Train" in Table 3, are applied to serve as antigens. After the optimal parameters have been obtained, other 11 different pulsed loads are used to verify the performance of the optimal controller, which are labeled as "Test".

Table 3. Pulsed load training and testing sets

Duration / Pulsed load	100 ms	200 ms	400 ms	1000 ms
2.65 kW	Test	Test	Test	Test
5.29 kW	Test	Test	Test	Search
7.94 kW	Test	Test	Search	
13.23 kW	Test	Test		

IV. PSO BASED OPTIMAL EXCITATION CONTROLLER DESIGN

Particle swarm optimization is a swarm intelligence technique (a search method based on nature inspired systems), which is widely used in electric power system [11]. It is an efficient method for solving one or more large scale nonlinear optimization problems [7]. The system initially has a population of random particles which are given some random positions and velocities in the search space. The particles have memory

which is used to keep track of their previous best position local best (P_{best}) and the corresponding fitness. The swarm has a memory which is used to keep track of best value of all P_{best}. The search process is aimed at accelerating each particle towards its P_{best} and the swarm's global best (G_{best}). The velocity and position update equations of the particles are given by

$$v_i(j+1) = w \cdot v_i(j) + c_1 \cdot R_1 \cdot \left(P_{best}(j) - x(j)\right) + c_2 \cdot R_2 \cdot \left(G_{best} - x(j)\right) \quad (8)$$

$$x_i(j+1) = x_i(j) + v_i(j+1) \quad (9)$$

where w is the inertia constant, c_1 and c_2 are two positive numbers referred to the cognitive and social acceleration constants, and $R_1$and R_2 are two random numbers with uniform distribution in the interval [0,1].

The detailed procedure for the development of optimal excitation controllers is given in below.

Initialization: Randomly initialize a population N of particles positions and velocity. To have a fast PSO search performance, in the laboratory setup, N is set to be 20 and the values of w, c_1 and c_2 are kept fixed at 0.8, 2.0 and 2.0 [11].

Evaluation: The objective of the PSO algorithm is to find optimal parameters in order to restore and stabilize the terminal voltage quickly; especially after pulsed loads of different magnitudes and durations. The fitness function is using (3).

Update: The position and velocity of the i^{th} particle is updated using (8) and (9).

V. RESULTS

The CSA and PSO algorithms for comparison have been implemented on two testing systems: 1). Matlab based testing system; 2) a MSK2812 DSP hardware platform system. The comparison is made under the following conditions: same value and dimension of initialized antibodies or particles, same number of allowed generations/iterations for searching the optimal parameters under the same constrains. By doing, the influence introduced by the randomly updating process could be minimized.

A. Matlab Based Testing System

In this paper, a generator with parameters shown in Table 1 and power system in Fig. 1 (b) are built in Matlab Simulink using SimPowerSystem blocks. A variable load is used to simulate the propulsion loads. The load is gradually changing from 1.65kW to 2.65kW during the pulsed load in order to simulate fire weapons while accelerating. In this case, the operation point is changing during the pulsed load, which make the simulated operating conditions closer to ship's real operation conditions, which is shown in Fig. 4. A pulsed load of 5.29kW with 0.75s duration is used for tuning controller parameters using CSA and PSO shown in Section III and IV respectively.

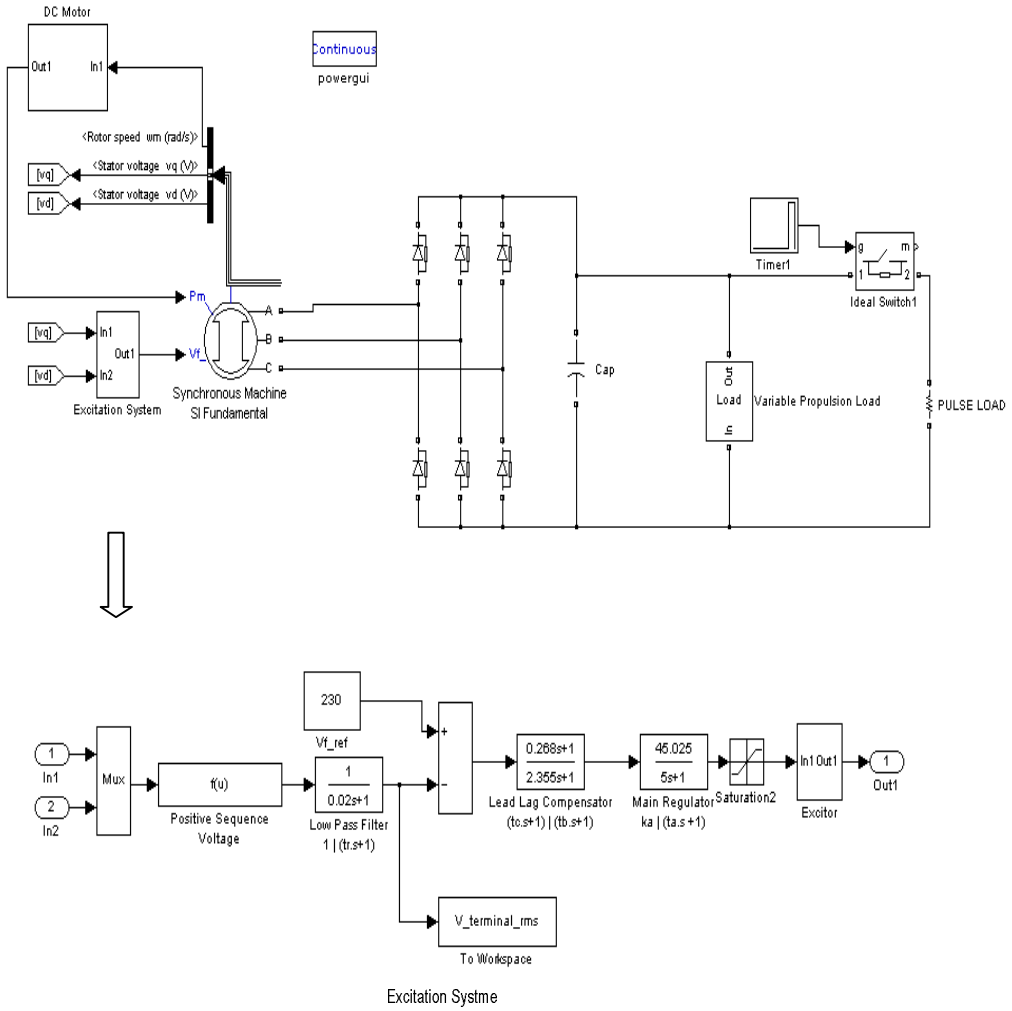

Fig. 4. Test ship power system for Matlab implementation

Furthermore, a pole placement method [2] is also applied in this study. A first order generator model is obtained using equations in [22, 23] with gain taken 0.7012 and the time constant taken 0.274 while assuming negligible amortisseur effects. Voltage overshoot of at least 1%-20% is anticipated with the pole-placement method with 2s total voltage recovery time, although its voltage rise time can be less than 1s [2]. In this case, the range of damping ratio is from 0.456 to 0.8261 [24]. In this study, damping ratio is chosen to be around 0.707. Both CSA and PSO are run for 30 trials. Among these 30 trials, one best antibody and one best particle are chosen as the parameters for the CSA-based controller and PSO-based controller respectively. And parameters obtained by pole placement, PSO and CSA are shown in Table 4.

Table 4. Parameters of the Excitation Controllers

	Ka	Ta	Tb	Tc
Pole-placement	885.609	0.001	2.356	0.268
PSO	398.524	0.998	0.0001	0.467
CSA	424.723	0.0001	3.084	1.056

The average fitness of best parameters using PSO and CSA over 100 iterations based on 30 trials is shown in Fig. 5. A statistical analysis based on standard deviation is evaluated using (10).

$$\sigma = \sqrt{\frac{1}{n}\sum_{i=1}^{n}\left(F_i - F_{ave}\right)^2} \tag{10}$$

where i = 1 for the first trial, 2 for the second trial and so on

n = total number of trials which is 30

F_{ave} = average best fitness for 30 trials

F_i, = the ith trial best fitness value for selected algorithm

In (10), σ is the standard deviation for the best solution for selected algorithm, which are 0.0317 and 0.0185 for PSO and CSA respectively. It is clear that CSA's accuracies around their corresponding best solution are higher than PSO's.

A performance comparison of these three methods under 5.29kW pulsed load with 0.75s duration is shown in Fig. 6. In Fig. 6 (a), the start-up performance comparison is shown. The overshoot of pole-placement based controller is 15.2% and the 2% settling time is 0.52s, which meet the design requirements. In Fig. 6 (b), a performance comparison of these three methods under a 5.29kW, 0.75s duration pulsed load is shown. It is clear that the performance of CSA based controller is very close to the performance of PSO based controller, which means both of them can do a good exploitation. However, according the fitness standard deviation value and Fig. 5, CSA has a better convergence.

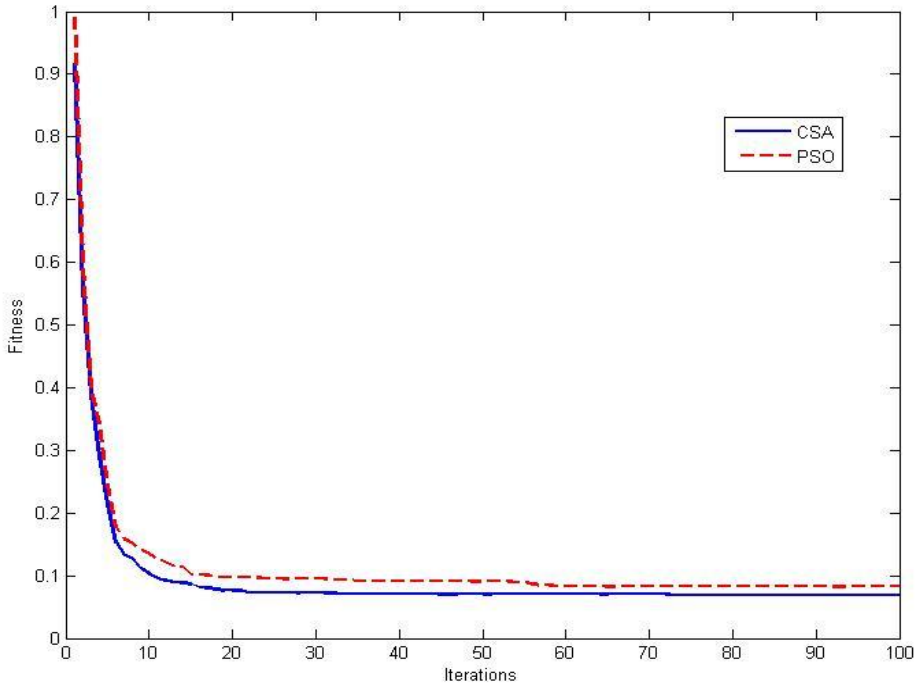

Fig. 5. Average fitness of best particle/antibody using PSO and CSA over 100 iterations based on 30 trials based on Matlab simulation.

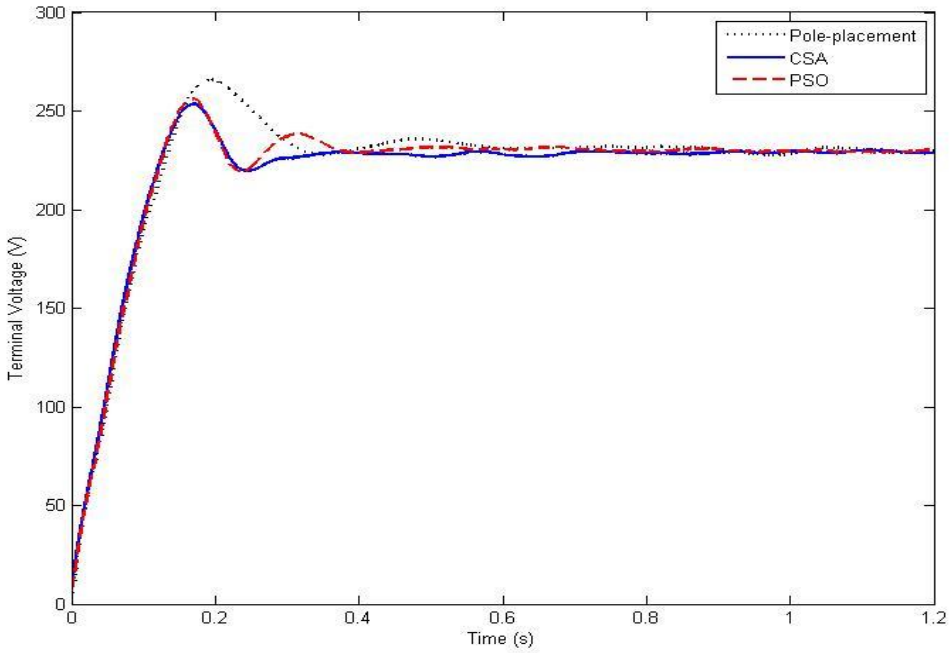

(a)

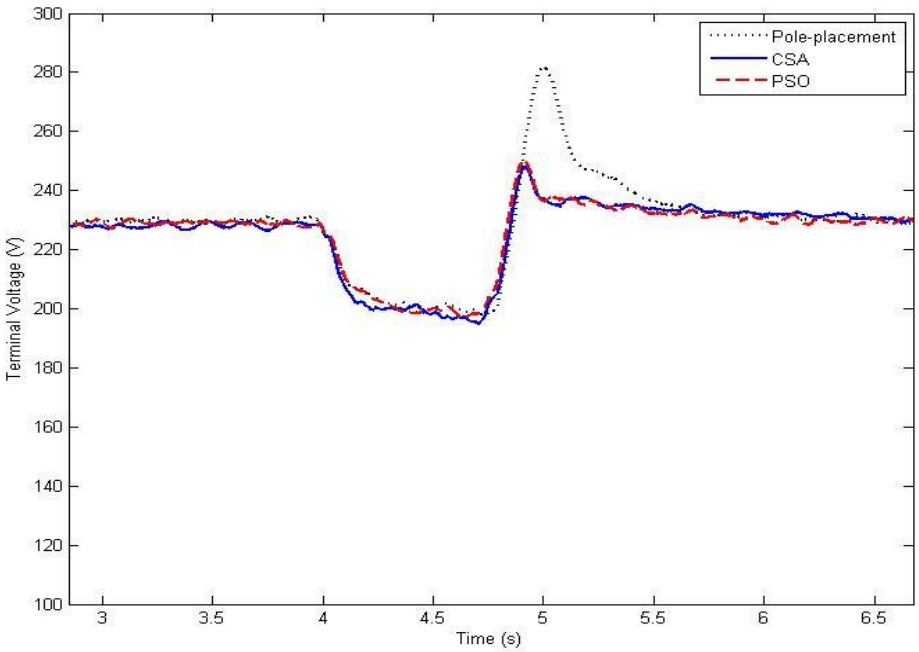

(b)

Fig. 6. The performance comparison of pole-placement, PSO and CSA based controllers based on Matlab simulation. (a) start up performance, (b) under 5.29kW and 0.75s duration pulsed load

B. Hardware Results

The hardware testbed is described in Section 1.2. The CSA and PSO algorithms are implemented in a MSK2812 DSP with 150MHz frequency.

Execution Time and Convergence Characteristics: The convergence of CSA and PSO algorithm during the search process over 40 iterations/generations based on 10 trials is shown in Fig. 7.

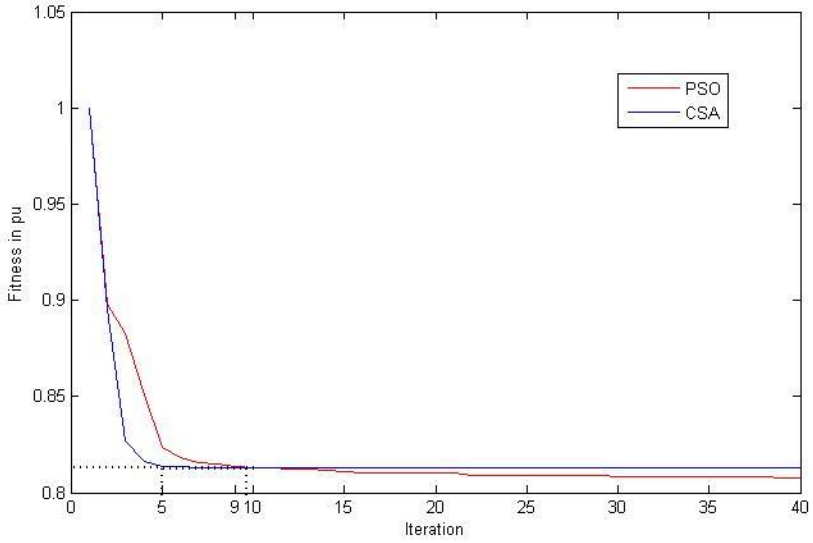

Fig. 7. Average fitness of best particle using PSO and CSA over 40 iterations based on 10 trials for hardware testbed.

The computational time taken by PSO and CSA using MSK2812 DSP is presented in Table 5. A single generation code execution time of for an Ab in CSA is nearly three times (0.064s) that of a PSO particle (0.022s). However, for this controller design application, when comparing the total time taken by CSA and PSO algorithms, difference in the code execution time is negligible.

Transient Performance: Both CSA and PSO are running for 10 times with 40 iterations every time. Among these 10 trials, one best antibody and one particle are chosen as the parameters of the CSA-based controller and PSO-based controller respectively. The parameters of excitation controller designed using CSA and PSO optimal strategies are gained given in Table 6. The comparative performance between the

CSA-based controller and PSO-based controller are shown in Figs. 8 to 10 respectively. The comparative performance of the excitation controllers under pulsed loads (including search and test sets) is shown in Table 7. For settling time calculation, because it is hard to compare settling time if the stable range is set to be 2%, the stable range is defined as from 228V to 232V, which is 0.87%.

Based on the analysis above, a comparison of CSA and PSO algorithms for excitation controller design is given in Table 8, which includes computation complexity, storage space demand, hardware demand, convergence, and time consuming. With a code optimization, the clock cycles for PSO and CSA can be reduced. But their ratio will not change a lot. Two three dimension performance analysis are shown in Fig. 11. Fig. 11 (a) shows settling time with different pulsed load values and durations while Fig. 11 (b) shows overshoot performance.

Table 5. Computational Time Taken by PSO and CSA

	PSO	CSA
Code time for each particle/Ab (one iteration/generation)	0.022s	0.064s
Evaluation time for each particle/ Ab (one iteration/generation)	7.400s	7.400s
Search time for each particle/Ab (one iteration/generation)	7.422s	7.464s

Table 6. Parameters of the Excitation Controllers for Lab Setup

	Ka	Ta	Tb	Tc
PSO	4359.000	0.119	0.691	0.732
CSA	5966.908	0.158	0.019	0.045

Table 7. Comparative Performance of the Excitation Controllers

		Setting Time ts (s)	Maximum Overshoot (%)
Pulsed load = 2.65KW; Duration = 1s	CSA	0.26	2.31
	PSO	0.64	5.09
Pulsed load = 2.65KW; Duration = 0.4s	CSA	0.24	2.26
	PSO	0.55	5.09
Pulsed load = 2.65KW; Duration = 0.2s	CSA	0.21	2.13
	PSO	0.42	4.35
Pulsed load = 2.65KW; Duration = 0.1s	CSA	0.18	2.10
	PSO	0.32	4.30
Pulsed load = 5.29KW; Duration = 1s	CSA	0.39	2.33
	PSO	0.84	5.93
Pulsed load = 5.29KW; Duration = 0.4s	CSA	0.38	2.33
	PSO	0.78	5.22
Pulsed load = 5.29KW; Duration = 0.2s	CSA	0.33	2.31
	PSO	0.71	4.57
Pulsed load = 5.29KW; Duration = 0.1s	CSA	0.27	2.20
	PSO	0.48	4.35
Pulsed load = 7.94KW; Duration = 0.4s	CSA	0.44	2.36
	PSO	0.88	5.54
Pulsed load = 7.94KW; Duration = 0.2s	CSA	0.41	2.34
	PSO	0.80	5.09
Pulsed load = 7.94KW; Duration = 0.1s	CSA	0.33	2.22
	PSO	0.55	4.36
Pulsed load = 13.23KW; Duration = 0.2s	CSA	0.45	2.22
	PSO	0.85	5.13
Pulsed load = 13.23KW; Duration = 0.1s	CSA	0.38	2.26
	PSO	0.75	4.75

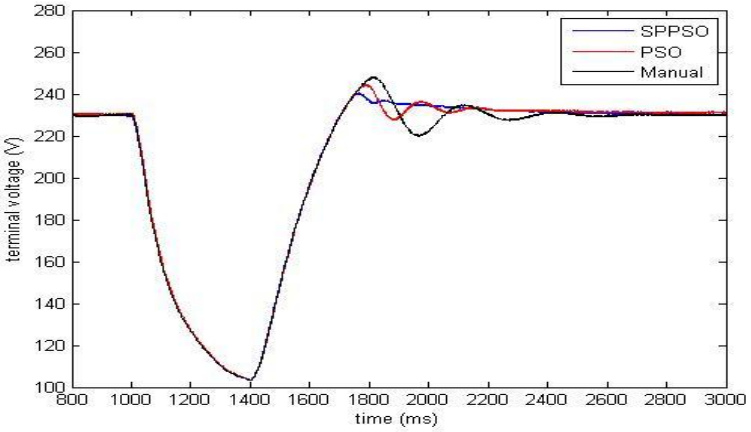

(a)

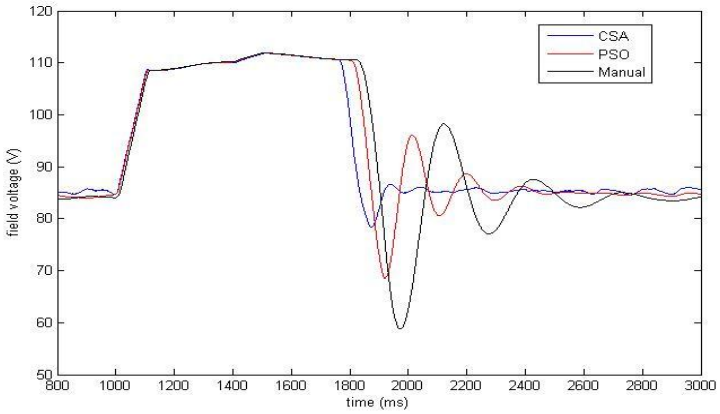

(b)

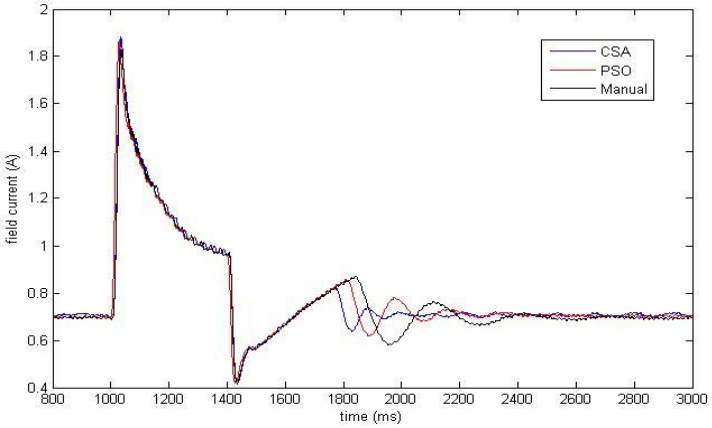

(c)

Fig. 8. Pulsed load at 7.94kW with 0.4s duration. (a) terminal voltage, (b) field voltage, (c) field current.

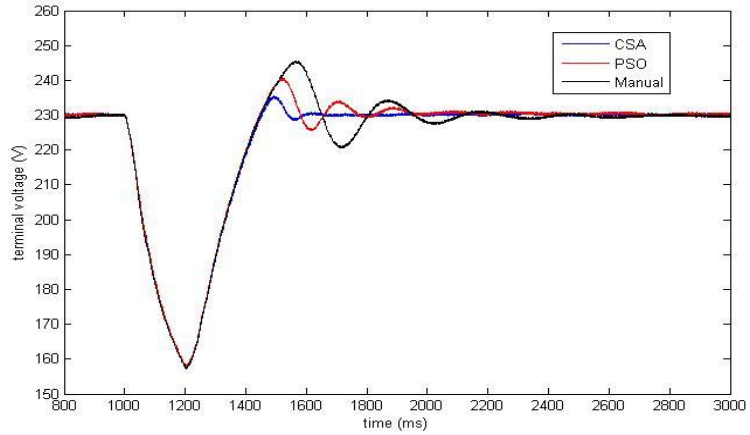

(a)

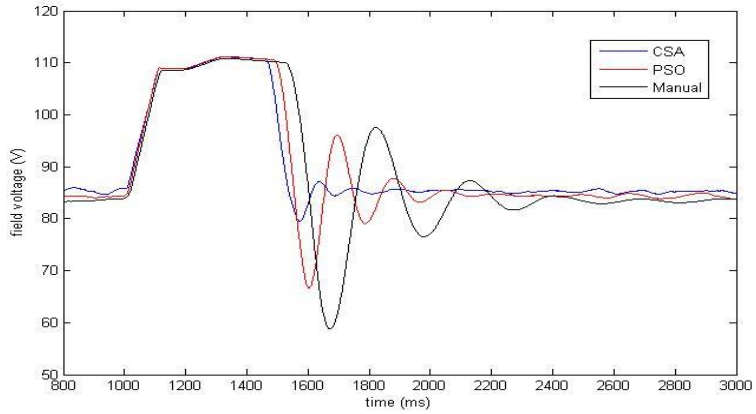

(b)

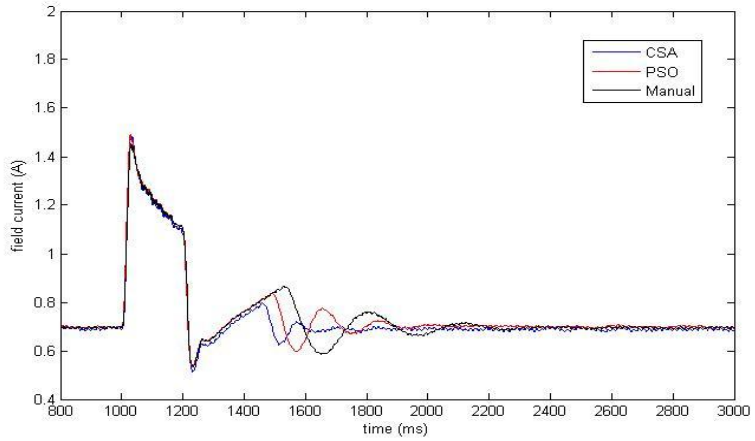

(c)

Fig. 9. Pulsed load at 5.29kW with 0.2s duration. (a) terminal voltage, (b) field voltage, (c) field current.

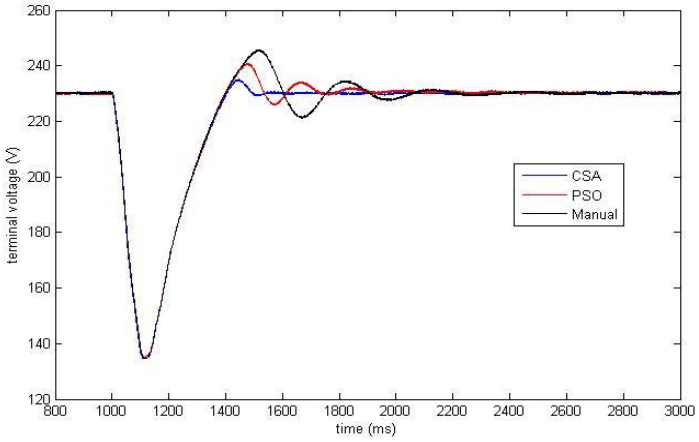

(a)

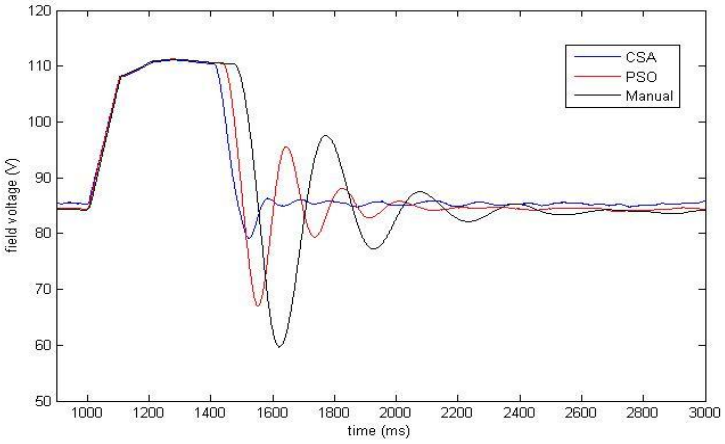

(b)

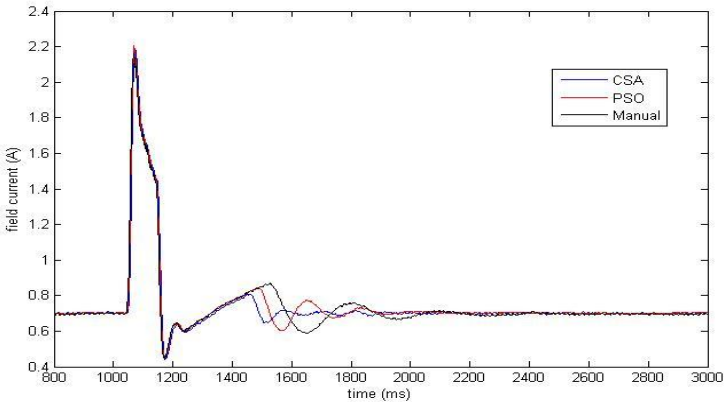

(c)

Fig. 10. Pulsed load at 13.23kW with 0.1s duration. (a) terminal voltage, (b) field voltage, (c) field current.

Table 8. Comparison of CSA and PSO Algorithms for Excitation Controller Design

	PSO	CSA
Computational complexity	Small, mainly "+, -, × operation"	Large, contains "sorting, round, exponential, and division operation"
Storage space	Small, mainly "particles position and velocity"	Medium, "antibody, affinity, new group of antibody and affinity"
Hardware demand	Low. Many microcontrollers such as PIC, DSP are available to be implemented on; No extend memory needed for most cases.	High. High processing speed is needed; Memory problem need to be considered.
Cost	Medium	High
Convergence	Fast	Faster
Explore ability	Better	Good
Time consuming for algorithm (without evaluation)	Small	Large, nearly 3 times larger than PSO

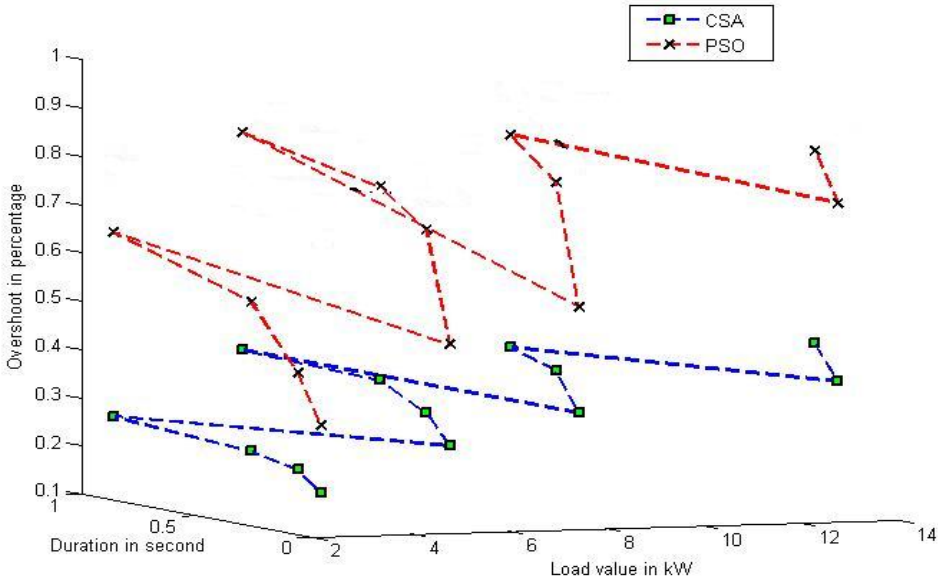

(a)

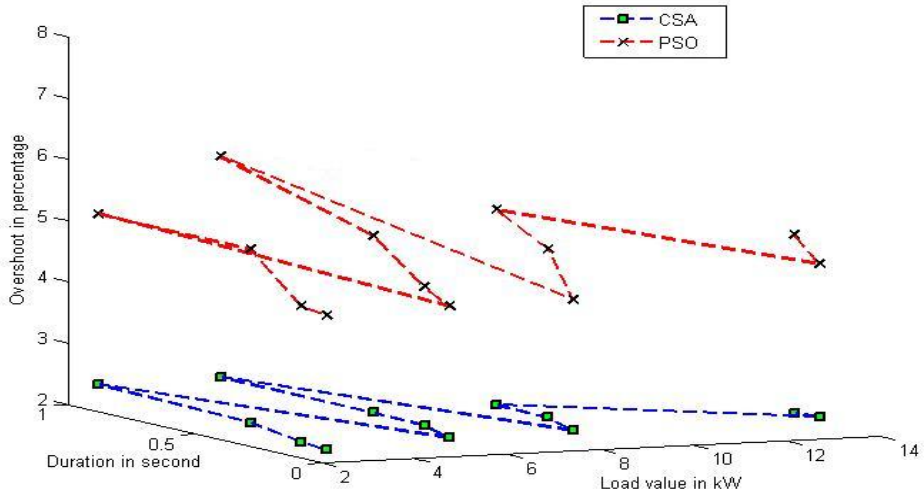

(b)

Fig. 11. Controller performance analysis with different load value and different duration (a) settling time performance, (b) overshoot performance

VI. CONCLUSION

An online designed optimal excitation controller using a clonal selection algorithm, from artificial immune systems, has been presented in this paper. The CSA has been implemented on a MSK2812 DSP hardware platform to control a laboratory scaled down version of the Navy's future electric ship power system. This controller has advantages including optimal oriented, no generator parameters needed and minimal human involvement. The objective for the CSA algorithm is to minimize the voltage deviations when pulsed loads are directly energized by shipboard power system, thus reducing energy storage devices capacity. Comparing CSA with PSO, both simulation and hardware results show that CSA-based controller can restore and stabilize the terminal voltage effectively and quickly with little disturbance introduced after high power pulsed loads are experienced.

VII. REFERENCE

[1] L. N. Domaschk, Abdelhamid Ouroua, Robert E. Hebner, "Coordination of Large Pulsed Loads on Future Electric Ships," *IEEE Transaction on Magnetics*, vol. 43, no.1, January 2007.

[2] K. Kim, R. C. Schaefer, "Tuning a PID Controller for a Digital Excitation Control System," *IEEE Transactions on Industry Application*, no.2, vol.41, pp.485-492, March/April 2005.

[3] K. Kim, A. Godhwani, M. J. Basler and T. W. Eberly, "Commissioning experience with a modern digital excitation system," *IEEE Transaction on Energy Conversion*, vol.13, no.2, pp.183-187, June 1998.

[4] J. Machowski, S. Robak, J. W. Bialek, J. R. Bumby, N. AbiSamra, "Decentralized Stability-Enhancing Control of Synchronous Generator," *IEEE Transactions on Power Systems*, no.4, vol.15, November 2000.

[5] Feng Zheng, Qingguo Wang, Tong H. Lee, Xiaogang Huang, "Robust PI Controller Design for Nonlinear Systems via Fuzzy Modeling Approach," *IEEE Transactions on Systems, Man, and Cybernetics*, no.6, vol.31, November 2001.

[6] Ali Karimi, Ali Feliachi, "PSO-tuned Adaptive Backstepping Control of Power Systems," *IEEE Power Systems Conference and Exposition*, Page(s):1315-1320, October 2006.

[7] Zwe-Lee Gaing, "A particle swarm optimization approach for optimum design of PID controller in AVR system," *IEEE Transaction on Energy Conversion,* vol.19, pp.384-391, June 2004.

[8] G. K. Venayagamoorthy, R. G. Harley, "A Continually Online Trained Neurocontroller for Excitation and Turbine Control of a Turbogenerator," *IEEE Transactions on Energy Conversion*, no.3, vol.16, pp.261-269, September 2001.

[9] G. K. Venayagamoorthy, R. G. Harley, "Two Separate Continually Online-Trained Neurocontrollers for Excitation and Turbine Control of a Turbogenerator," *IEEE Transactions on Industry Applications*, no.3, vol.38, pp.887-893, May/June 2002.

[10] P. Mitra, C. Yan, L. Grant, G. K. Venayagamoorthy and K. Folly, "Comparative Study of Population Based Techniques for Power System Stabilizer Design," *International Conference on Intelligent System Applications to Power Systems*, pp.1-6, 2009.

[11] Y. del Valle, G.K. Venayagamoorthy, S. Mohagheghi, J.C. Hernandez, and R.G. Harley, "Particle Swarm Optimization: Basic Concepts, Variants and Applications in Power Systems," *IEEE Transactions on Evolutionary Computation*, vol.12, no.2, pp.171-195, 2008.

[12] A. Ouroua, L. Domaschk, and J.H. Beno,"Electric Ship Power System Integration Analyses Through Modeling and Simulation," *IEEE Electric Ship Technologies Symposium*, 2005.

[13] IEEE Standard 421.5, *2005 IEEE Recommended Practice for Excitation System Models for Power System Stability Studies*, pages 1-85, 2006.

[14] L.N. de Castro and F.J. Von Xuben, "Learning and Optimization Using the Clonal Selection Principle," *IEEE Transactions on Evolutionary Computation*, volume 6, number 3, June 2002.

[15] H. Lou, C. Mao and D. Wang, "PWM optimization for three-level voltage inverter based on clonal selection algorithm," *IET Electric Power Applications*, vol. 1, no. 6, pages 870–878, 2007.

[16] F. Campelo, F.G. Guimaraes, H. Igarashi and J.A. Ramirez, "A Clonal Selection Algorithm for Optimization in Electromagnetics," *IEEE Transactions on Magnetics*, vol.41, no.5, pp.1736-1739, 2005.

[17] X. Wang, "Clonal Selection Algorithm in Power Filter Optimization," *IEEE Mid-Summer Workshop on Soft Computing in Industrial Applications*, June 2005.

[18] S.A. Panimadai Ramaswamy, G.K. Venayagamoorthy and S. N. Balakrishnan, "Optimal Control of Class of Non-linear Plants Using Artificial Immune Systems:

Application of the Clonal Selection Algorithm." *IEEE International Symposium on Intelligent Control*, October 2007.

[19] L. Zhang, Y. Zhong, B. Huang, J. Gong and P. Li, "Dimensionality Reduction Based on Clonal Selection for Hyperspectral Imagery," *IEEE Transaction on Geoscience and Remote Sensing*, vol. 45, no 12, pp.4172-4186, 2007.

[20] P. Mitra and G.K. Venayagamoorthy, "An Adaptive Control Strategy for DSTATCOM Applications in an Electric Ship Power System," *IEEE Transactions on Power Electronics*, vol.25, no.1, pp.95-104, 2010.

[21] E.R.C. Viveros, G. N. Taranto and D.M. Falcao, "Tuning of Generator Excitation Systems using meta-heuristics," *IEEE Power Engineering Society General Meeting*, pp. 1-6, 2006.

[22] F.P. Demello and C. Concordia, "Concepts of Synchronous Machine Stability as Affected by Excitation Control," *IEEE Transaction on Power Apparatus and Systems*, vol. PAS-88, no.4, pp.316-329, 1969.

[23] P. Kundur, *Power System Stability and Control*. New York: McGraw-Hill, 1993.

[24] Stanley M. Sinners, *Modern Control System Theory and Design*, 2nd edition, Wiley-Interscience, 1998.

PAPER

2. ANALYSIS AND APPLICATION OF THE SPPSO ALGORITHM FOR THE DEVELOPMENT OF AN OPTIMAL EXCITATION CONTROLLER

Chuan Yan, Ganesh K. Venayagamoorthy and Keith A. Corzine

Real-Time Power and Intelligent Systems Laboratory, Missouri University of Science & Technology, Rolla, MO -65409, USA

Abstract:

Operation of high energy loads on future Navy electric ships will cause disturbance on the main bus voltage and impact the operation of the rest of the system; especially if the pulsed loads are directly powered from the main dc bus. An optimal excitation controller can be designed to minimize the effects of pulsed loads and reduce energy storage device capacities. Since exact system parameters and disturbances experienced are unknown, a fast online excitation controller design approach is preferred. Small population based particle swarm optimization (SPPSO) has been recently introduced to address the long search time needed to attain good solutions and the problem of getting trapped in local minimum associated with the PSO algorithm. SPPSO overcomes these problems with concepts of a small population and regeneration of particle positions at regular intervals. A study on the number of particles to be regenerated, and what interval, is investigated in this paper for the online design of an excitation controller for a synchronous generator. The SPPSO is studied for an optimal excitation controller design in both Matlab/Simulink and on a laboratory hardware platform. Both simulation and implementation results show that for time critical application, the SPPSO optimized controller provides effective control of a generator's terminal voltage during pulsed loads; restoring and stabilizing it quickly.

*Keywords***:** Electric ship, optimal excitation controller, small population particle swam optimization (SPPSO), pulsed loads.

1. INTRODUCTION

The Navy's future electric ship power system is based on the integrated power system (IPS) architecture consisting of four main elements: power generation, propulsion systems, hydrodynamics, and DC zonal electric distribution system (DC-ZEDS) [1]. In order to maintain power quality in IPS, immediate energy storage devices with their corresponding charging systems are proposed to make the pulsed power required compatible with the supply system [1]. However, this will increase the system cost. To some extent, the generator field excitation control can be used along with energy storage to maintain the system voltage. The excitation control is one of the most effective and economical techniques to stabilizing the terminal voltage of the synchronous generators. An optimally tuned excitation system offers benefits in overall operating performance during transient conditions caused by system faults, disturbance, or motor starting [2]. In order to optimize them, many algorithms are extended to the design of the optimal excitation controller for the synchronous generators. Two methods are predominantly used, one being the pole-placement method and the other being the cancellation approach [2, 3]. However, for these methods to be applied, the system transfer function and machine parameters are needed. Furthermore, these techniques are not optimal oriented. In other literature [4], Lyapunov's direct method has been used to optimize excitation controller. But again, knowledge of the machine parameters is required.

Recently, computational intelligence (CI) methods have been used in optimizing excitation controllers. Types of CI techniques include fuzzy set theory [5], particle swarm optimization (PSO) [6, 7], genetic algorithms (GAs) [7] and online trained neurocontroller [8, 9]. These techniques all have good performance at maintaining the terminal voltage. However, there are two main difficulties with most of the CI methods. First, the search time is relatively long, mainly as a result of large number of fitness evaluations. Therefore, it is unpractical for online controller development using heuristic search algorithms. For example, a PSO based optimal excitation controller search process with 20 particles and 100 iterations will require 2000 evaluations which means that 2000

disturbances are applied to the generator. Therefore, these CI based optimal excitation controller search process are not implemented in hardware which means that detailed machine parameters and system specifications are needed in order to build the simulation system. Second, although the search process for these CI based optimal excitation controller have a good convergence, they have a premature or local minimum trapping problem.

SPPSO was first introduced by Das and Venayagamoorthy [10] and has two distinguishing features from the standard PSO. The first feature is the small population, resulting in reduction of the number of fitness evaluations to be carried out per iteration. Fitness evaluations for online design of an excitation controller are found to be most time tasking [25]. The other feature of SPPSO is the regeneration concept, which overcomes the problem of particles getting trapped in local minima and not finding the global optimum. As a result of these advantages, SPPSO has been shown to be useful in time critical power system optimization problems [10-12]. However, the effectiveness of the SPPSO algorithm for online optimization problems can be only observed and even enhanced if the optimal number of particles to be regenerated and at what interval of the search iterations is carefully determined. This is studied in this paper for online excitation controller design based on a Matlab/Simulink model of a synchronous generator connected a propulsion motor with some loads (a portion of the IPS). Based on an optimized SPPSO algorithm, a real-time implementation is carried out on the MSK2812 DSP hardware platform to minimize the voltage deviations in scaled-down laboratory setup of electric ship power system. Both Matlab simulation and laboratory implementation results show that the online SPPSO-based controller improves the dynamic performance and the stability of the synchronous generator.

The rest of the paper is organized as follows: Section 2 describes the power system model for the electric ship and the laboratory hardware implementation/setup; Section 3 presents the SPPSO algorithm, the studies to determine the optimal regeneration scheme, and its application to the design of an optimal controller; Section 4 presents typical simulation and laboratory implementation results, and finally, the conclusion is given in Section 5.

2. ELECTRIC SHIP POWER SYSTEM MODEL AND LABORATORY HARDWARE SETUP

The power system of the all-electric ship system mainly consists of four parts: prime movers, advanced propulsion induction motors, dc zonal distribution loads, and other auxiliary loads which are shown in Fig. 1. All prime mover power is first converted into electric power, and then it is distributed and allocated between propulsion, pulsed power weapons, ship service power and other electrical loads as required. In order to study the proposed controller, a scaled down testbed is needed. In the laboratory setup, four parts (power generation, Propulsion loads, DC zonal loads and excitation system) are implemented. The detailed implementation can be found in [25].

In the laboratory setup, a small-scale power generation system is used to emulate the gas turbine-generator sets of the electric ship. This small-scale system consists a three-phase 60Hz 5kVA synchronous generator coupled to a 15kW dc motor to supply mechanical torque.

In the notional electric ship, a propulsion system consists of a transformer, a rectifier, an inverter, and a propulsion motor [1]. In the laboratory setup, a 2.65kW resistive load in the dc side is used to emulate the load impact of the propulsion motors on the IPS.

In the laboratory setup, a diode rectifier is used along with a passive filter to realize the power conversion model and three IGBT-controlled resistive loads are used to represent three different energy-level loads on the dc side (2.65kW, 5.29kW, 5.29kW).

In the laboratory setup, the proposed excitation system is simplified so that some parts such as the power system stabilizer and under-excitation limiter are not considered. A simple functional block diagram for the excitation controller is shown in Fig. 2.

As is shown in Fig. 2, V_s^* is the rms terminal voltage reference of the synchronous generator and V_s is the measured value. The subtraction of V_s^* and V_s produces error voltage signal, which is amplified in the regulator. The overall equivalent gain and the time constant associated with the regulator are simulated by K_a and T_a, respectively. The time constants, T_b and T_c, may be used to model equivalent time constants inherent in the voltage regulator. $V_{r,max}$ and $V_{r,min}$ defines the maximum and minimum voltage regulator output respectively [13]. In this case, the key element in the design of the optimal

excitation controller is finding the optimal controller parameters (K_a, T_a, T_b and T_c) to provide optimal performance during the pulsed loads.

In the laboratory setup, the excitation controller consists of a sensor board, an A/D conversion board, a MSK2812 DSP board consisting of the TMS320F2812 processor, and a D/A conversion board. The A/D conversion board receives terminal voltage signal form the sensor board and output digital signal to the central controller. The D/A conversion board receives the PWM signals from the central controller and outputs them to the IGBTs. The field of the synchronous generator is connected with a four-quadrant PWM dc drive. The field voltage is regulated by a central controller through switch on and off the IGBTs.

In this paper, an online optimal excitation design approach is presented. Here 'online' means that the parameters of excitation controller are determined via iterative approach, in other words, in an incremental manner, using the optimal SPPSO algorithm.

3. IMPLEMENTATION OF AN ONLINE SPPSO BASED OPTIMAL EXCITATION CONTROLLER

A. SPPSO Algorithm

Particle swarm optimization is widely used in electric power systems today [14]-[19], and SPPSO is a variant of PSO developed for quasi-online applications by Das and Venayagamoorthy [10]. SPPSO has two distinguishing features from the standard PSO. The first feature is the use of a small population, which means fewer fitness evaluations compared to the standard PSO. Fitness evaluations are found to be most computational expensive task in the optimization process, especially when it comes to power system applications. The other feature of the SPPSO algorithm is the regeneration concept, which addresses the problem of particles getting trapped in local minima, and not finding the global optimum. The velocity and position update equations of the particles in SPPSO are the same as that of the standard PSO, and are given by (1) and (2) respectively.

$$v_i(k+1) = w \cdot v_i(k) + c_1 \cdot rand_1 \cdot \left(P_{best}(k) - x(k)\right) + c_2 \cdot rand_2 \cdot \left(G_{best} - x(k)\right) \quad (1)$$

$$x_i(k+1) = x_i(k) + v_i(k+1) \quad (2)$$

where w is the inertia constant, c_1 and c_2 are two positive numbers referred to the cognitive and social acceleration constants, and $rand_1$ and $rand_2$ are two random numbers with uniform distribution in the interval [0,1]. The values of w, c_1 and c_2 are kept fixed at 0.8, 2.0 and 2.0 [19]. The movement of a SPPSO particle in two dimensions is illustrated in Fig. 4. P_{best} is a particle's best position and G_{best} is the best global position in the swarm.

Every M iterations, the position and velocity for R out of 5 particles is regenerated in the case of the SPPSO algorithm. The new position and velocity is obtained from a random uniform. Prior to regeneration, the P_{best} and G_{best} are updated. The number of particles to be regenerated and at what frequency is explained for the online controller development problem in Section 3C.

B. On-line Optimal Controller Design using SPPSO

The procedure for the online design of an optimal excitation controller is illustrated in the flowchart given in Fig. 5. Positions and velocity of N particles are randomly initialized. According to [10] and [19], N is set to be 5 and 20 for SPPSO and PSO algorithms, respectively.

In the excitation control loop of Fig. 2, the proportional gain K_a, and time constants T_a, T_b, and T_c have to be carefully tuned to provide satisfactory performance under both normal and pulsed load conditions. The objective of the SPPSO algorithm is to find these parameters in order to restore and stabilize the generator's terminal voltage quickly; especially after pulsed loads of different magnitudes and durations. Most objective functions used for excitation controllers design in literature is function of the settling time, rise time and overshoot. In this paper, the objective function associated with the controller performance is obtained by calculating the transient response area, given by (3) [20], [21]. This can be used as a fitness function to guide search algorithms to find the corresponding controller parameters that provide the desirable time response characteristics such as rise time, overshoot and settling time. In other words the parameters that results in the minimum transient area can be found.

$$Fitness = \frac{1}{2}\sum_{i=1}^{n}\left\{\sqrt{\left[V_s^* - V_s(i)\right]^2 + \left[V_s^* - V_s(i+1)\right]^2}\right\}\Delta t \qquad (3)$$

where

V^*_s reference terminal voltage value;

k sampling instant;

Δt sampling interval;

V_s measured terminal voltage;

A sampling frequency of 500Hz and a sampling window of 1s is used in carrying the fitness evaluation.

Due to the high computational overhead involved in computing the square root function on a digital signal processor, (3) is modified to (4) for the controller design. The term ($i\Delta t$) is a weighting factor that puts an increasing penalty as oscillations persist for a longer time; thus guiding the search algorithm to minimize the settling time of the system oscillations in addition to the maximum overshoot after a disturbance.

$$Fitness = \frac{1}{2}\sum_{i=1}^{n}\left(\left[V_s^* - V_s(i)\right]^2 + \left[V_s^* - V_s(i+1)\right]^2\right)(i\Delta t)\Delta t \qquad (4)$$

In hardware, the pulsed load magnitudes and duration used in controller development and evaluation phases are shown in Table 1. Two pulsed loads, which are labeled "Search" in Table 1, are applied to serve as disturbance to system when both PSO and SPPSO algorithms are searching for optimal parameters. After the optimal parameters have been obtained, eleven other different pulsed loads are used to evaluate the performance of the optimal controller, which are labeled as "Evaluate".

C. 'Optimal' SPPSO for Excitation Controller Development

To maximize SPPSO performance for online tuning of controller parameters, careful selection of the number of particles to be regenerated, *R* and frequency *M* (the number of iteration interval for regeneration) is critical. *R* and *M* are determined in this study using a Matlab and Simulink/SimuPowerSystem implementation (Fig. 6) of the electric ship power system model in Fig. 1. In order simulate ship's acceleration characteristic, a variable load is used to simulate the propulsion loads. The propulsion load is gradually changed from 1.65kW to 2.65kW during the pulsed load application. In this case, the operating point of the IPS is changing which makes the simulated operating conditions closer to ship's real operation conditions. A pulsed load of 5.29kW with 0.75s

duration is used for tuning controller parameters. Fitness evaluation is carried out using (2).

In order to analyze the *R* and *M* parameter sensitivity, the range of the parameter *R* is from 1 to 5 with a step of 1, and the possible values for *M* are selected to be 5, 10 and 20, based on experience that most improvements with the standard PSO takes place in the first 10 to 20 iterations. Therefore, there are totally 15 combinational studies with the different values of *R* and *M*. The optimal values of *R* and *M* are obtained based on average fitness computed over 50 trials, and each trial has 100 iterations. The average performance is shown in Figs. 7 to 11 for different values of *R*. It is clearly shown that the lowest fitness is achieved with *M* = [5, 5, 10, 20, 20] for *R* = [1, 2, 3, 4, 5] respectively, which is summarized in Fig. 12. The number of fitness evaluation for 5 particles in 100 iterations is 500. Therefore, the total number of regeneration for each combination study is shown in Table 2. For example, when *R* = 1 and *M* = 5, there are 20 regenerations taking place, which is 4% of the total 500 fitness evaluations. It is clearly shown that the best performance is observed when the regeneration percentage is in range of 4% to 8% of the total fitness evaluations.

The best average performance evaluated using the average fitness function is obtained when the numbers of particles to participation in the regeneration process is two, and frequency of regeneration is five. Two particles are chosen at random every five generations, and positions and velocities are randomized from a uniform distribution. Therefore, for the online development of the optimal excitation controller, both in simulation and laboratory implementation studies, the ‘optimal’ SPPSO has R set to two and M set to 5.

A statistical analysis based on standard deviation is used to evaluate the convergence for PSO and SPPSO using the standard deviation, defined as (5).

$$\sigma_{ave} = \sqrt{\frac{1}{n}\sum_{i=1}^{n}\left(F_i - F_{ave}\right)^2} \tag{5}$$

where i = 1 for the first trial, 2 for the second trial, and so on, n = total number of trials which is 30, F_{ave} = average best fitness over 30 trials, and $F_{i,}$ = the i^{th} trial best fitness value.

As is shown in Figs. 7 to 11, the average performance of PSO is better than SPPSO, which means PSO has better exploitation capability than SPPSO. Using (5), the standard deviation is 0.00577 and 0.0037 for PSO and SPPSO, respectively. It is clear that SPPSO's accuracies around their corresponding average solution are higher than PSO's. Furthermore, since the particle population for PSO is 20 and the search is over 100 iterations, the total number of fitness evaluations for PSO is four times more than that with SPPSO. Therefore, it is clearly shown that SPPSO overcomes the local minimum trapping problem with much less fitness evaluations, in other words in a shorter time.

4. ONLINE CONTROLLER DEVELOPMENT RESULTS

The SPPSO and PSO algorithms for comparison purposes have been implemented on two platforms: i) Simulation based on Matlab/Simulink/SimuPowerSystems; and ii) a laboratory hardware system. In order to minimize the effects of the randomness in the search algorithms, SPPSO and PSO start with the same initialization. This is true for population size of SPPSO. The search space boundaries and limits are the same for the positions and velocities of the particles. The two algorithms are allowed the same number of fitness evaluations, in other words the respective number of iterations is fitness evaluations allowed divided by the population size. The following subsections present results obtained from the simulation and hardware implementations.

A. Matlab Simulation

The SPPSO and PSO algorithms based online controller design are carried out for 30 trials. At the end of the 30 trials, two best particles (G_{best} solutions) are chosen as the parameters for the SPPSO based controller and PSO based controller respectively. A pole placement based controller design is also carried out in this study for comparison with online heuristic approaches [2]. A first order generator model is obtained with gain taken 0.7012 and the time constant taken 0.274 while assuming negligible amortisseur effects [22], [23]. Voltage overshoot of at least 1-20% and 2s total voltage recovery time is

anticipated with the pole-placement method, although the voltage rise time can be less than 1s [2]. The range of damping ratio can be from 0.456 to 0.8261 [24]. For the study in this paper, damping ratio is chosen to be around 0.707. And parameters obtained by pole placement, SPPSO and PSO methods are shown in Table 3.

A performance comparison of the three controllers above is shown in Fig. 13. In Fig. 13 (a), the start-up performance comparison is shown. The overshoot of pole-placement based controller is 12.2% and the 2% settling time is 0.52s, which meets the design requirements. In Fig. 13 (b), a performance comparison is shown under a 5.29kW, 0.75s duration pulsed load. It is clear that the performance of the SPPSO based controller is comparable to the performance of PSO based controller, which means both can perform good exploitation. However, according the standard deviation of the fitness values, SPPSO has a consistent convergence around the same average value while PSO has a better exploitation capability.

B. Hardware Results

A MSK2812 DSP with 150MHz clock frequency and laboratory setup described in Section 2 is used to implement the 'optimal' SPPSO and PSO algorithms for online excitation controller development. The parameters of the excitation controllers found by SPPSO and PSO algorithms are shown in Table 4. These parameters are obtained based on the global best fitness over 40 iterations and 10 trials. The convergence of the SPPSO and PSO algorithms during the search is shown in Fig. 14. This figure shows the fitness convergence of SPPSO and PSO versus iterations averaged over ten trials. The fitness has been normalized. As is shown in Fig. 14, the SPPSO attains convergence on average in the first set eleven iterations (55 fitness evaluations) while PSO attains in the first nine iterations (180 fitness evaluations). The comparative performance for all data sets (search and evaluate) of the SPPSO and PSO design based excitation controllers in terms of the time domain responses (settling time and maximum overshoot) is shown in Table 5. For settling time calculation, because it is hard to compare settling time to within 2% of the reference value, the settling time is computed for oscillation constrained to the range -228V to 232V, which is 0.87%. Typical time domain responses for different pulsed loads are shown in Figs. 15 to 17. It can be observed clearly that the damping provided by the 'optimal' SPPSO based controller is better than that of PSO in terms maintaining a

smaller overshoot and a faster settling time. In addition, it can be seen that variations in the field voltage and current is minimized faster by SPPSO controller. This means heat losses are reduced in the field circuit and extended life. Fig. 18 shows typical magnitudes of overshoots and settling times for pulsed loads of different magnitudes and durations when the excitation controller parameters are found using the 'optimal' SPPSO and PSO algorithms. Again, it is clear that 'optimal' SPPSO finds a better set of parameters.

C. Computation Overhead and Summary

As is shown in Fig. 14, SPPSO and PSO algorithms attend the same fitness after 11 and 9 search iterations, respectively. With 40 iterations allowed online for the search, it is clear that no significant improvements can result. A computational time analysis taking the stalling of fitnesses after 11 and 9 iterations with SPPSO and PSO, respectively, is presented in Table 6. The code execution time per particle for SPPSO and PSO are of the same order and comparable. However, the SPPSO algorithm on overall is at least three times faster than the PSO. Reconfiguration of parameters of an excitation controller within seven minutes is preferred to over 22 minutes for mission critical application on a Navy's electric ship. An overview comparison of SPPSO and PSO algorithms for the online development of optimal excitation controller for electric ship is given in Table 7.

5. CONCLUSION

An online optimal excitation controller using 'optimal' SPPSO algorithm has been proposed and demonstrated on two platforms of a Navy's electric ship power system, namely, a Matlab/Simulink simulation and on an laboratory scaled down power system. The objective for the SPPSO algorithm based controller design is to minimize the voltage deviations at the generator terminals when pulsed loads are directly energized by shipboard power system, thus reducing energy storage devices capacity. The SPPSO algorithm based controller development has numerous advantages for time critical tuning including optimal oriented, no generator parameters needed and no human involved. The number of particles to participate in the regeneration process and the frequency at which they do have been determined to provide the most effective SPPSO algorithm for online controller tuning.

Matlab simulation results show that SPPSO has consistent convergence around the average value although PSO has a better average value. SPPSO based design can greatly reduce search time which means less number of fitness evaluations to find good controller parameters. This translates to less strain on the machine rotor and extended life. Parameters obtained from the 'optimal' SPPSO algorithm can restore and stabilize the terminal voltage effectively and very quickly after high-power pulsed loads are experienced. Therefore, the SPPSO has potential for time critical controller tuning and reconfiguration.

6. ACKNOWLEDGMENT

The finance support by the US Office of Naval Research under the Young Investigator Program (N00014-07-1-0806) and the US NSF CAREER grant (ECCE #0348221) are gratefully acknowledged.

7. REFERENCE

[1] L. N. Domaschk, Abdelhamid Ouroua, Robert E. Hebner, "Coordination of Large Pulsed Loads on Future Electric Ships," *IEEE Transaction on Magnetics*, vol. 43, no.1, January 2007.

[2] K. Kim, R. C. Schaefer, "Tuning a PID Controller for a Digital Excitation Control System," *IEEE Transactions on Industry Application*, no.2, vol.41, pp.485-492, March/April 2005.

[3] K. Kim, A. Godhwani, M. J. Basler and T. W. Eberly, "Commissioning experience with a modern digital excitation system," *IEEE Transaction on Energy Conversion*, vol.13, no.2, pp.183-187, June 1998.

[4] J. Machowski, S. Robak, J. W. Bialek, J. R. Bumby, N. AbiSamra, "Decentralized Stability-Enhancing Control of Synchronous Generator," *IEEE Transactions on Power Systems*, no.4, vol.15, November 2000.

[5] Feng Zheng, Qingguo Wang, Tong H. Lee, Xiaogang Huang, "Robust PI Controller Design for Nonlinear Systems via Fuzzy Modeling Approach," *IEEE Transactions on Systems, Man, and Cybernetics*, no.6, vol.31, November 2001.

[6] Ali Karimi, Ali Feliachi, "PSO-tuned Adaptive Backstepping Control of Power Systems," *IEEE Power Systems Conference and Exposition*, Page(s):1315-1320, October 2006.

[7] Zwe-Lee Gaing, "A particle swarm optimization approach for optimum design of PID controller in AVR system," *IEEE Transaction on Energy Conversion*, vol.19, pp.384-391, June 2004.

[8] S. Vachirasricirikul, I. Ngamroo and S. Kaitwanidvvilai, "Coordinated SVC and AVR for Robust Voltage Control in a Hybrid Wind-diesel System," *Energy Conversion and Management*, available online June 2010.

[9] G. K. Venayagamoorthy, R. G. Harley, "Two Separate Continually Online-Trained Neurocontrollers for Excitation and Turbine Control of a Turbogenerator," *IEEE Transactions on Industry Applications*, no.3, vol.38, pp.887-893, May/June 2002.

[10] T. K. Das, G. K. Venayagamoorthy, " Bio-Inspired Algorithms for the Design of Multiple Optimal Power System Stabilizers: SPPSO and BFA," *IEEE Transaction on Industry applications*, vol.44, pp.1445-1457, September 2008.

[11] P. Mitra and G.K. Venayagamoorthy, "Real-time implementation of an intelligent algorithm for electric ship power system reconfiguration," *Electric Ship Technologies Symposium*, pp.219-226, 2009.

[12] P. Mitra, C. Yan, L. Grant, G. K. Venayagamoorthy and K. Folly, "Comparative Study of Population Based Techniques for Power System Stabilizer Design," *International Conference on Intelligent System Applications to Power Systems*, pp.1-6, 2009.

[13] IEEE Standard 421.5, 2005 IEEE Recommended Practice for Excitation System Models for Power System Stability Studies, pages 1-85, 2006.

[14] P. Acharjee, S.K. Goswami, "A Decoupled Power Flow Algorithm using Particle Swarm Optimization Technique," *Energy Conversion and Management*, vol.50, no.9, pp.2351-2360, September 2009.

[15] L.D.S. Coelho and V.C. Mariani, "Particle Swarm Approach based on Quantum Mechanics and Harmonic Oscillator Potential Well for Economic Load Dispatch with Valve Point Effects," *Energy Conversion and Management*, vol.49, no.11, pp.3080-3085, November 2008.

[16] H. Shayeghi, H.A. Shayanfar, A. Safari and R. Aghmasheh, "A Robust PSSs Design Using PSO in a multi-machine environment," *Energy Conversion and Management*, vol.51, no.5, pp.696-702, April 2010.

[17] R.L. Welch and G.K. Venayagamoorthy, "Energy Dispatch Fuzzy Controller for a Grid-independent Photovoltaic System," *Energy Conversion and Management*, vol.51, no.5, pp.928-937, May 2010.

[18] B.K. Panigrahi, V.R. Pandi and S. Das, "Adaptive Particle Swarm Optimization Approach for Static and Dynamic Economic Load Dispatch," *Energy Conversion and Management*, vol.49, no.6, pp.1407-1415, June 2008.

[19] Y. del Valle, G.K. Venayagamoorthy, S. Mohagheghi, J.C. Hernandez and R.G. Harley, "Particle Swarm Optimization: Basic Concepts, Variants and Applications in Power Systems," *IEEE Transactions on Evolutionary Computation*, no. 2, vol. 12, pp.171-195, April 2008.

[20] P. Mitra and G.K. Venayagamoorthy, "An Adaptive Control Strategy for DSTATCOM Applications in an Electric Ship Power System," *IEEE Transactions on Power Electronics*, vol.25, no.1, pp.95-104, 2010.

[21] E.R.C. Viveros, G. N. Taranto and D.M. Falcao, "Tuning of Generator Excitation Systems using meta-heuristics," *IEEE Power Engineering Society General Meeting*, pp. 1-6, 2006.

[22] F.P. Demello and C. Concordia, "Concepts of Synchronous Machine Stability as Affected by Excitation Control," *IEEE Transaction on Power Apparatus and Systems*, vol. PAS-88, no.4, pp.316-329, 1969.

[23] P. Kundur, Power System Stability and Control. New York: McGraw-Hill, 1993.

[24] Stanley M. Sinners, Modern Control System Theory and Design, 2nd edition, Wiley-Interscience, 1998.

[25] Chuan Yan; Venayagamoorthy, G.K.; Corzine, K.A, "Implementation of a PSO based online design of an optimal excitation controller," *IEEE Swarm Intelligence Symposium*, Oct. 2008, pp. 1–8.

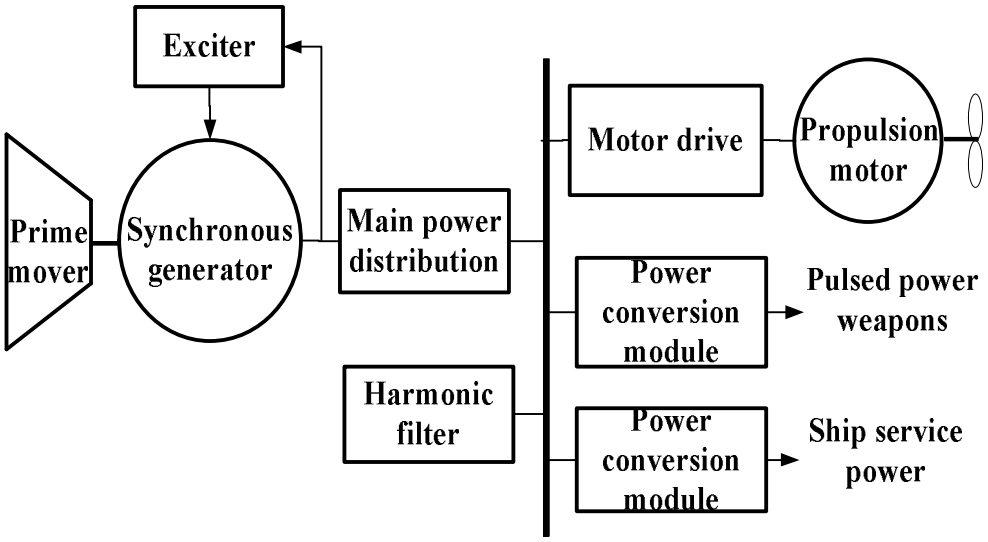

Fig. 1. Simplified power system of an electric ship.

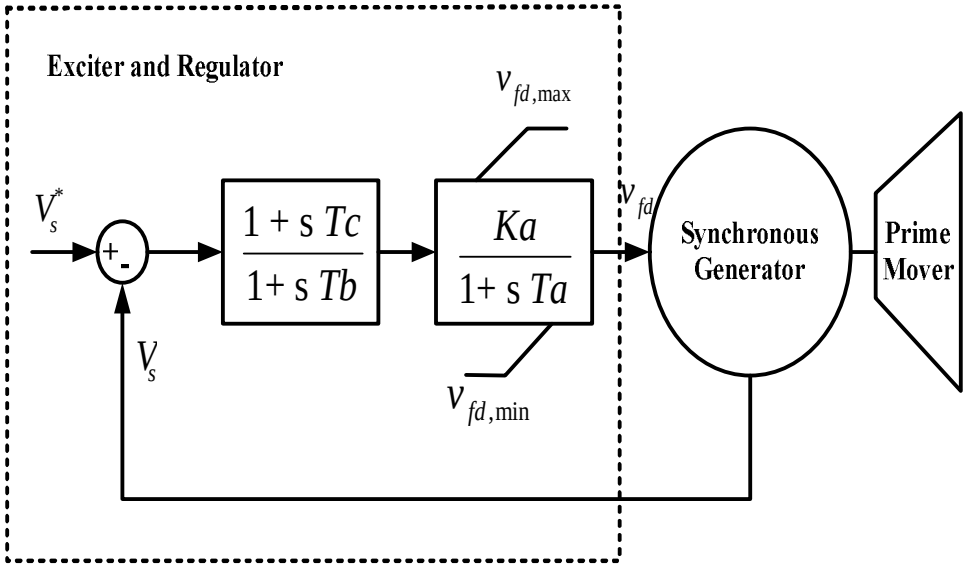

Fig. 2. Simple functional block diagram for synchronous machine excitation control system.

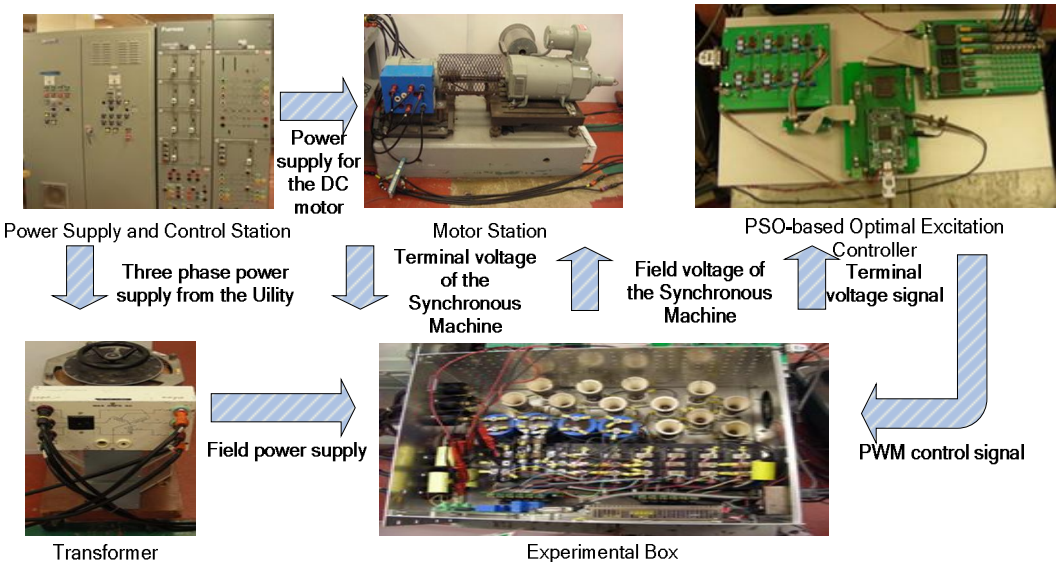

Fig. 3. Laboratory hardware setup of a scaled down electric ship power system and the excitation controller design using SPPSO.

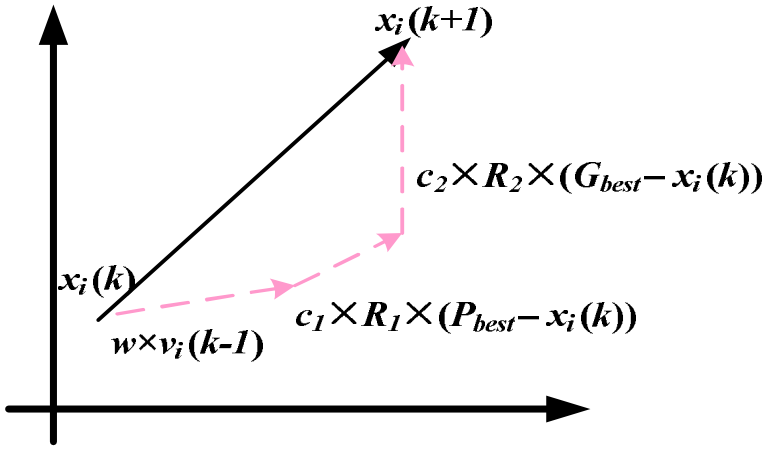

Fig. 4. Movement of a SPPSO particle in two dimensions from one instant k to another instant $k+1$.

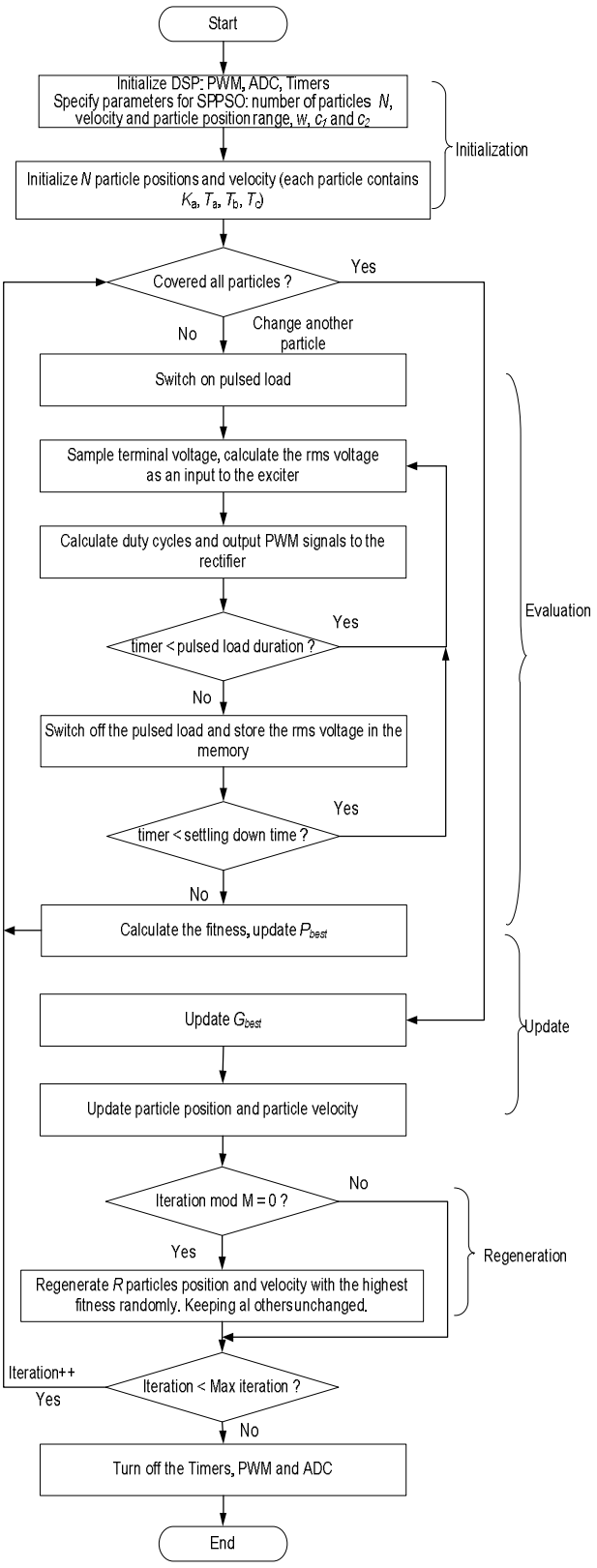

Fig. 5. Flowchart of the SPPSO based design of an optimal excitation controller.

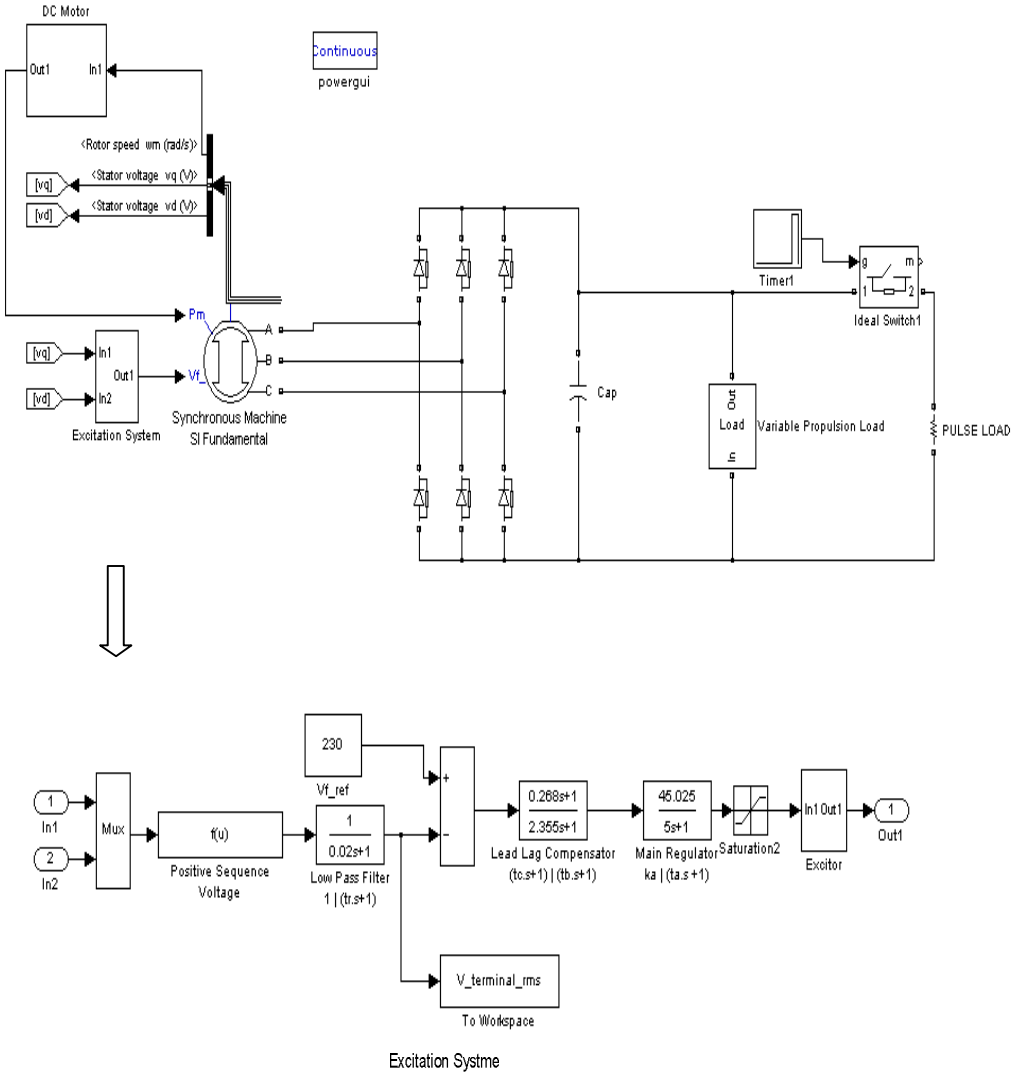

Fig. 6. Test ship power system for Matlab implementation

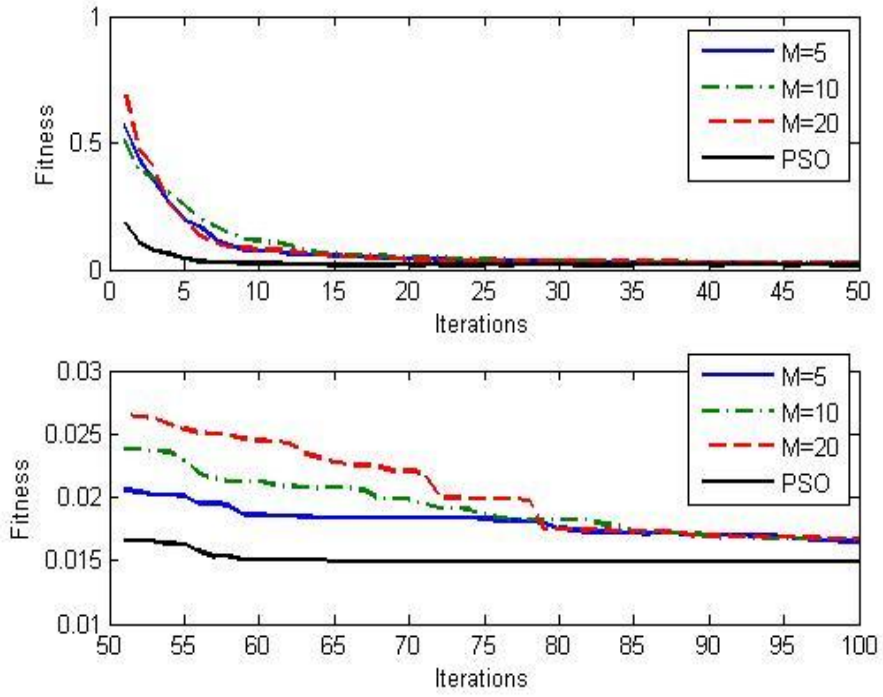

Fig. 7. Average performance of *M* when *R* is set to be 1.

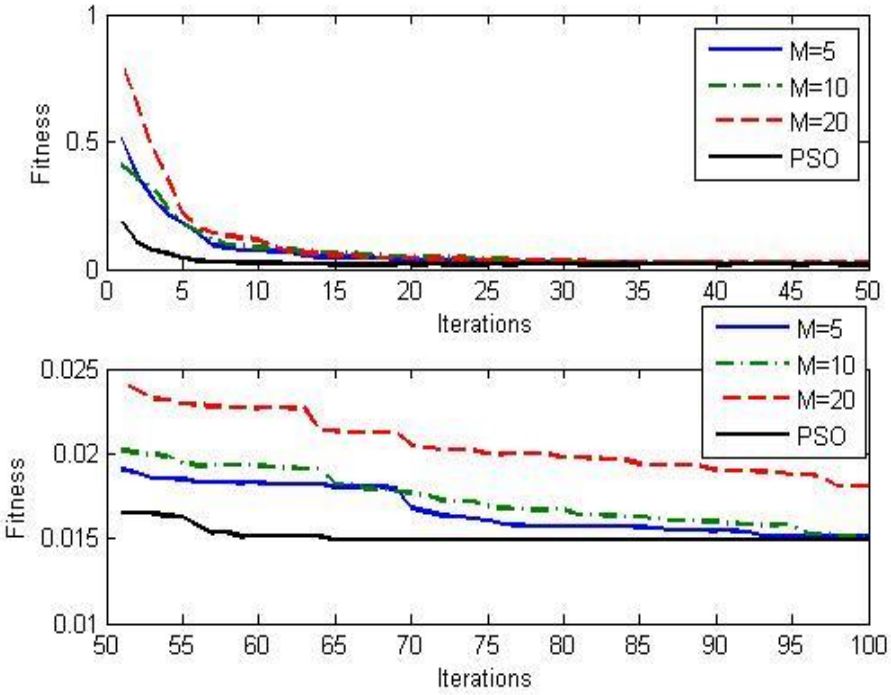

Fig. 8. Average performance of *M* when *R* is set to be 2.

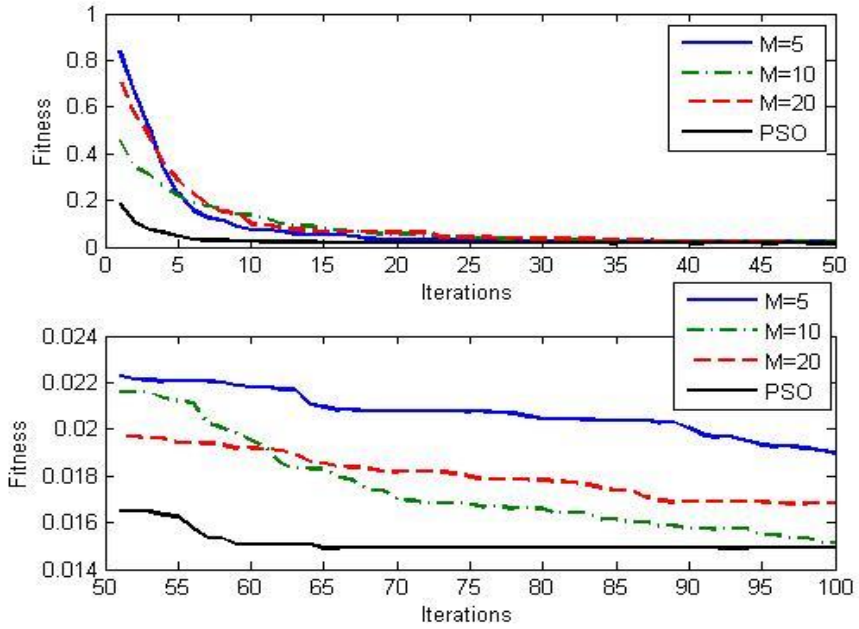

Fig. 9. Average performance of *M* when *R* is set to be 3.

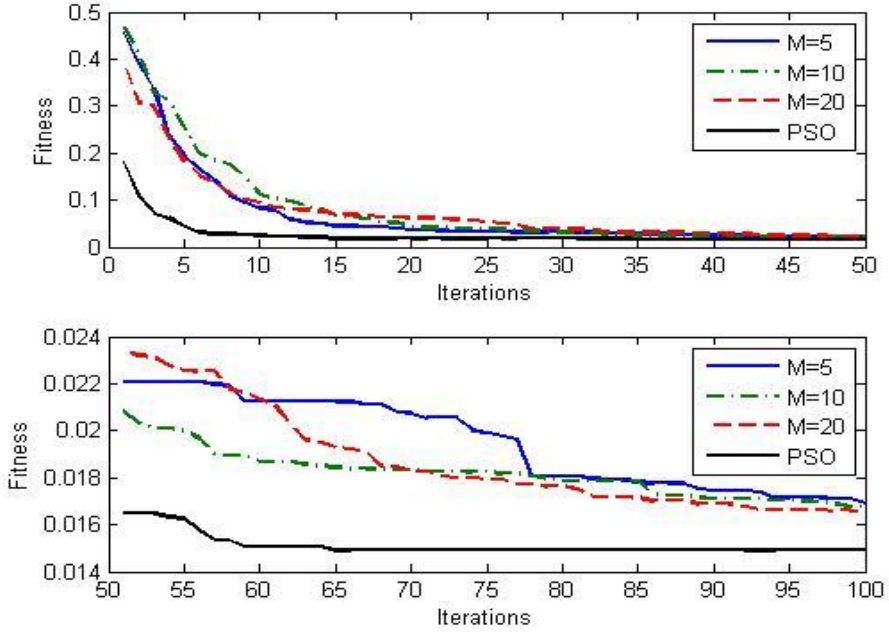

Fig. 10. Average performance of *M* when *R* is set to be 4.

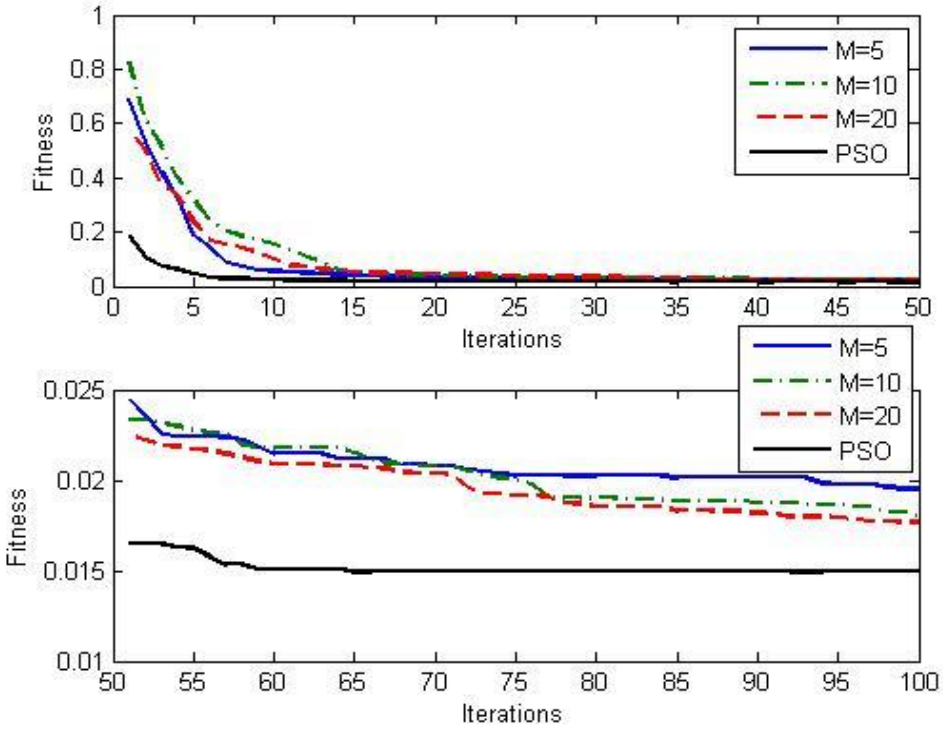

Fig. 11. Average performance of *M* when *R* is set to be 5.

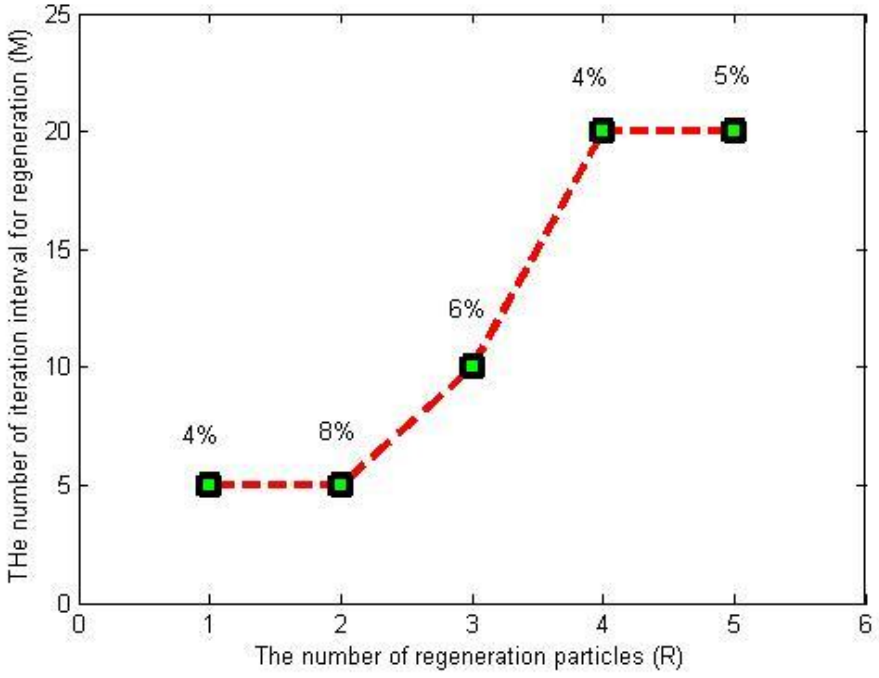

Fig. 12. The best *M* value for different *R* values.

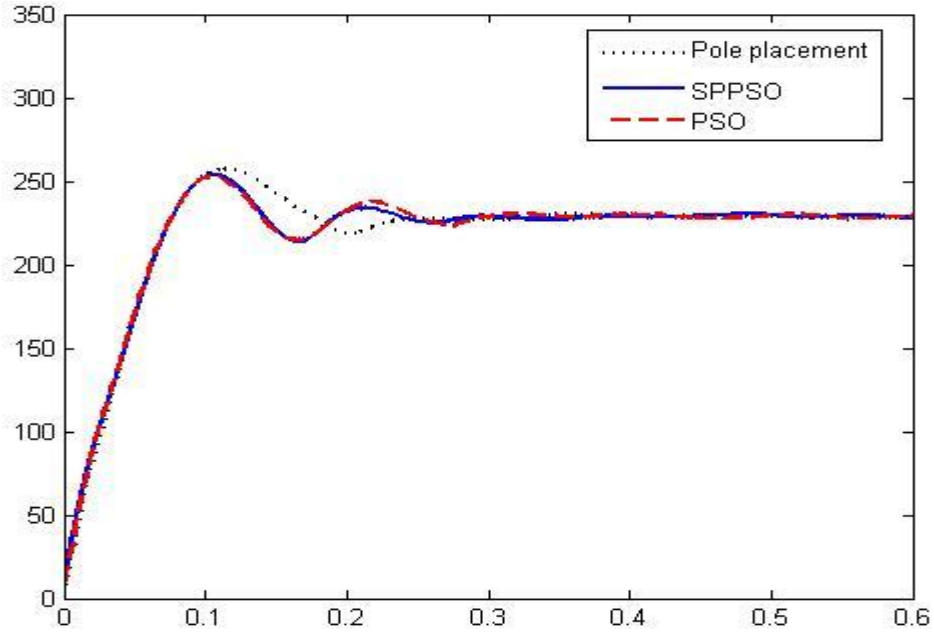

(a)

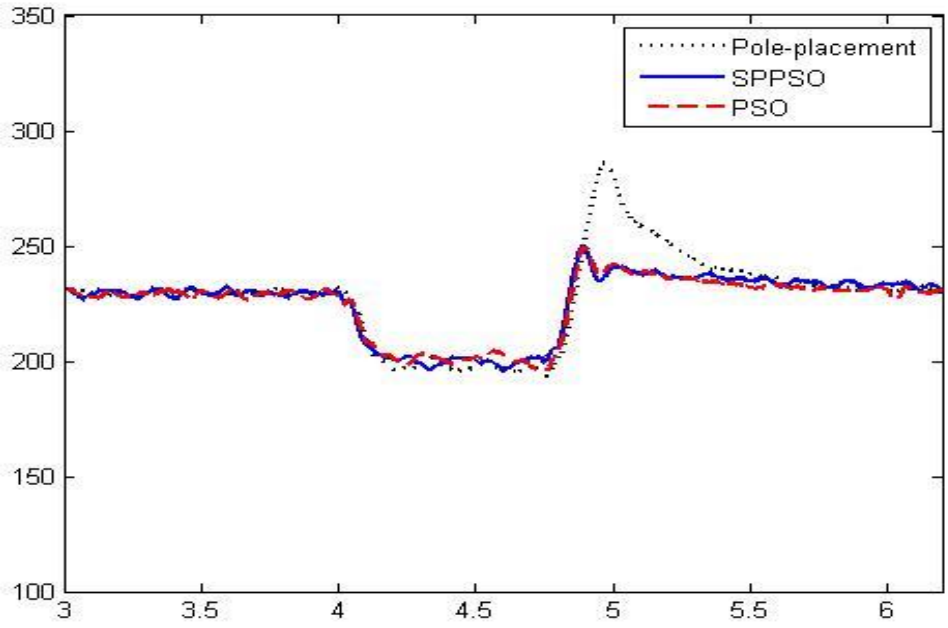

(b)

Fig.13. The performance comparison of pole-placement, PSO and SPPSO based controllers based on Matlab simulation. (a) start up performance, (b) under 5.29kW and 0.75s duration pulsed load

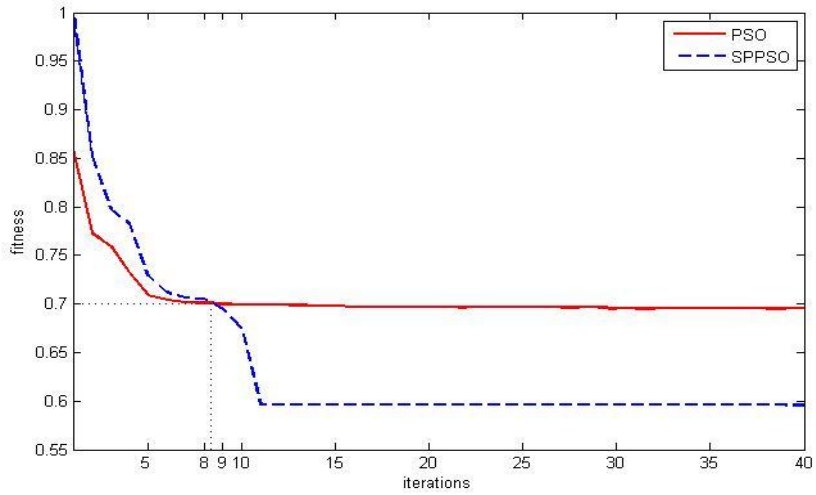

Fig. 14. Average fitness of the best particle in SPPSO and PSO during 40 iterations

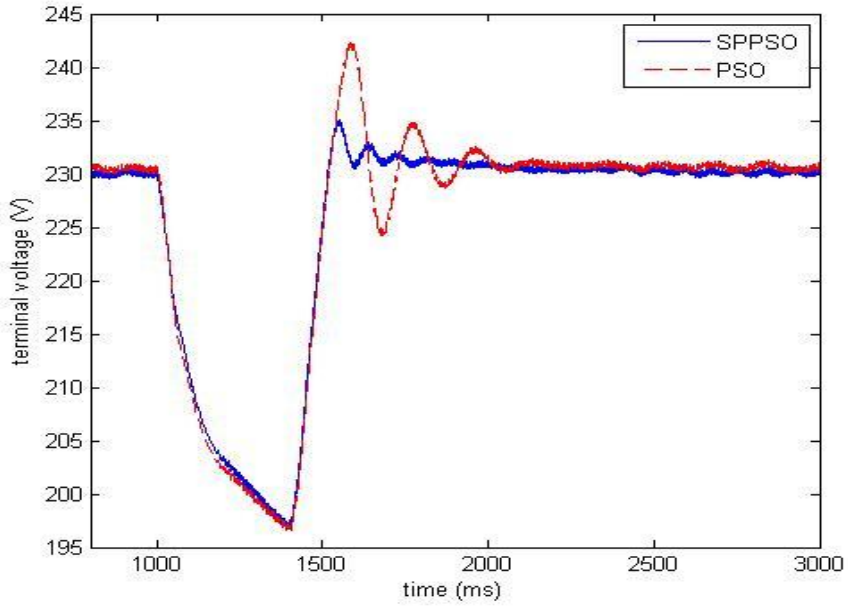

(a)

Fig 15. 2.65kW and 0.4s duration with (a) terminal voltage, (b) field voltage, (c) field current

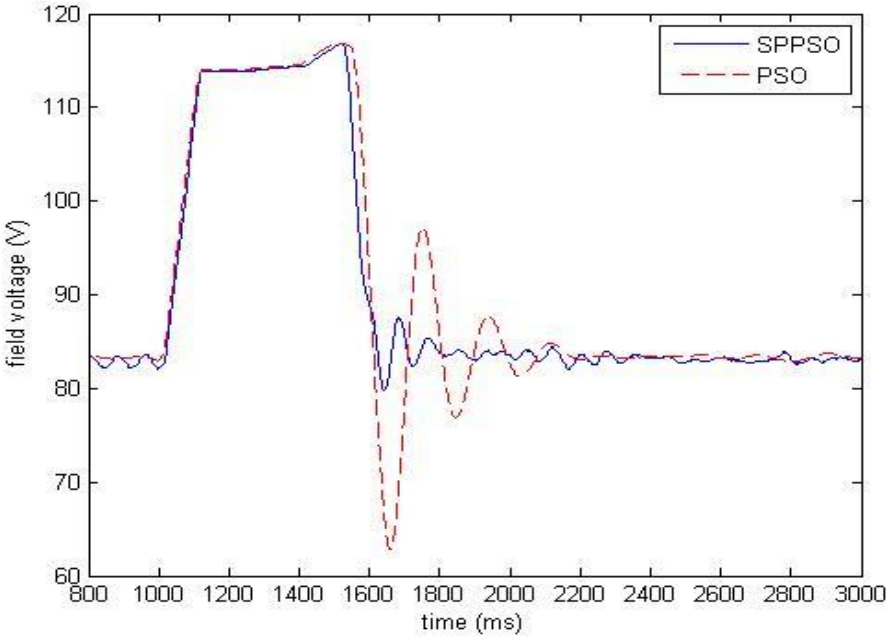

(b)

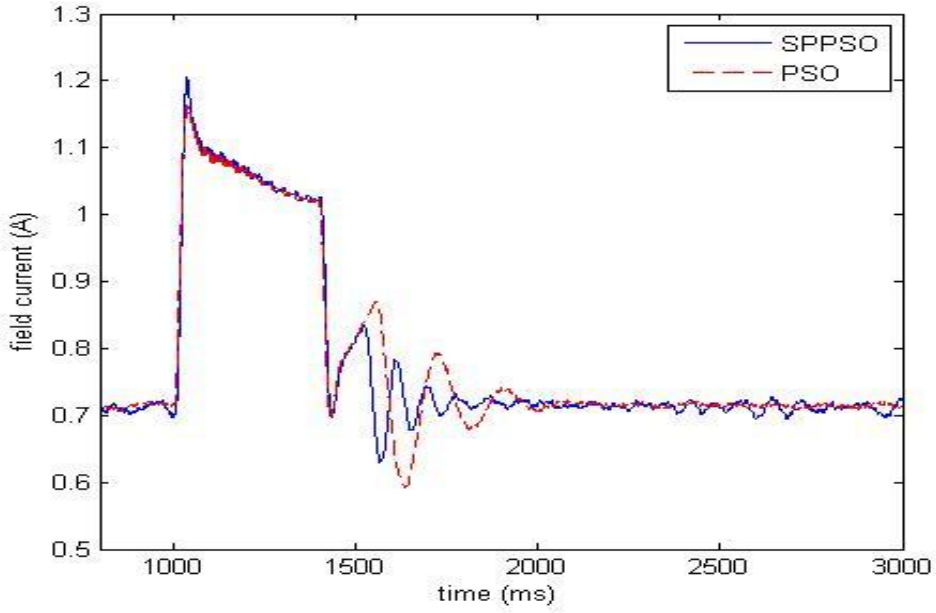

(c)

Fig 15. (Continued) 2.65kW and 0.4s duration with (a) terminal voltage, (b) field voltage, (c) field current

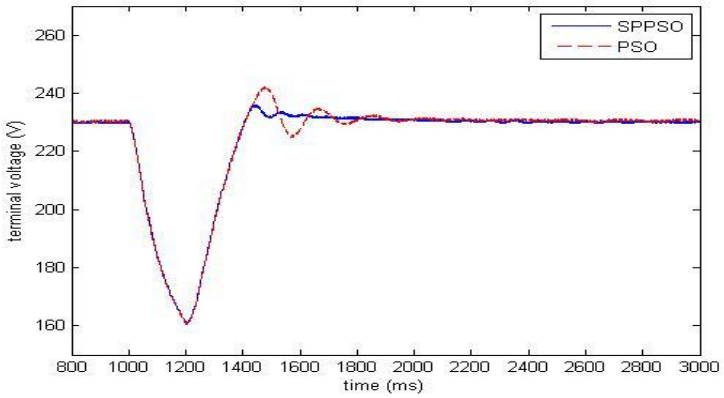

(a)

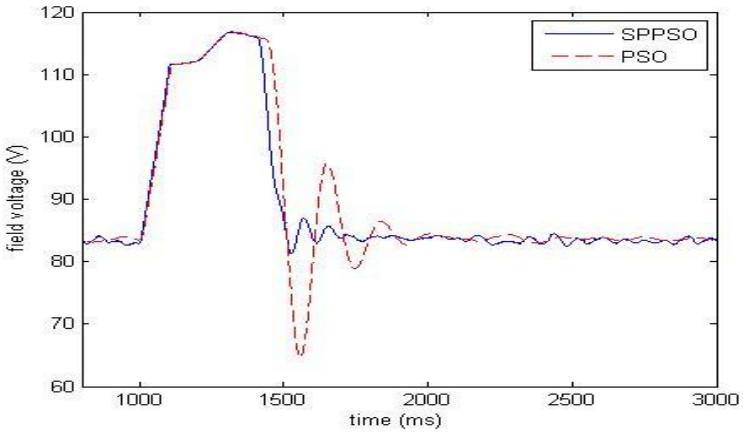

(b)

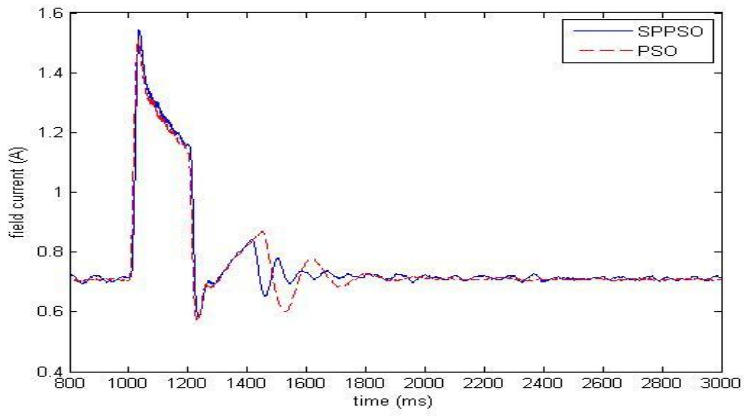

(c)

Fig 16. 5.29kW and 0.2s duration with (a) terminal voltage, (b) field voltage, (c) field current

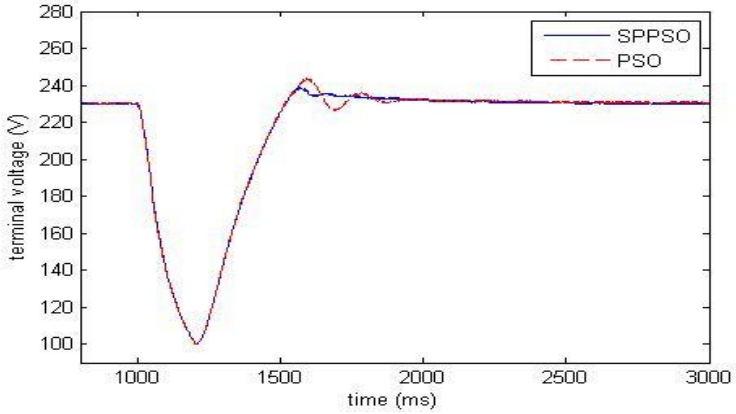

(a)

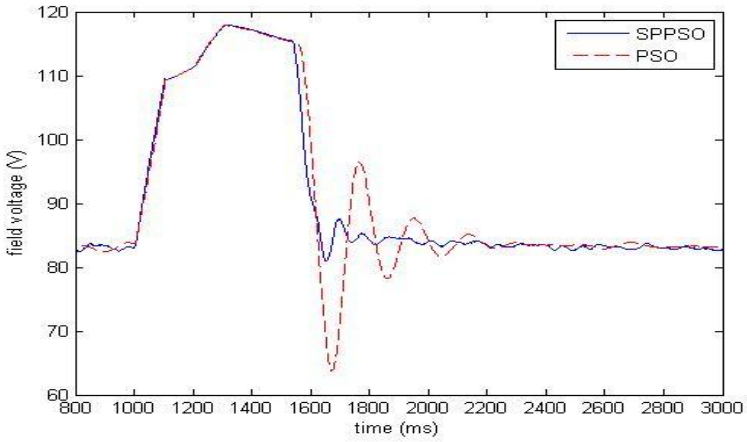

(b)

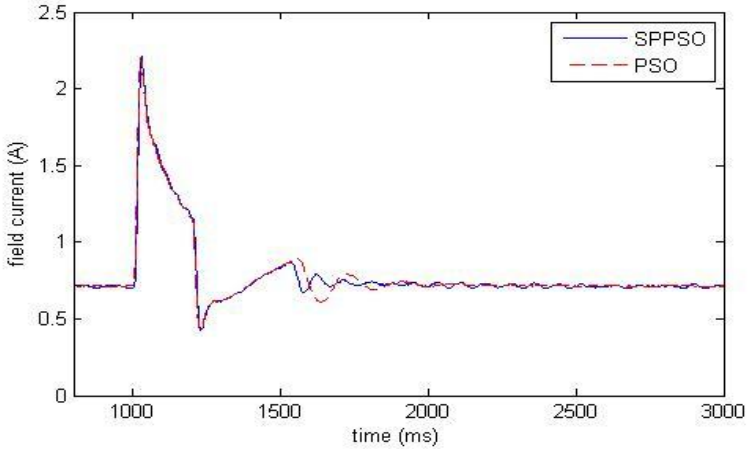

(c)

Fig 17. 13.23kW and 0.2s duration with (a) terminal voltage, (b) field voltage, (c) field current

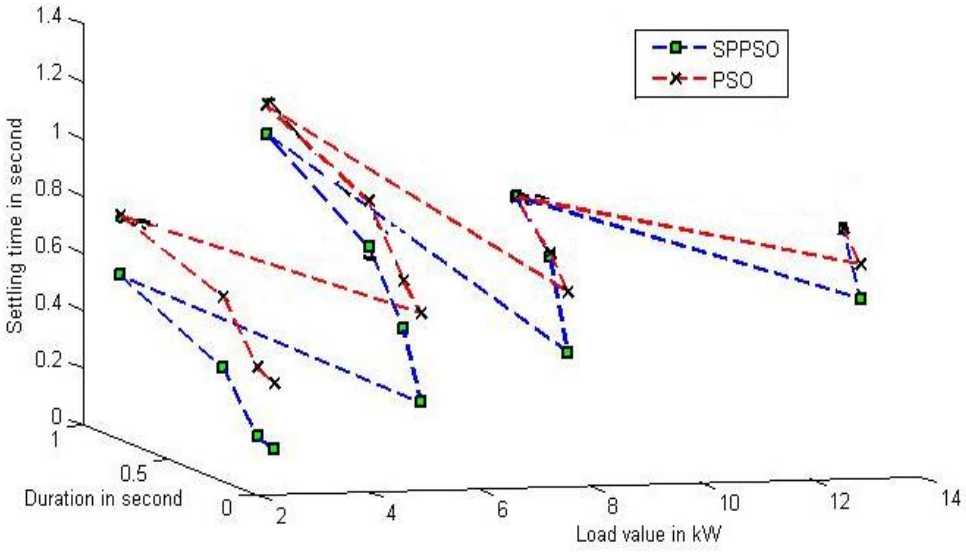

(a)

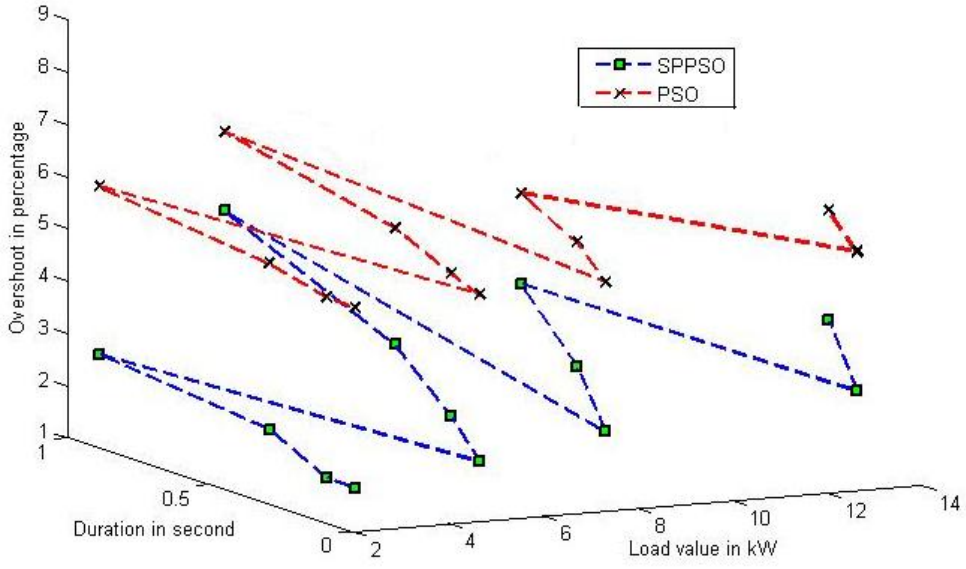

(b)

Fig 18. Controller performance analysis with different load value and different duration (a) settling time performance, (b) overshoot performance

Table 1. Pulsed Load Training and Testing Sets

Duration / Pulsed load	100 ms	200 ms	400 ms	1000 ms
2.65 kW	Test	Test	Test	Test
5.29 kW	Test	Test	Test	Training
7.94 kW	Test	Test	Training	
13.23 kW	Test	Test		

Table 2. Value of the Parameters for the Sensitivity Analysis

M \ R		*R* = 1	*R* = 2	*R* = 3	*R* = 4	*R* = 5
M = 5	No. of regeneration	20	40	60	80	100
	Percentage of No. of regeneration among total evaluation	4%	8%	12%	16%	20%
	Best average fitness value	16.4 e -3	15.1 e -3	19.0 e -3	17.0e-3	19.5e-3
M = 10	No. of regeneration	10	20	30	40	50
	Percentage of No. of regeneration among total evaluation	2%	4%	6%	8%	10%
	Best average fitness value	16.7 e -3	15.2 e -3	15.2 e -3	16.8 e -3	18.0e-3
M = 20	No. of regeneration	5	10	15	20	25
	Percentage of No. of regeneration among total evaluation	1%	2%	3%	4%	5%
	Best average fitness value	16.8 e -3	18.0 e -3	15.8 e -3	16.5 e -3	17.7e-3

Table 3. Parameters of the Excitation Controllers

	K_a	T_a	T_b	T_c
Pole-placement	885.609	0.001	2.356	0.268
PSO	398.524	0.998	0.0001	0.467
SPPSO	423.354	0.0001	2.265	0.87

Table 4. Parameters of the Excitation Controller

	K_A	T_A	T_B	T_C
PSO	4425.003	0.119	0.695	0.631
SPPSO	4021.027	0.024	0.444	0.375

Table 5. Comparative Performance of the Excitation Controller

		Setting Time ts (s)	Maximum Overshoot (%)
Pulsed load = 2.65KW; Duration = 1s	SPPSO	0.52	2.55
	PSO	0.73	5.77
Pulsed load = 2.65KW; Duration = 0.4s	SPPSO	0.34	2.19
	PSO	0.59	5.37
Pulsed load = 2.65KW; Duration = 0.2s	SPPSO	0.15	1.63
	PSO	0.39	5.08
Pulsed load = 2.65KW; Duration = 0.1s	SPPSO	0.13	1.60
	PSO	0.36	5.05
Pulsed load = 5.29KW; Duration = 1s	SPPSO	1.13	5.10
	PSO	1.10	6.62
Pulsed load = 5.29KW; Duration = 0.4s	SPPSO	0.75	3.61
	PSO	0.91	5.86
Pulsed load = 5.29KW; Duration = 0.2s	SPPSO	0.51	2.60
	PSO	0.68	5.34
Pulsed load = 5.29KW; Duration = 0.1s	SPPSO	0.28	1.91
	PSO	0.59	5.11
Pulsed load = 7.94KW; Duration = 0.4s	SPPSO	0.91	4.59
	PSO	0.91	6.32
Pulsed load = 7.94KW; Duration = 0.2s	SPPSO	0.75	3.36
	PSO	0.76	5.74
Pulsed load = 7.94KW; Duration = 0.1s	SPPSO	0.44	2.29
	PSO	0.65	5.15
Pulsed load = 3.23KW; Duration = 0.2s	SPPSO	0.82	3.85
	PSO	0.82	5.95
Pulsed load = 3.23KW; Duration = 0.1s	SPPSO	0.60	2.67
	PSO	0.72	5.35

Table 6. Computation Time Comparison of SPPSO and PSO

	SPPSO	PSO
Particle population	5	20
Code time for each particle (one iteration)	0.024s	0.022s
Evaluating time for each particle (one iteration)	7.4s	7.4s
Time cost for one interation	37.12s	148.44s
Training iterations	11	9
Total training time	6min48s	22m16s

Table 7. An Overview Comparison of SPPSO and PSO Based Controller

	SPPSO	PSO
The average performance of Convergence	Better	Good
Storage space	Small, only “5 particles position and velocity”	Medium, “20 particles position and velocity are needed”
Time consuming	Because of small population, SPPSO could get good results using less time than PSO	Medium
Computational Complexity	Small, mainly “+, -, × operation”;	Small, mainly “+, -, × operation”;
Hardware demand	Low. Ease to implement. Many microcontrollers such as PIC, DSP are available to be implemented on; No extend memory needed for most cases.	Same as SPPSO

PAPER

3. AIS-BASED COORDINATED AND ADAPTIVE CONTROL OF GENERATOR EXCITATION SYSTEMS FOR AN ELECTRIC SHIP

Chuan Yan, Ganesh K. Venayagamoorthy, *Senior Member, IEEE*, Keith Corzine, *Senior Member, IEEE*

Abstract - An artificial immune system (AIS) based control of generator excitation systems for the Navy's electric ship is presented in this paper to solve power quality problems caused by high-energy loads such as direct energy weapons. The coordinated development of the AIS controllers mainly consists of two parts – an innate immunity (optimal) and adaptive immunity. The parameters of the controllers for the first part, to provide optimal performance, are determined simultaneously using the particle swarm optimization (PSO). For dramatic changes in the ship power system, an adaptive control based on the immune system feedback law is developed. The feedback law adapts the controllers' parameters only during transient disturbances. Post-disturbance, the controllers' parameters are restored to their innate values. A real-time ship power system and the proposed AIS control of all excitation systems have been implemented on a real-time digital simulator (RTDS) and DSP, respectively. Results from the hardware-in-the-loop studies show that the AIS controllers can provide effective control of all generators' terminal voltages during pulsed loads, restoring and stabilizing them quickly.

Index Terms - Automatic voltage regulator (AVR), artificial immune system (AIS), electric ship, pulsed load.

I. INTRODUCTION

The future Electric ships power system is based on the integrated power system (IPS) architecture consisting of four parts: power generation, propulsion systems, hydrodynamics, and DC zonal electric distribution system (DC-ZEDS), all of which provide benefits on flexibility, survivability, capability for high energy loads and

maintainability [1]. In order to maintain power quality in IPS, immediate energy storage devices with their corresponding charging systems are proposed to make the pulsed power required compatible with the supply system [1]. However, this will increase the system cost and demand larger ship space. The excitation control is one of the most effective and economical techniques to stabilizing the terminal voltage of the synchronous generators. An optimally tuned excitation system offers benefits in overall operating performance during transient conditions caused by system faults, disturbance, or motor starting [2]. In order to optimize them, many algorithms are extended to the design of the optimal excitation controller for the synchronous generators. Two methods are predominantly used, one being the pole-placement method and the other being the cancellation approach [2, 3]. However, transfer function and parameters of machines are needed. And they are not optimal oriented. In [4], Lyapunov's direct method has been used to optimize excitation controller. But again, machine parameters are needed.

Recently, computational intelligence methods are widely used in optimizing excitation controllers such as fuzzy set theory [5], particle swarm optimization (PSO) theory [6], and online trained neurocontroller [7, 8] all of which have good performance at maintaining the terminal voltage. However, computational intelligence (CI) based controller designs use fitness functions mainly based on rise time, settling time and overshoot. Reactive power control in a multimachine power system is essential for improved system performance and minimization of power losses. Besides, an optimal excitation controller developed using CI techniques can only provide optimal performance for the range of operation conditions considered in the design, however, its performances degrades when the operation condition changes. Therefore, adaptive excitation controllers are used [9, 10]. Furthermore, the design of multiple excitation controllers to provide optimal performance with changing operating conditions is a challenging task, and critical for Navy applications. This requires coordinated development of the excitation controllers and adaptive online-operation.

In this paper, an artificial immune system (AIS) based control of excitation controllers for the electric ship is presented. There are two parts in the AIS-based excitation control design, namely innate immunity and adaptive immunity. The parameters of the controllers for the first part, to provide optimal performance, are

determined simultaneously using the particle swarm optimization (PSO). For dramatic changes in the ship power system, an adaptive control based on the immune system feedback law is developed. The feedback law adapts the controllers' parameters only during transient disturbances. Post-disturbance, the controllers' parameters are restored to their innate values. A ship power system, consisting of four generators, and the proposed AIS control of all excitation systems have been implemented on a real-time digital simulator (RTDS) and DSP, respectively. Results of the hardware-in-the-loop (HIL) studies are presented to show that four AIS controllers can provide effective control of voltages on the ship power system during pulsed loads, restoring and stabilizing them quickly.

The rest of the paper is organized as follows: Section II describes the ship power system; Section III provides a detailed description of the AIS-based excitation control development; Section IV presents the HIL results and finally, Section V provides a conclusion.

II. EXCITATION CONTROL SYSTEM ON AN ELECTRIC SHIP

A. Integrated Power System (IPS) for the Electric Ship

The power system of the all-electric ship system mainly consists of two 36MW main turbine generators (MTGs), two 4MW auxiliary turbine generators (ATGs), two 36.5MW advanced induction motors (IM), ship service loads, pulsed loads and other auxiliary loads [1]. In this system, four 2MW DC zonal loads and two pulsed loads namely rail gun with 40MW and 0.75s duration and EM launcher with 10MW and 3s duration are implemented as are shown in Fig. 1 [11].

B. Excitation System

The ship power system is a small isolated power system. The transmission distance is too small so that the inductance could be neglected. In this case, the terminal voltage of four generators is the same, which means all four excitation controllers are coordinated with the same input. For reducing maintenance, all four generators are equipped with brushless exciters [12]. The excitation is controlled by an automatic voltage regulator (AVR) that senses the terminal voltage of the generator and compares it

with a reference value in order to regulate terminal voltage of generators. A simplified AVR block diagram is shown in Fig. 2 [13].

As is shown in Fig. 2, Vs* is the rms terminal voltage reference of the synchronous generator and Vs is the measured value. The rms line-to-neutral terminal voltage is calculated in terms of instantaneous quantities using

$$V_s = \frac{\sqrt{v_{as}^2 + v_{bs}^2 + v_{cs}^2}}{\sqrt{3}} \qquad (1)$$

The subtraction of V_s^* and V_s produces error voltage signal, which is amplified in the regulator. The overall equivalent gain and the time constant associated with the regulator are simulated by K_a and T_a, respectively. The time constants, T_b and T_c, may be used to model equivalent time constants inherent in the voltage regulator. $V_{r,max}$ and $V_{r,min}$ defines the maximum and minimum voltage regulator output respectively [13].

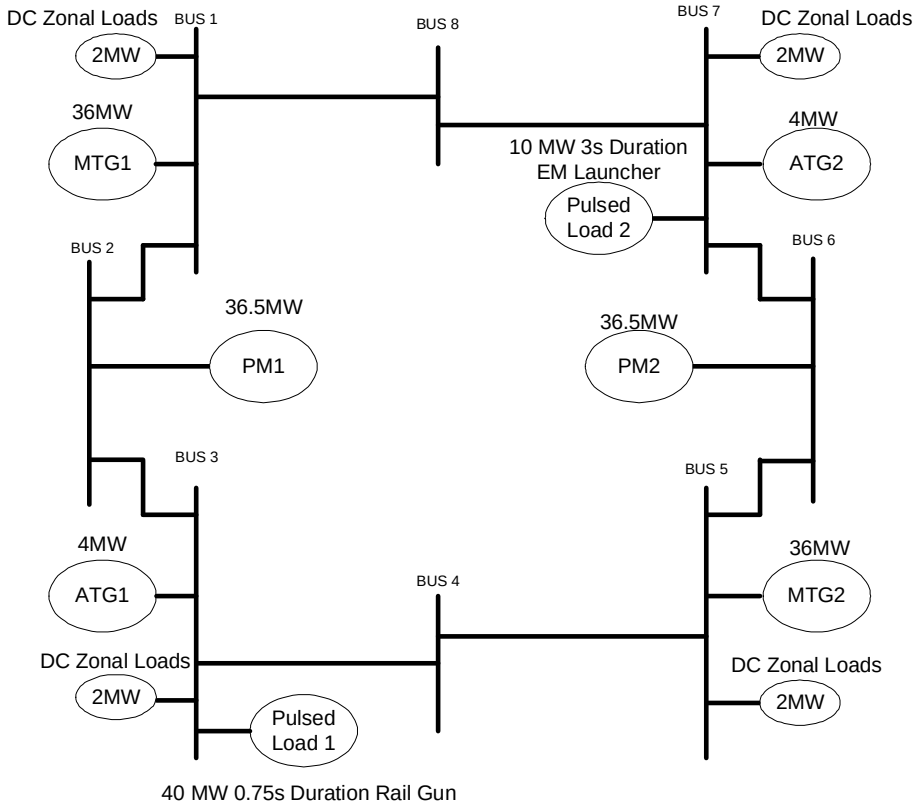

Fig. 1. IPS of an electric ship. (ATG: auxiliary turbine generator; MTG: main turbine generator; PM: Propulsion motor)

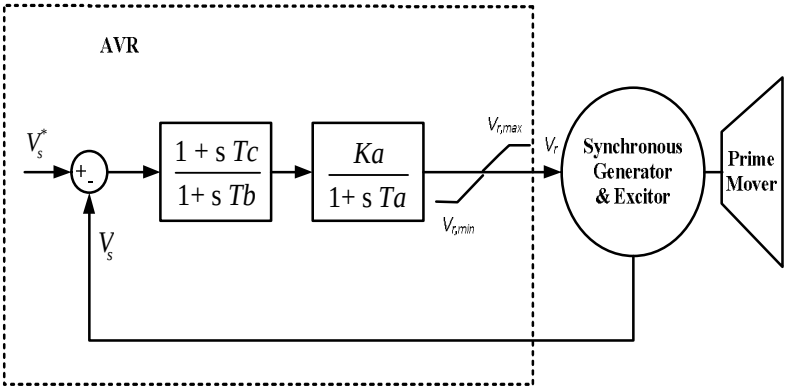

Fig. 2. Laboratory setup of the hardware in loop devices including RTDS and DSP.

C. Hardware-in-the-Loop Laboratory Setup

In order to validate the proposed AIS excitation controls, a detailed model of an electric ship IPS is simulated in real-time on a RTDS which can replicate the dynamics almost as close as the physical ship power system. The RTDS is equipped with D/A cards and A/D cards with a range from -10V to +10V. AIS controllers are implemented on an Innovative M67 DSP. A HIL system between the RTDS and the DSP is built as shown in Fig. 3 is developed. This is realized using the RTDS 16-bit D/A cards to send the four generators' terminal voltage and reactive power signals to the DSP 16-bit A/D cards at a 1 KHz sampling frequency. The digital excitation controllers of the four generators are implemented on the DSP. The DSP 16-bit D/A cards send calculated field voltages for the respective generators to RTDS 16-bit A/D cards at a 1 KHz sampling frequency.

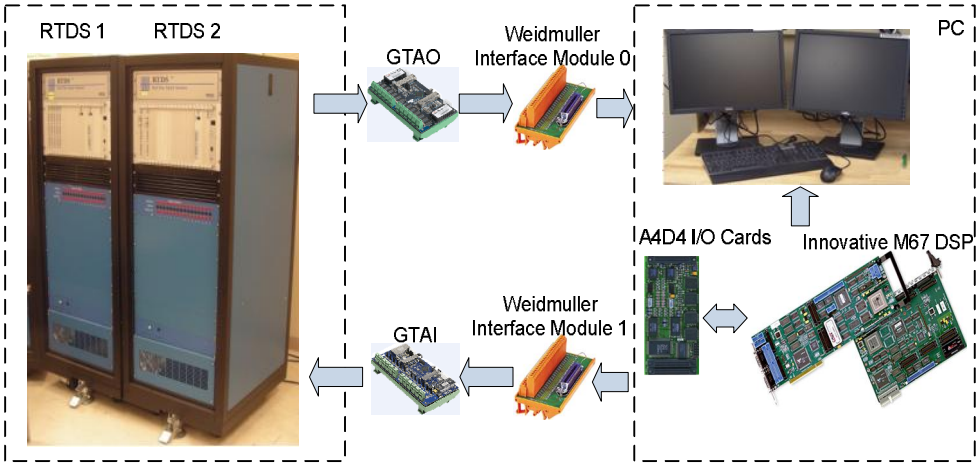

Fig. 3. HIL laboratory setup including RTDS and DSP.

III. AIS BASED EXCITATION CONTROLLER

A. Biological Immune System and Artificial Immune System

Biological immune system of human beings is a complex adaptive system that has evolved in interaction of various cells to protect them from invading pathogens. Antigen presenting cells (*APC*) identifies the invading antigen, and activates *CD4+T* cells to clone and differentiate into activated helper T cells (*TH Cell*), which stimulate the *B Cells.* Then *B* Cells will produce antibody (A_b) to kill antigens. When the number of antigens is reduced, Suppressor T cells (*TS Cell*) are activated to suppress the action of *TH Cell*. The process of the biological immune system is illustrated in Fig. 4 [14-18].

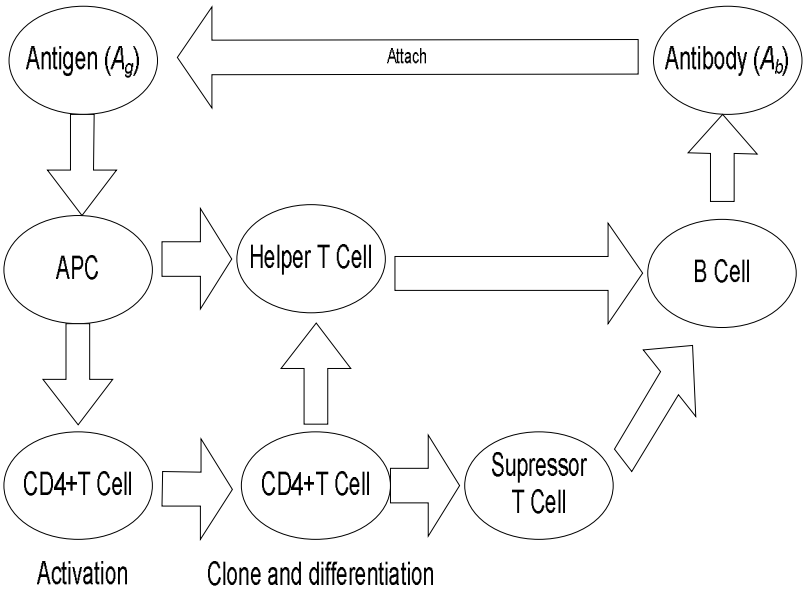

Fig. 4. Schematic showing the process in a typical biological immune system

The AIS is a biologically motivated information processing system, which has many superior characteristics in optimization, such as flexible adaptability, clone selection, pattern recognition and distributed multi-level structure [17]. There are two parts in an AIS-based controller design, namely innate immunity and adaptive immunity which are described in following two subsections. The innate immunity provides optimal control with the fixed parameters and the adaptive immunity provides adaptive control with parameter variation.

B. AIS Based Excitation Control: Innate Immunity Design

The innate immunity for excitation systems requires optimal controllers. In this paper, particle swarm optimization is used to find the optimal AVR parameters. PSO is a swarm intelligence technique (a search method based on nature inspired systems). It is an efficient method for solving complex nonlinear optimization problems [19-22] and has been widely used in power electronics applications to power systems [23-26]. PSO initially has a population of random particles which are given some random positions and velocities in the search space. The particles have memory which is used to keep track of their previous best position local best (P_{best}) and the corresponding fitness. The swarm has a memory which is used to keep track of best value of all P_{best}. The search process is aimed at accelerating each particle towards its P_{best} and the swarm's global best (G_{best}). The velocity and position update equations of the particles are given by

$$v_i(j+1) = w \cdot v_i(j) + c_1 \cdot R_1 \cdot \left(P_{best}(j) - x(j)\right) + c_2 \cdot R_2 \cdot \left(G_{best} - x(j)\right) \quad (2)$$

$$x_i(j+1) = x_i(j) + v_i(j+1) \quad (3)$$

where i is the particle number, w is the inertia constant, c_1 and c_2 are the cognitive and social acceleration constants respectively, and $R_1$and R_2 are two random numbers with uniform distribution in the interval [0,1].

Due to the symmetry of the IPS, two excitation controllers' parameters for the main generators are the same and likewise those of the two auxiliary generators. Therefore, two AVRs consisting of eight parameters are to be the PSO particle dimensions. The detailed procedure for the development of optimal excitation controllers is given in below.

Initialization: Randomly initialize a population N of particles positions and velocity. To have a fast PSO search performance, in the laboratory setup, N is set to be 30 and the values of w, c_1 and c_2 are kept fixed at 0.8, 2.0 and 2.0 [27]. The initialization range for parameters is obtained by trial and error which can make system stable. K_a is from 0 to 1000; T_a ranges from 0 to 2; T_b ranges from 0 and 20; T_c ranges from 0 to 5.

Evaluation: In the excitation control loop of Fig. 2, the proportional gain K_a and time constants T_a, T_b and T_c have to be carefully selected to provide satisfactory performance under normal and pulsed load conditions. The objective of the PSO algorithm is to find these parameters in order to restore and stabilize the terminal voltage quickly; especially after pulsed loads of different magnitudes and durations.

Most objective functions used for excitation controllers design in literature involve settling time, rise time and overshoot [18, 28]. The area under the voltage curve during and post-pulsed load can be calculated using (4). This can be used as a fitness function to guide the PSO design process to minimize the time response characteristics such as rising time, overshoot and settling time.

$$Fitness = \frac{1}{2}\sum_{k=1}^{n}\{\sqrt{[V_s^* - V_s(k)]^2 + [V_s^* - V_s(k+1)]^2}\}\Delta t \tag{4}$$

where

V^*_s	reference terminal voltage value;
k	sampling instant;
Δt	sampling interval;
V_s	measured terminal voltage;

However, it is possible that some generators can output negative reactive power while the others output positive reactive power if terminal voltage is the only factor considered during tuning excitation controllers. In this case, the current in the transmission line could be much higher, which means thicker wire and more heat. Therefore, a fitness function (5) which involves both terminal voltage and reactive power is preferred.

$$\begin{aligned} Fitness = \frac{1}{2}\sum_{k=1}^{n}\{\sqrt{[V_s^* - V_s(k)]^2 + [V_s^* - V_s(k+1)]^2}\}\Delta t \\ + |Q_{MTG1}| + |Q_{MTG2}| + |Q_{ATG1}| + |Q_{ATG2}| \end{aligned} \tag{5}$$

where

Q_{MTG1} reactive power of MTG_1 in steady state;

Q_{MTG2} reactive power of MTG_2 in steady state;

Q_{ATG1} reactive power of ATG_1 in steady state;

Q_{ATG2} reactive power of ATG_2 in steady state;

Update: The position and velocity of the i^{th} particle is updated using (2) and (3).

In order to tune AVR parameters, three different kinds of pulsed loads are applied. The first one is a 40MW pulsed load with 0.75 second duration; the second one is a 10MW pulsed load with 3 seconds duration; the third one is an overlap of the first two pulsed loads. In this case, the ship excitation controller will achieve an innate immunity toward these three pulsed loads or some pulsed loads close to this range.

C. AIS Based Excitation Control: Adaptive Immunity Design

From the previous section, all innate immunity parameters (K_{a_main}, T_{a_main}, T_{b_main}, T_{c_main}, K_{a_aux}, T_{a_aux}, T_{b_aux}, T_{c_aux}) are found using PSO. Based on them, the adaptive immune controller is designed. The input of the AIS controller is the deviation of the bus voltage $\Delta V(k)$ at time instant k, which can be regarded as the antigens. The objective of AIS is to minimize the antigens. Therefore, it activates helper T cells to eliminate antigens. The mathematical representation of this process can be shown using (6):

$$TH(k) = m_1 \times \Delta V(k) \tag{6}$$

where

m_1 stimulating factor of the helper *T* cells;

In order to balance AIS and suppress the action of *TH* cells, the *TS* cells are introduction, which mathematical representation is shown in the (7).

$$TS(k) = m_2 \times \Delta V_b(k) \times \exp\left(-\frac{\Delta V_b(k)}{\Delta V_b(k-1)}\right) \tag{7}$$

where

m_2 suppressor factor of the suppress *T* cells;

The B cells activated by *TH* cells and *TS* cells can be represented as (8).

$$B(k) = TH(k) - TS(k) \tag{8}$$

Biological immune system cannot only defend invading antigens but also have a killing effect on self-antigens when the immune responses are inappropriately too high or too low [14]. Therefore, a limitation function is added and the antibody can be represented as (9).The upper limit value and lower limit value are the upper range and lower range of initialization range of parameters respectively.

$$A_b(k) = Limitation\big(IN + B(k)\big) \tag{9}$$

where

IN Innate immunity parameter value;

Since there are four excitation controllers on the ship power system, four AIS controllers has been implemented. The schematic of the AIS controller for ship power system could be shown in Fig.. 6. In Fig. 6, the input for AIS controller of MGT_1, MGT_2, AGT_1 and AGT_2 are the deviation terminal voltage (pu) of bus 1, 5, 3 and 7 respectively. Since two main generators should perform the same as well as two auxiliary generators, the innate immunity parameters and their constrains for AIS controller for MTG_1 and MTG_2 are the same, as well as those of AIS controller for ATG_1 and ATG_2.

In this paper, PSO has been employed for tuning all eight *TS* scaling factors (m_2, m_4, m_6, m_8, m_{10}, m_{12}, m_{14}, m_{16}) and eight *TH* scaling factors (m_1, m_3, m_5, m_7, m_9, m_{11}, m_{13}, m_{15}). The detailed tuning process is shown in Fig. 5.

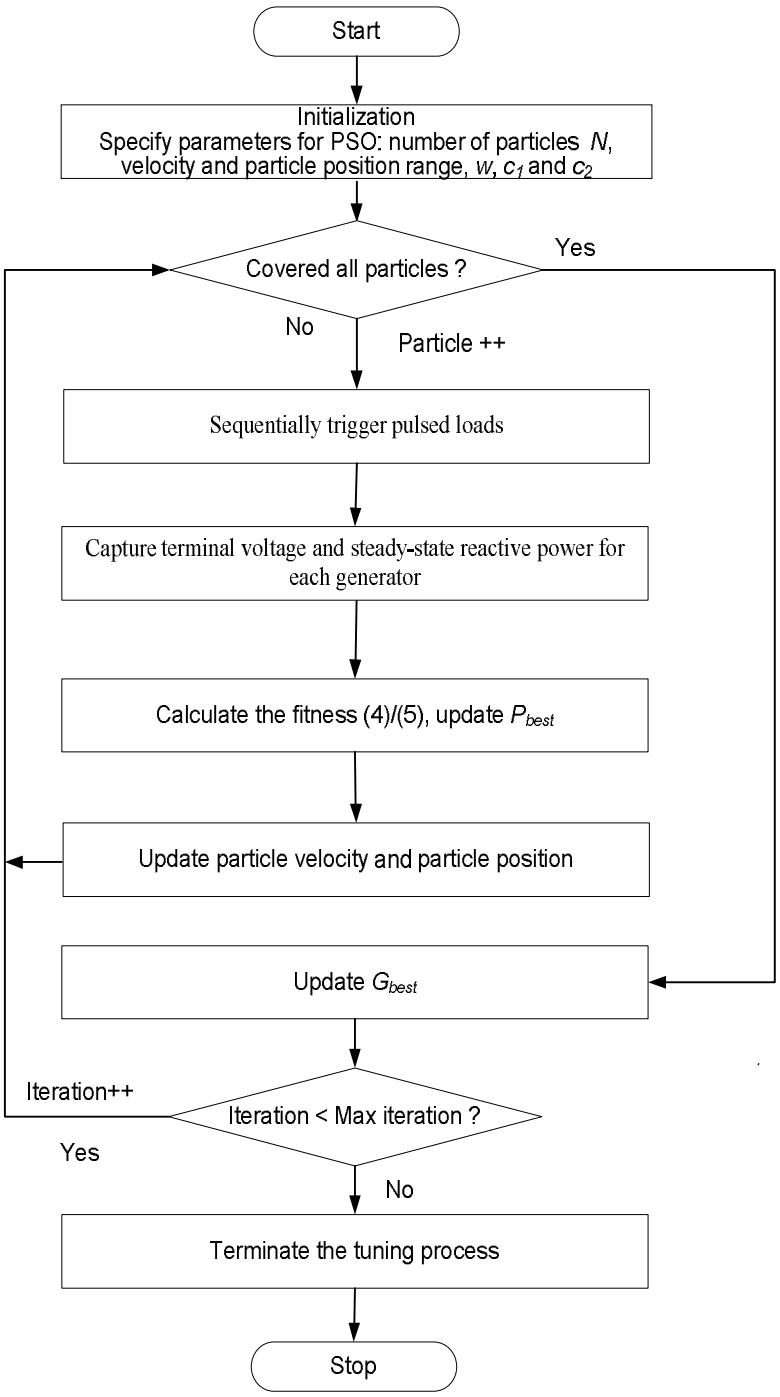

Fig. 5. Schematic of AIS controller tuning process using PSO.

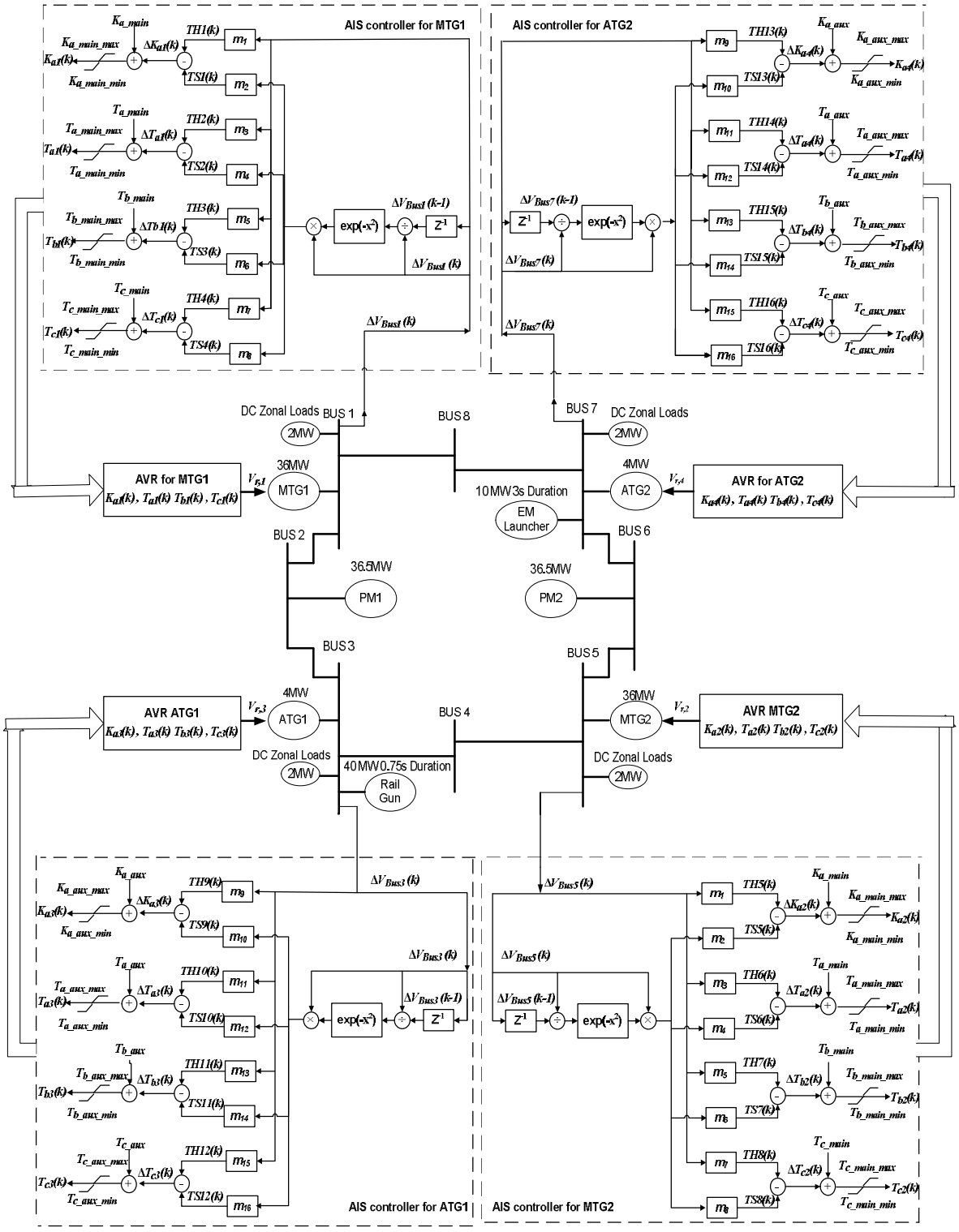

Fig. 6. Schematic of AIS based excitation controller for ship power system.

IV. RESULTS

A. AIS Based Excitation Control: Innate Immunity

To verify the effectiveness of the presented fitness function for the PSO based optimal excitation controller, two case studies have been made.

Case One Study: Case one study uses PSO with fitness function (4) to tune the excitation controllers while the parameters of excitation controllers for two main generators are not set to be same, as well as those for two auxiliary generators. The results of case one study under a 40MW and 0.75s duration pulsed load are shown in Figs. 7 to 11. Terminal voltage for four generators is shown in Fig. 7. The field voltage and current are shown in Fig.8 and 9 respectively while the active power and reactive power for four generators are shown in Figs.10 and 11 respectively. In Figs.8 and 9, field voltage and field current for four generators are different with each other, which lead to different reactive power. In this case, although the terminal voltage shows a good performance, the power system is not balanced. Some machines work in a heavy duty while others not, which is not desired. Therefore, it is necessary to set excitation controllers for two main generators to be the same, as well as those for two auxiliary generators. In Fig.11, because of no reactive power constrains, although the terminal voltage perform good and the active and reactive loads are constant, auxiliary generator 2 is absorbing reactive power, which means other generators need to send more reactive power. In this case, the current on the transmission line will be higher and the heat and power loss will be more. Therefore, reactive power must be taken into consideration in the fitness function. The tuned parameters of four excitation controllers for case one study are shown in Table 1.

Table 1. Parameters of the Optimal Excitation Controllers Using (4)

	Excitation controller for MTG 1	Excitation controller for MTG 2	Excitation controller for ATG 2	Excitation controller for ATG 2
Ka	430.422	676.4943	594.107	301.825
Ta	0.0675	0.001	0.230	0.574
Tb	16.603	10.515	10.000	10.000
Tc	1.010	1.000	1.000	1.000

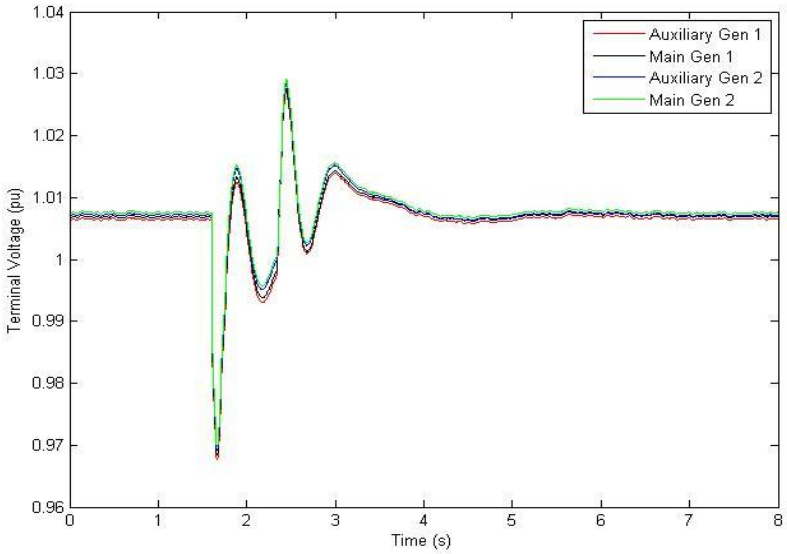

Fig. 7. Terminal voltage using PSO based optimal excitation controller and (4) under a rail gun load.

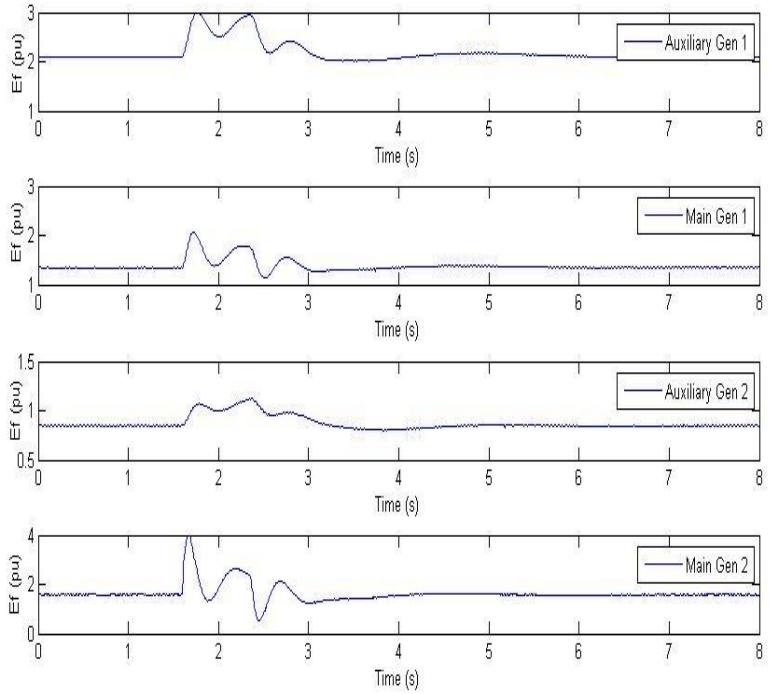

Fig. 8. Field voltage using PSO based optimal excitation controller and (4) under a rail gun load.

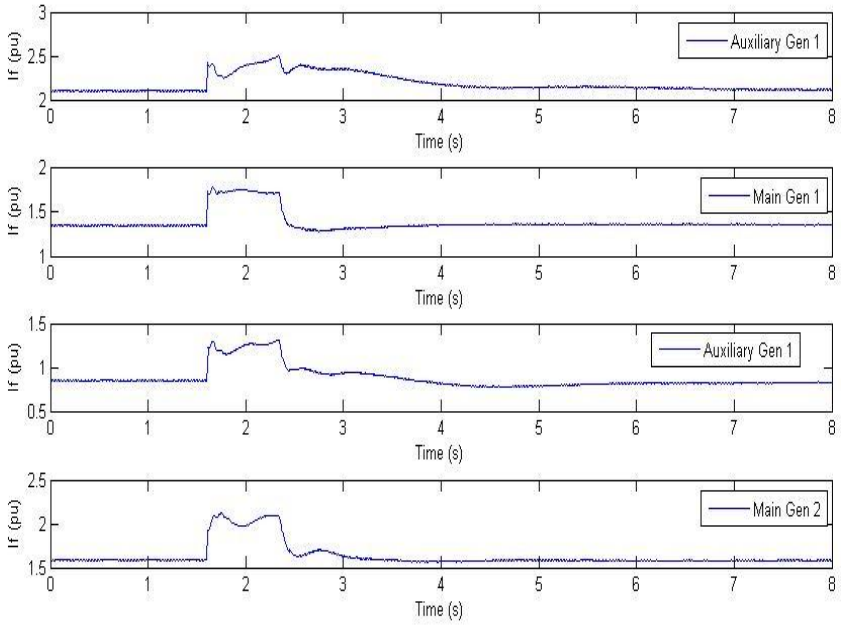

Fig. 9. Field current using PSO based optimal excitation controller and (4) under a rail gun load.

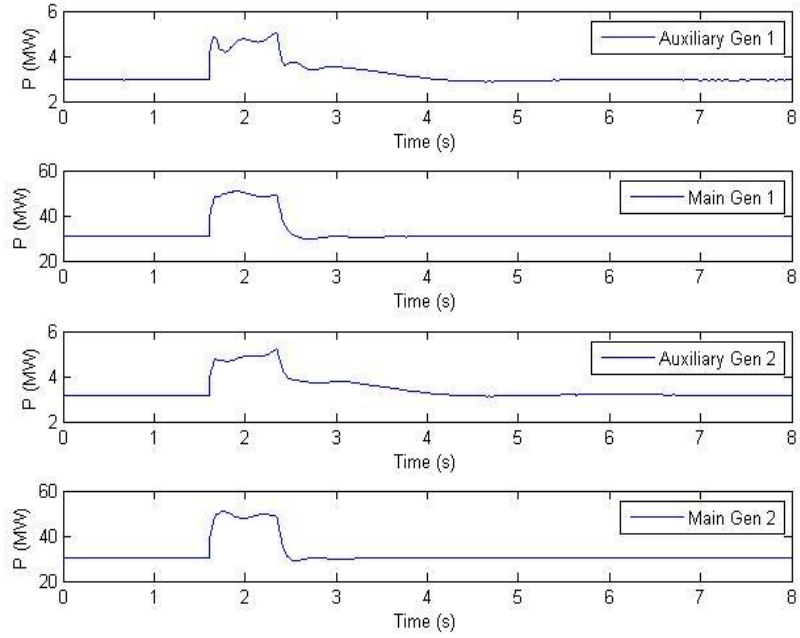

Fig. 10. Active power using PSO based optimal excitation controller and (4) under a rail gun load.

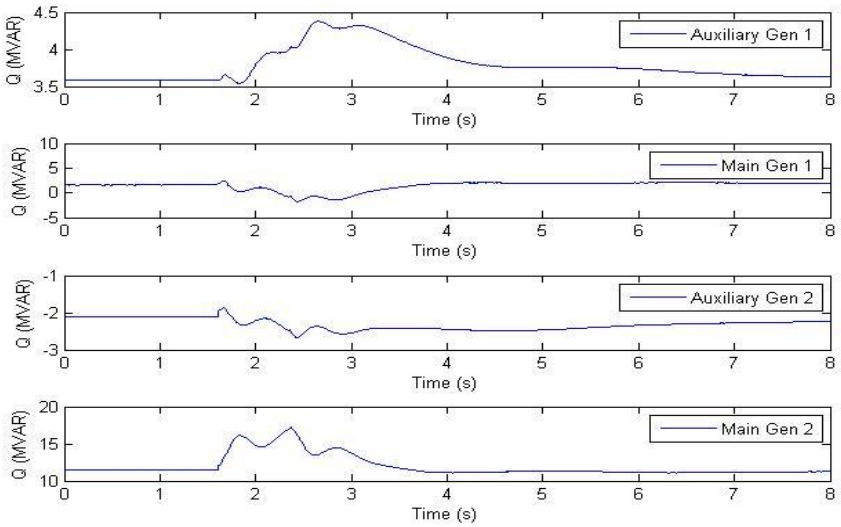

Fig. 11. Reactive power using PSO based optimal excitation controller and (4) under a rail gun load.

Case Two Study: Case two study uses PSO with fitness function (5) while the parameters of excitation controllers for two main generators are set to be the same, as well as those for two auxiliary generators. The results of case one study under a 40MW and 0.75s duration pulsed load are shown in Figs. 12 to 16. Both case one and two employs PSO to tune the parameters with the same particle number, iterations and initialization, which are given in Section III. Terminal voltage for four generators is shown in Fig. 12. The field voltage and current are shown in Figs. 13 and 14 respectively while the active power and reactive power for four generators are shown in Figs. 15 and 16 respectively. And in Fig. 16, all reactive power for four generators is positive and the system is balanced. Therefore, fitness function (5) is preferred. The tuned parameters of four excitation controllers for case two are shown in Table 2.

Table 2. Parameters of the Optimal Excitation Controllers Using (4)

Excitation controller for MTG 1&2		Excitation controller ATG 1&2	
Ka_main	501.5	Ka_aux	498.6
Ta_main	0.001	Ta_aux	0.246
Tb_main	8.106	Tb_aux	12.168
Tc_Main	1.299	Tc_aux	1.305

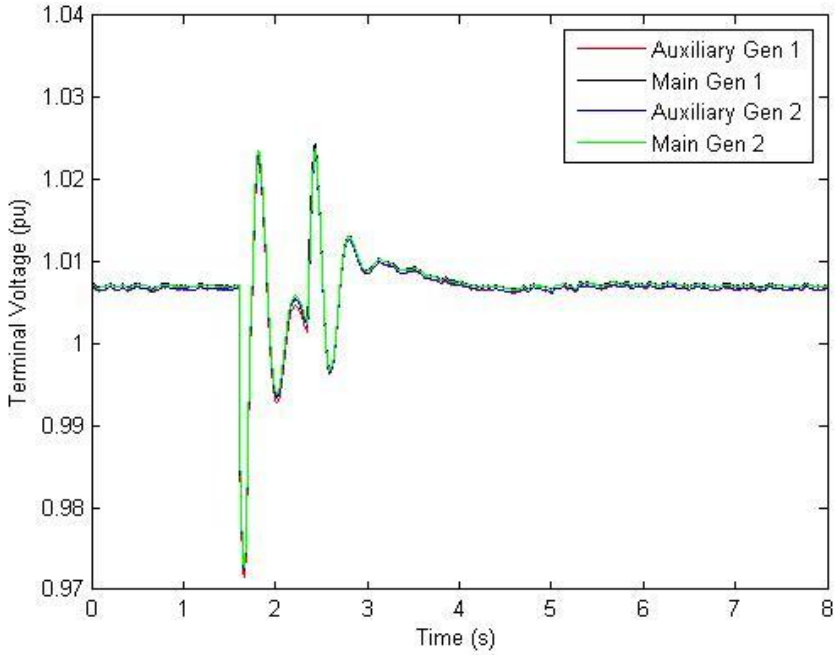

Fig. 12. Terminal voltage using PSO based optimal excitation controller and (5) under a rail gun load.

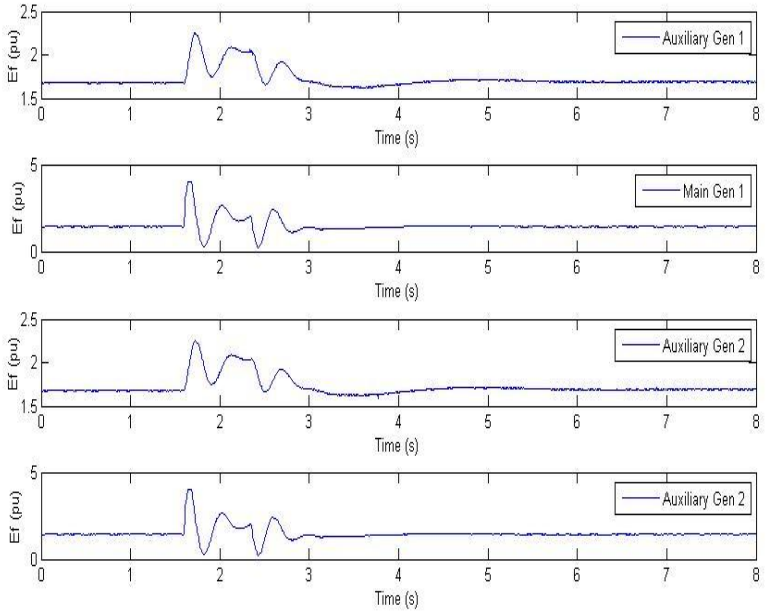

Fig. 13. Field voltage using PSO based optimal excitation controller and (5) under a rail gun load.

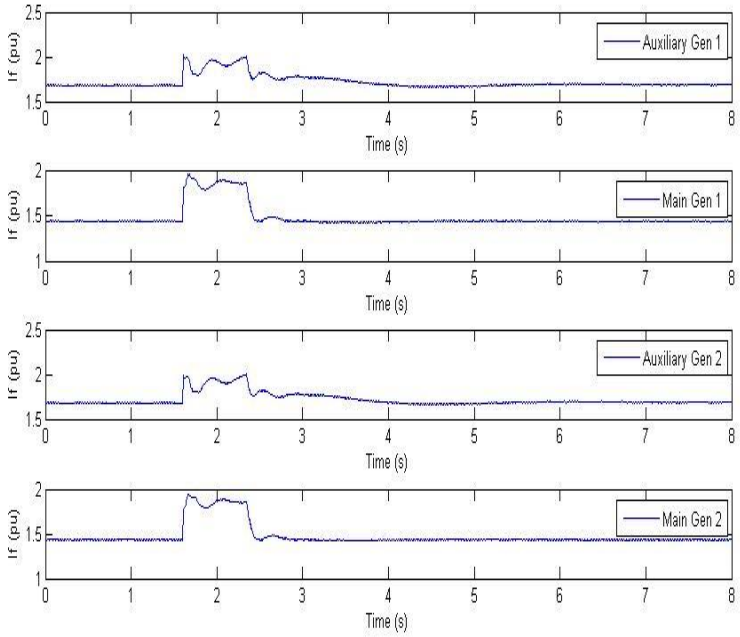

Fig. 14. Field current using PSO based optimal excitation controller and (5) under a rail gun load.

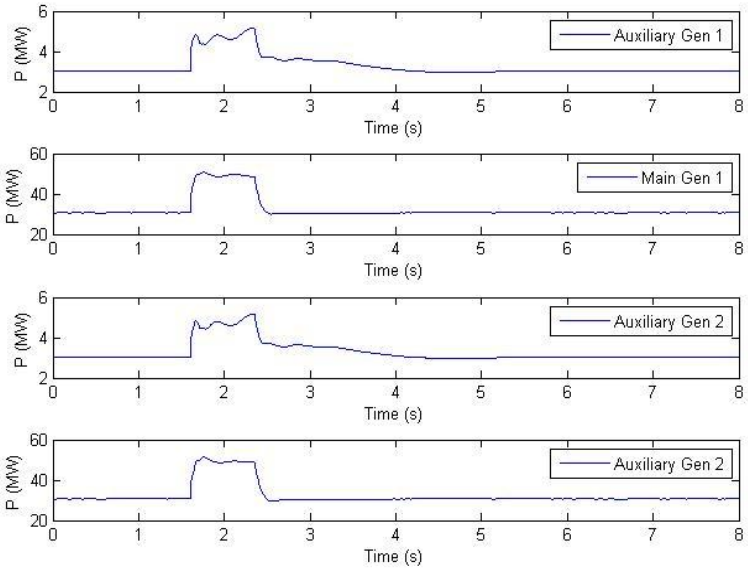

Fig. 15. Active power using PSO based optimal excitation controller and (5) under a rail gun load.

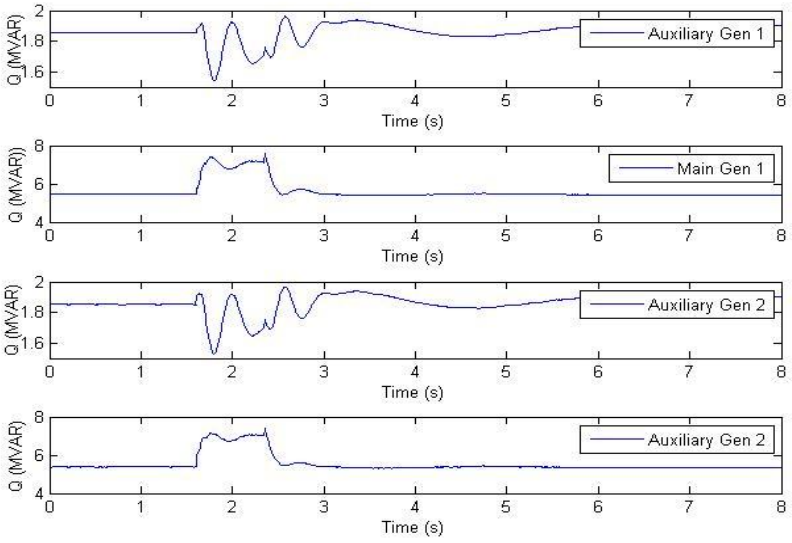

Fig. 16. Reactive power using PSO based optimal excitation controller and (5) under a rail gun load.

B. AIS Based Excitation Controller: Adaptive Immunity

To verify the effectiveness of the AIS based controllers, several comparison between AIS based controllers and PSO based optimal excitation controllers in Table 2 have been made. And the *m* constants parameters obtained by PSO are shown in Table 3.

Table 3. Parameters for TH stimulating Factors and TS Suppressor Factors

TH stimulating factors		TS suppressor factors	
m1	5785.394	m2	27918.073
m3	3.052	m4	8.3012
m5	112.832	m6	149.644
m7	15.715	m8	12.244
m9	5987.508	m10	28731.390
m11	100	m12	91.528
m13	135.809	m14	99.147
m15	16.235	m16	13.470

A detailed comparison using 40MW pulsed load with 0.75s duration has been made in Figs. 17 to 21. The comparison of terminal voltage for two controllers is shown in Fig.17, from which is clearly observed that the AIS based controllers can reduce oscillation caused by pulsed load better than PSO based controller. In Figs.18 and 19, the dynamic variation of parameter for AVR of two main generators and those of two auxiliary generators has been given respectively. It is clearly showed that parameters adaptively vary away from their optimal innate immunity values during the pulsed load which is regarded as invading antigen. And the variation magnitude for each parameters are well-controlled by stimulating factors and suppressor factors of AIS controller based on the invading antigen. After the disturbance, parameters again settle down to their optimal innate immunity values. The comparisons of field voltage and current have been shown in Figs.20 and 21 respectively, all of which show the effect of variation for parameters.

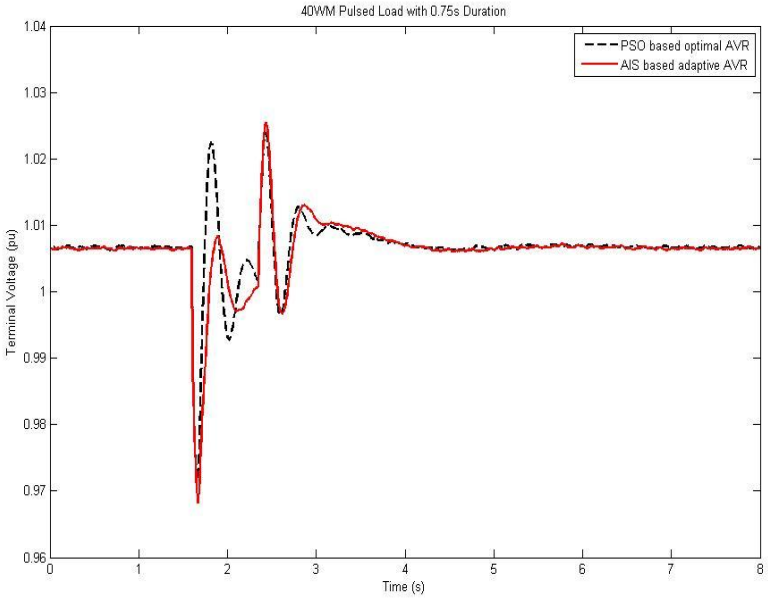

Fig. 17. Comparison of terminal voltage using PSO based optimal controller and AIS based controller under rail gun load.

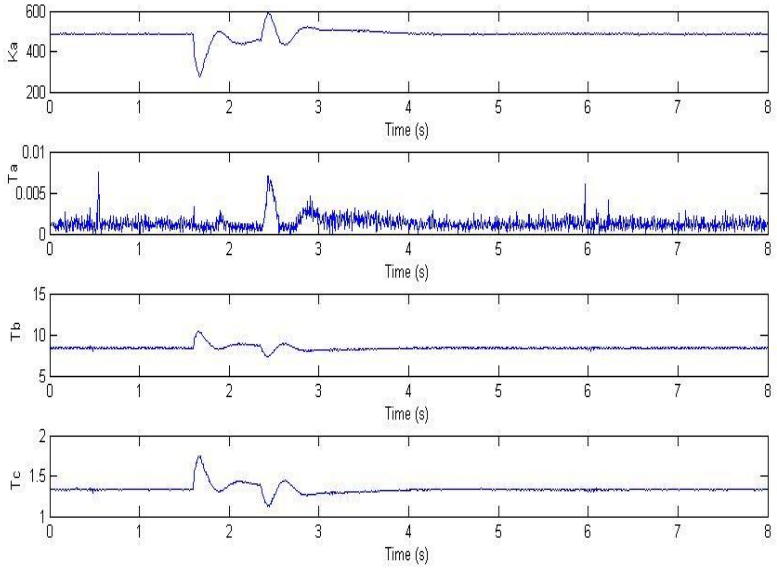

Fig. 18. Dynamic variation of parameters for excitation controllers of two main generators using AIS based controller under rail gun load.

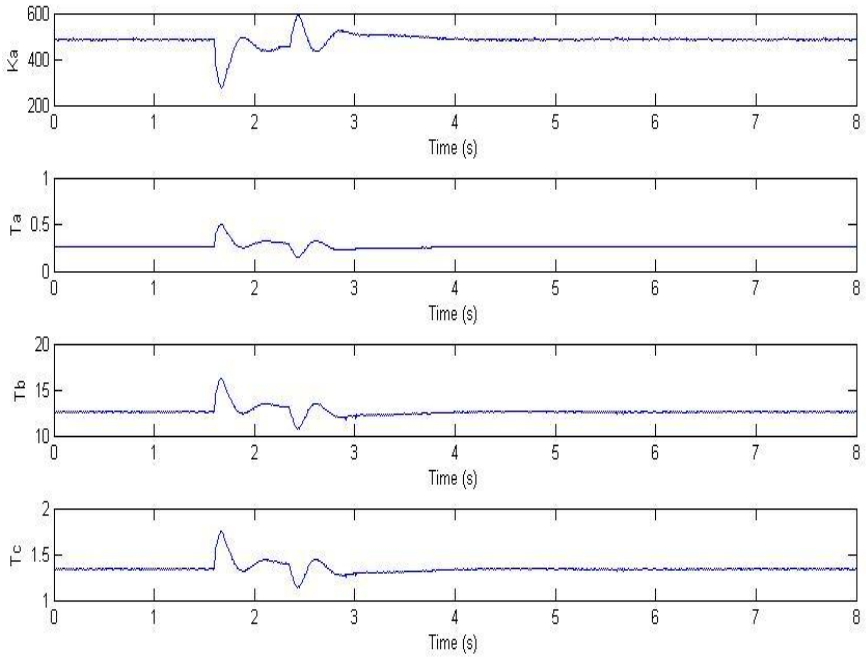

Fig. 19. Dynamic variation of parameters for excitation controllers of two auxiliary generators using AIS based controller under rail gun load.

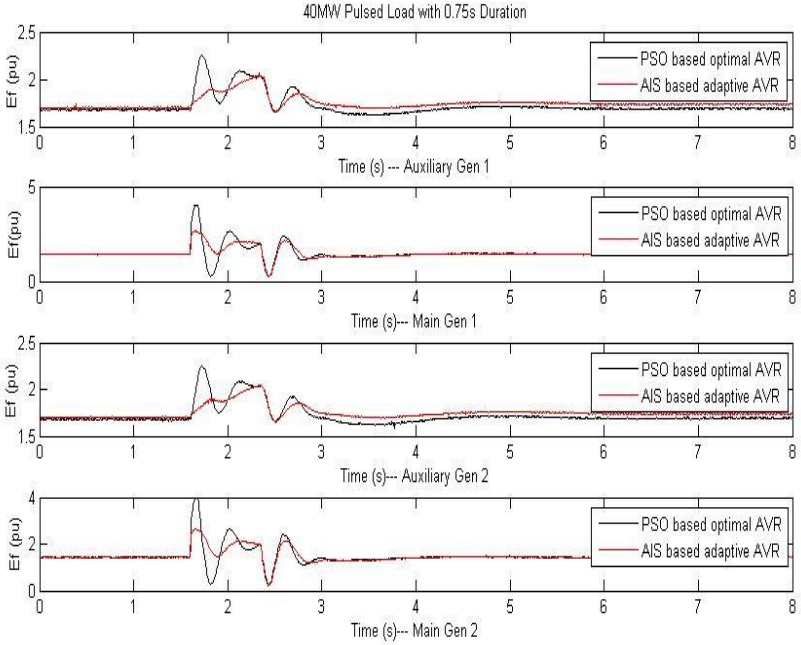

Fig. 20. Comparison of field voltage using PSO based optimal controller and AIS based controller under rail gun load.

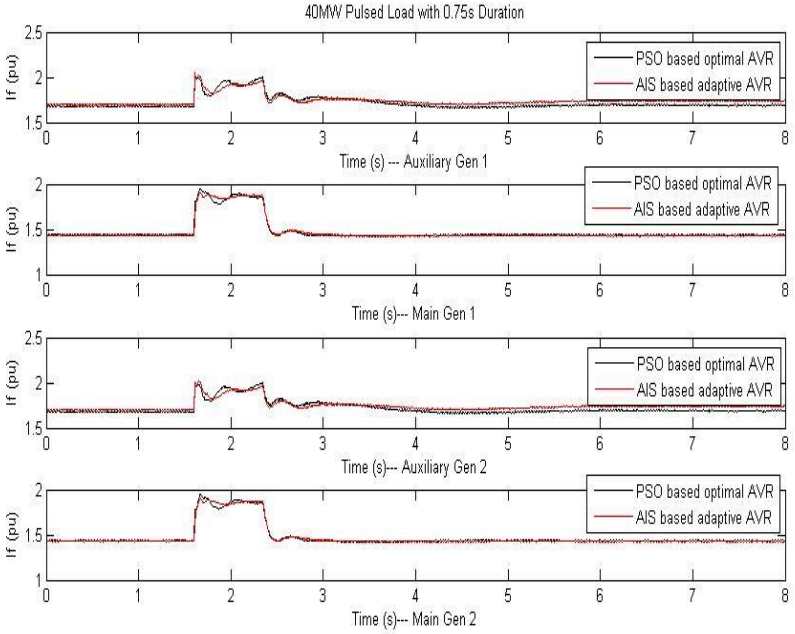

Fig. 21. Comparison of field current using PSO based optimal controller and AIS based controller under rail gun load.

A comparison using 10MW pulsed load with 3s duration (EM launcher) has been made in Fig. 22. It can be seen that AIS controller performs better than PSO controller. Two more comparisons with different pulsed load have been shown in Figs. 23 and 24. In Fig. 23, an overlap of an EM launcher pulsed load and a 40WM 0.75s duration pulsed load. The EM launcher pulsed load is fired first, and after 2.25s, the second one is fired. And they are switched off at the same time. In Fig. 24, a comparison using 0.75s duration pulsed load with different magnitude has been made. From Figs. 17 to 24, it can be seen that AIS based excitation controller can perform better than PSO based excitation controller.

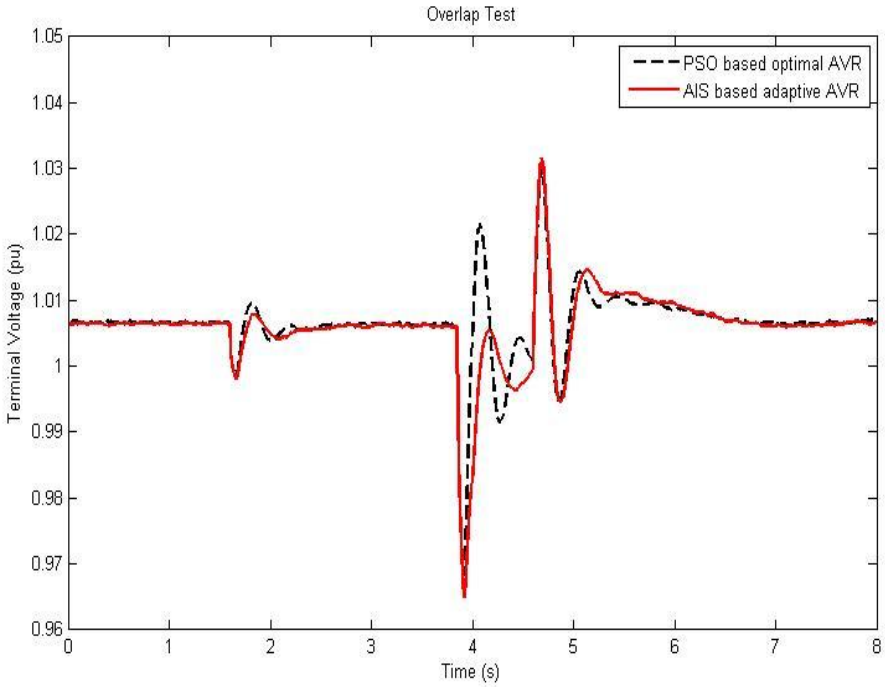

Fig. 22. Comparison of terminal voltage using PSO based optimal controller and AIS based controller under an overlap load.

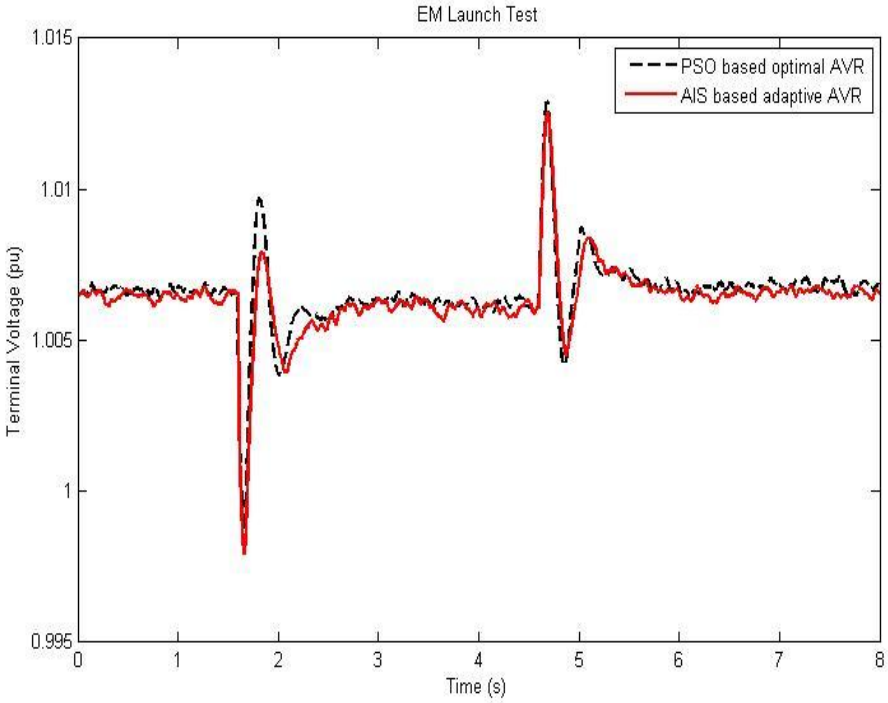

Fig. 23. Comparison of terminal voltage using PSO based optimal controller and AIS based controller under EM launcher load.

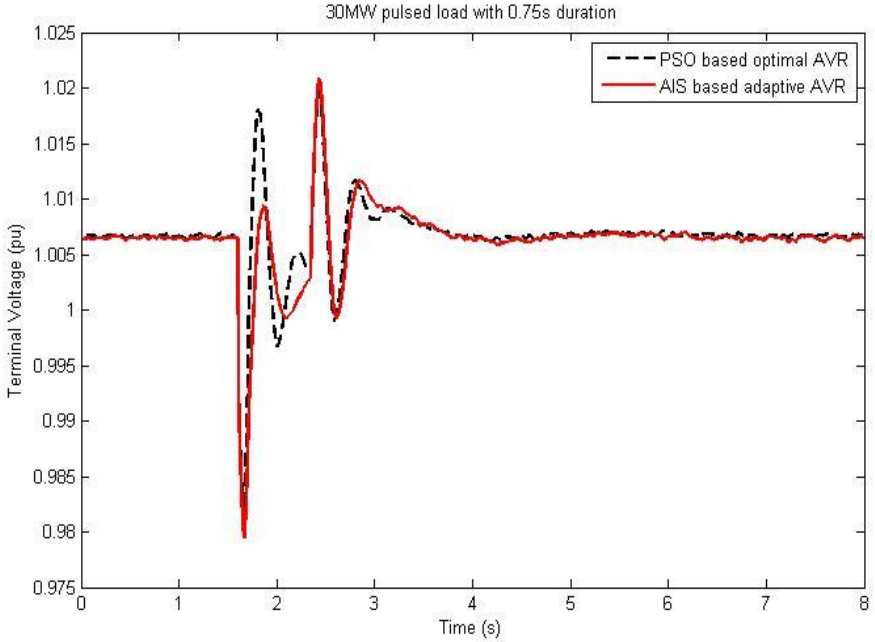

Fig. 24. Comparison of terminal voltage using PSO based optimal controller and AIS based controller under 30MW and 0.75s duration pulsed load.

V. CONCLUSION

An artificial immune system based excitation controller has been proposed and implemented on innovative M67 DSP and RTDS hardware platform to control the power system for the Navy's Future Electric ship. This controller has advantages including optimal oriented with innate immunity, no generator parameters needed and no human involved, and adaptive immunity. The objective for the presented controller is to minimize the voltage deviations when pulsed loads are directly energized by shipboard power system. Compared with PSO based optimal controller, the hardware simulation results show that AIS-based controller can restore and stabilize the terminal voltage effectively and very quickly after high power pulse loads are experienced.

VI. REFERENCE

[1] L. N. Domaschk, Abdelhamid Ouroua, Robert E. Hebner, "Coordination of Large Pulsed Loads on Future Electric Ships," *IEEE Transaction on Magnetics*, vol. 43, no.1, January 2007.

[2] K. Kim, R. C. Schaefer, "Tuning a PID Controller for a Digital Excitation Control System," *IEEE Transactions on Industry Application*, no.2, vol.41, pp.485-492, March/April 2005.

[3] K. Kim, A. Godhwani, M. J. Basler and T. W. Eberly, "Commissioning experience with a modern digital excitation system," *IEEE Transaction on Energy Conversion*, vol.13, no.2, pp.183-187, June 1998.

[4] J. Machowski, S. Robak, J. W. Bialek, J. R. Bumby, N. AbiSamra, "Decentralized Stability-Enhancing Control of Synchronous Generator," *IEEE Transactions on Power Systems*, no.4, vol.15, November 2000.

[5] Feng Zheng, Qingguo Wang, Tong H. Lee, Xiaogang Huang, "Robust PI Controller Design for Nonlinear Systems via Fuzzy Modeling Approach," *IEEE Transactions on Systems, Man, and Cybernetics*, no.6, vol.31, November 2001.

[6] Ali Karimi, Ali Feliachi, "PSO-tuned Adaptive Backstepping Control of Power Systems," *IEEE Power Systems Conference and Exposition*, Page(s):1315-1320, October 2006.

[7] G. K. Venayagamoorthy, R. G. Harley, "A Continually Online Trained Neurocontroller for Excitation and Turbine Control of a Turbogenerator," *IEEE Transactions on Energy Conversion*, no.3, vol.16, pp.261-269, September 2001.

[8] G. K. Venayagamoorthy, R. G. Harley, "Two Separate Continually Online-Trained Neurocontrollers for Excitation and Turbine Control of a Turbogenerator," *IEEE Transactions on Industry Applications*, no.3, vol.38, pp.887-893, May/June 2002.

[9] K. Wang, H. Xin and D. Gan, "Robust adaptive excitation control based on a new backstepping approach," *IEEE Power & Energy Society General Meeting*, pp.1-5, 2009.

[10] O.P. Malik and G.S. Hope, "An Adaptive Generator Excitation Controller Based on Linear Optimal Control," *IEEE Transactions on Energy Conversion*, volume 5, number 4, December 1990.

[11] D. H. Clayton, S. D. Sudhoff, and G. F. Grater, "Electric Ship Drive and Power System," Conference Record of the 2000 Twenty-fourth International Modulator Symposium, pp.85-88, 2000.

[12] J. F. Gieras, (2009). *Advancements in Electric Machines*, Spinger.

[13] IEEE Standard 421.5, *2005 IEEE Recommended Practice for Excitation System Models for Power System Stability Studies*, pages 1-85, 2006.

[14] X. Zhou, "Research on Immune Pathology in Artificial Immune System", *Control and Decision Conference*, pp.1366-1370, 2009.

[15] D. Dasgupta, "Advances in Artificial Immune Systems" IEEE Computational Intelligence magazine, no.4, vol.1, pp.40-49, 2006.

[16] M. Hunjan and G. K. Venayagamoorthy, "Adaptive Power System Stabilizers Using Artificial Immune System", IEEE Symp. Artificial Life (CI-ALife 2007), pp.440-447.

[17] H.F. Wang, H. Li and H. Chen, "Power System Voltage Control by Mulitple STATCOMs Based on Learning Humorial Immune Response", *IEE Proceedings of Generation, Transmission and Distribution*, no. 4, vol. 149, pp. 416-426, 2002.

[18] P. Mitra and G.K. Venayagamoorthy, "An Adaptive Control Strategy for DSTATCOM Applications in an Electric Ship Power System," *IEEE Transactions on Power Electronics*, vol.25, no.1, pp.95-104, 2010.

[19] Y.X. Liao, J.H. She and M. Wu, "Integrated Hybrid-PSO and Fuzzy-NN Decoupling Control for Temperature of Reheating Furnace," *IEEE Transactions on Industrial Electronics*, no.7, vol.56, pp.2704-2714, July 2009.

[20] S.H. Ling, H. Lu, F.H.F. Leung and K.Y. Chan, "Improved Hybrid Particle Swarm Optimized Wavelet Neural Network for Modeling the Development of Fluid Dispensing for Electronic Packaging," *IEEE Transactions on Industrial Electronics*, no.9, vol.55, pp.1478-1489, September 2008.

[21] A. Chatterjee, K. Pulasinghe, K. Watanabe and K. Izumi, "A particle-swarm-optimized fuzzy-neural network for voice-controlled robot systems," *IEEE Transactions on Industrial Electronics,* no.6, vol.52, pp.1478-1489, December 2005.

[22] C. Dai, W. Chen and Y. Zhu, "Seeker Optimization Algorithm for Digital IIR Filter Design," *IEEE Transactions on Industrial Electronics*, accepted for future publication, pp. 1-1, 2009.

[23] M. R. AlRashidi, M. E. El-Hawary, "A Survey of Particle Swarm Optimization Applications in Electric Power Systems", *accepted for publication in IEEE Transactions on Evolutionary Computation.*

[24] S C.-H. Liu, Y. –Y. Hsu, "Design of a Self-Tuning PI Controller for a STATCOM Using Particle Swarm Optimization," *IEEE Transactions on Industrial Electronics*, accepted for future publication, pp. 1-1, 2009.

[25] N. He, D. Xu and L. Huang, "The Application of Particle Swarm Optimization to Passive and Hybrid Active Power Filter Design," *IEEE Transactions on Industrial Electronics*, no.8, vol.56, pp.2841-2851, August 2009.

[26] F.-J. Lin, L.-T. Teng, J.-W. Lin and S.-Y. Chen, "Recurrent Functional-Link-Based Fuzzy-Neural-Network-Controlled Induction - Generator System Using Improved Particle Swarm Optimization," *IEEE Transactions on Industrial Electronics*, no.5, vol.56, pp.1557-1577, May 2009.

[27] Y. del Valle, G.K. Venayagamoorthy, S. Mohagheghi, J.C. Hernandez and R.G. Harley, "Particle Swarm Optimization: Basic Concepts, Variants and Applications in Power Systems," *IEEE Transactions on Evolutionary Computation*, no. 2, vol. 12, pp.171-195, April 2008.

[28] E.R.C. Viveros, G. N. Taranto and D.M. Falcao, "Tuning of Generator Excitation Systems using meta-heuristics," *IEEE Power Engineering Society General Meeting*, pp. 1-6, 2006.

PAPER

4. OPTIMAL LOCATION AND SIZING OF ENERGY STORAGE MODULES ON AN ELECTRIC SHIP POWER SYSTEM

Chuan Yan, Ganesh K. Venayagamoorthy, *Senior Member, IEEE*, Keith Corzine, *Senior Member, IEEE*

Abstract - Energy storage modules are being considered for the Navy's next generation of electric ship power systems. Energy storage modules supply high energy loads as well as critical equipment and increase the overall quality of service. This paper describes an approach to evaluate the impact of energy storage module sizing and location for ship survivability and quality of service. Specifically, a multiple objective optimization algorithm, multiple objective particle swarm optimization, is used to obtain Pareto fronts for survivability, quality of service and cost. Simulation results show that optimal energy storage module sizing and location improves ships' survivability and quality of service greatly with a low cost.

Index Terms - Electric ship, multiple objective particle swarm optimization (MOPSO), survivability, quality of service (QOS).

I. INTRODUCTION

The Navy's future electric ships power system is based on the integrated power system (IPS) architecture consisting of four components, power generation, propulsion systems, hydrodynamics, and dc zonal electric distribution system (DC-ZEDS); all of which provide benefits of flexibility, survivability, capability to supply high energy loads, and maintainability [1]. In order to maintain power quality in IPS, energy storage modules (ESMs) are proposed to make the pulsed-power required compatible with the supply system [16]. In addition to high energy loads, EMSs are used to supply power for critical equipment, both potentially damaged by a threat and normal system transients, so

as to increase the ship's survivability and quality of service (QOS) [11]. Furthermore, ESMs can also be used to supply power peaks and to level the power demanded from main generators, leading not only to functional benefits, but also to operational benefits in terms of power quality and fuel economy [2]. There are mainly three aspects for ESM design for a shipboard power system: 1) type; 2) management and controls for ESM and auxiliary devices; 3) size and location. In the literature, a number of ESM sizing studies have been carried out [5-16].

The type of ESS depends on many factors such as reliability, efficiency, cost and rate of discharge, etc. [8]. A number of studies have been carried out in this aspect [5, 7, 8 and 10]. Four types of ESMs using different physical principles for energy storage that could apply to the Navy's future needs are considered as follows: advanced capacitors (electrostatic); batteries (chemical), flywheels (kinetic) and superconducting magnetic energy storage (SMES) (magnetic) [5-10]. Supercapacitors have extremely high power capability and much longer lifetime. However, main drawbacks are at the cost of low energy density, high self discharge, and insufficient discharge time [5]. Batteries are one of the most cost-effective and matured energy storage technologies available [6]. The U.S. Army has been a leader in the development of high-density, high-power, 6- to 12-V battery power systems for vehicles, pulsed-power weapons, remote power backup, and missile systems [10]. Flywheels have advantages such as fast response and great power delivery profile. However, its main drawbacks are energy density and safety [5, 10]. As for SMES, it has similar advantages as supercapacitors. However, its main disadvantages are relative high cost and significant auxiliary equipment requirements [5, 10].

As for management and control, studies are carried out at the power system level [13, 14]. In [13], a comprehensive approach is introduced to study the energy management for all electric ship. It describes some control challenges and ESS stability analysis. In [14], optimal generation scheduling with ESS is studied. Some studies are carried out at the power electronics level [15, 16].

However, few studies are carried out in relation to location and size. According to [9, 12], neither of Navy's current two software packages, Advanced Surface Ship and Submarine Evaluation Tool (ASSET) and the Electric Plant Load Analysis (EPLA), are capable of developing optimized ESS location design, and location study is still an open

issue [18]. Therefore, it is necessary to study the optimal ESS location evaluation and design.

In order to evaluate ESM location and size design, three main factors can be considered: survivability, QOS, and cost. Therefore, the design involves multiple objective optimization problems. Multiple objective particle swarm optimization (MOPSO) has been widely used for multiobjective optimization in recent years [26-28]. According to [26], MOPSO has a better average performance with respect to some of the best multiobjective evolutionary algorithms known to date. Therefore, in this paper, MOPSO is used to optimize ESM design.

II. INTEGRATED POWER SYSTEM FOR THE ELECTRIC SIHP

A. IPS Technical Architecture

Two power architectures are mainly studied to meet the power requirements: medium voltage as power (MVAC) and medium voltage dc power (MVDC). The current DDG1000 employs MVAC, while MVDC is the long-term goal [29]. In his paper, the MVDC architecture is studied, which is shown in Fig. 1. The architecture consists of power generation module (PGM), power distribution module (PDM), auxiliary turbine generator (ATG), main turbine generator (MTG) and propulsion motor module (PMM). The zonal electric distribution system design employs six zones, resulting in each zone being roughly 15% of the length of the ship [30]. Therefore, six zones based MVDC architecture is studied.

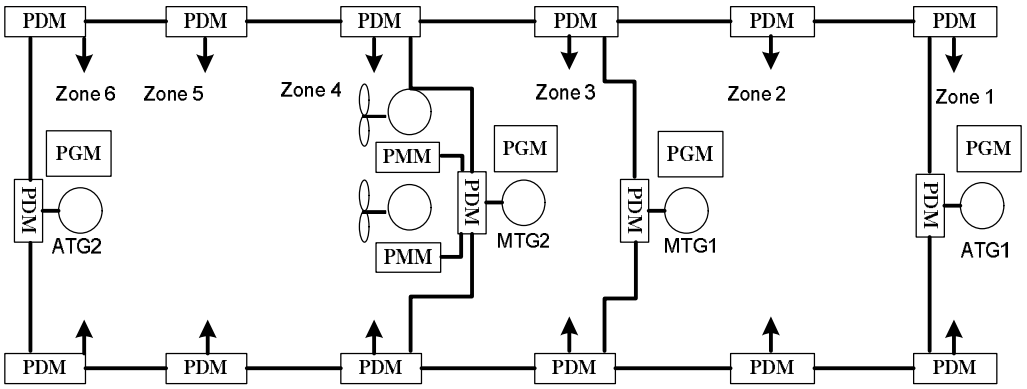

Fig. 1. MVDC architecture

B. Next Generation Integrated Fight Through Power (IFTP)

Fig. 2 shows a proposed next generation IFTP zonal architecture [29]. PCM-1A is the interface to ZEDS and converts power from the longitudinal bus to loads and PCM-2A. PCM-1A mainly consists of four types of modules: PCM-4A; ship service converter module (SSCM) with 800VDC; SSCM with 650VDC and ship service inverter module (SSIM) with 450VAC which are shown in Fig. 3 (a). PCM-2A consists of two types of modules: SSIM with 400Hz 450VAC and SSIM with 60Hz 450VAC, which are shown in Fig. 3 (b). Each SSCM and SSIM module are considered to have a rating of 300kW. To ensure adequate supply in the event of a SSCM/SSIM failure, an *N*+1 redundancy scheme was employed [20]. The SSCM and SSIM number are first calculated by dividing the capacity required for each module type by 300kW, then apply the *N*+1 redundancy scheme. According to loads the table in Appendix I in [20], the detailed SSCM/SSIM requirement for PCM-1A and PCM-2A are shown in Table 1 and 2 respectively.

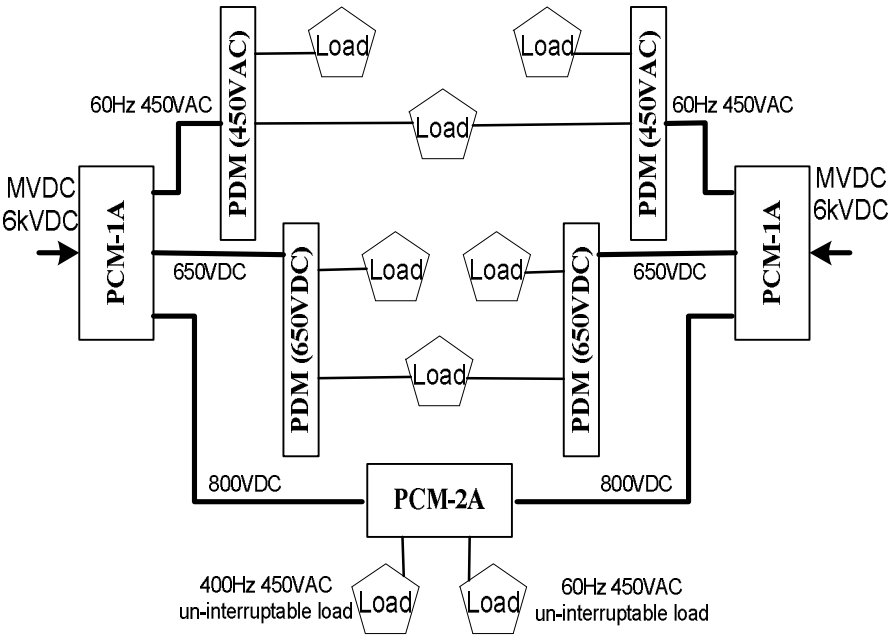

Fig. 2. Notational in-zone power system structure

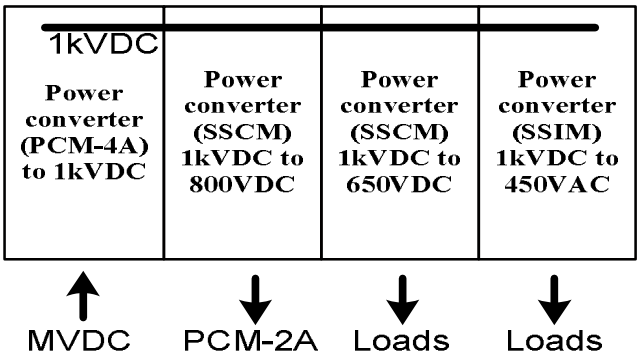

(a)

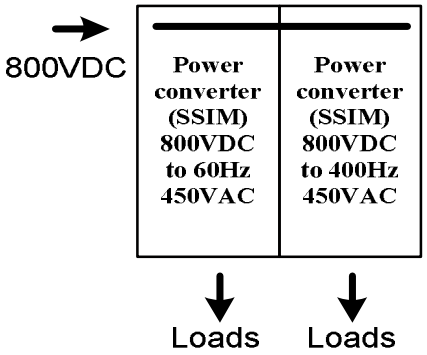

(b)

Fig. 3. Notational PCM-1A and PCM-2A structure. (a) PCM-1A structure. (b) PCM-2A structure.

Table 1. Zonal SSCM/SSIM Requirement for PCM-1A

Zone	PCM-1A	650VDC SSCM	800VDC SSCM	60Hz SSIM
1	Left	1	2	1
	Right	1	2	2
2	Left	1	2	3
	Right	2	2	2
3	Left	2	2	2
	Right	1	2	3
4	Left	2	2	3
	Right	1	3	2
5	Left	1	2	3
	Right	1	3	2
6	Left	1	2	3
	Right	1	2	2

Table 2. Zonal SSCM/SSIM Requirement for PCM-2A

Zone	PCM-1A	650VDC SSCM	800VDC SSCM 60Hz 450VAC SSIM
1	1	0	4
2	1	2	4
3	1	0	4
4	1	0	5
5	1	2	5
6	1	0	5

C. Electrical Loads

For electrical power systems, loads can be categorized into four QOS categories: uninterruptible (UI), short-term interruptable (STI), long-term interruptable (LTI), and exempt loads (EX) [19]. UI are defined as electrical loads can only tolerate power interruptions less than 2 seconds. The standby power systems should be capable of providing power to them up to 10 minutes while a interruption occurs. STI and LTI are defined as electrical loads that can tolerate power interruptions ranging from 2 seconds to 5 minutes and more than 5 minutes respectively [25].

Due to security issues, it is infeasible to obtain all ship electrical loads and their characteristics. In this study, 166 ship service loads from [20] are used and analyzed, which are listed in Appendix I. All electrical loads are categorized by QOS, power rating, ship operation mode, zones and power nodes.

D. ESM

As is described in Section I, four types of technologies are considered to apply for ESM application. Since this study mainly focus on a location and sizing study, all ESMs are considered to be battery modules. It is fair to assume that each ESM has a peak power of 250kW and multiple ESMs can work together to supply power for certain power node [29]. It is assumed that the battery working range is from 40% to 70% state-of-charge and can supply 250kW for 5 minutes. Therefore, each ESM has a capacity of 69.4kW·h.

Three main options to integrate ESMs within the in-zone power distribution system are proposed [5, 17, 18]. The first option is to incorporate an ESM within a PCM-2A, which is shown in Fig. 4. The primary purpose is to provide loads with the type of power they need with the requisite survivability and QOS. The main advantage of this

distribution is that they are near or within the vital loads they are supporting, which suggests a more reliable power source. The main drawback of this type is that some emergency loads connected to PCM-1A will not be supported. Furthermore, it cannot supply power for the PMM and generator startup.

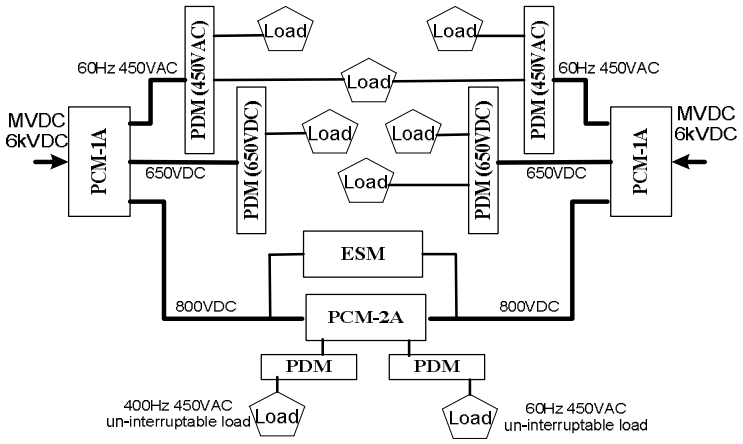

Fig. 4. Option 1 for ESM location strategy.

The second option is to incorporate ESM within PCM-1A, which is shown in Fig. 5. In this case, the ESM will connect to the 1kV dc side. Therefore, the ESM can supply power for all in-zone electrical loads. However, since the ESM is not near critical loads, QOS and survivability for critical loads are lower than the first option. Furthermore, it cannot supply power for the PMM and generator startup as well.

The third option is to incorporate ESMs with ports or starboards on the longitude bus with 6kV dc, which is shown in Fig. 6. In this case, ESMs can supply power for PMM and generator startup. Furthermore, it can provide potential economical savings by using a proper economic dispatch strategy. However, the main drawback is that the QOS and survivability for critical loads are lower than the first two options. In this paper, it is assumed that PDMs in Fig. 1 have no faults because they mainly consist of breakers and corresponding control software. Therefore, it is reasonable to combine all this option ESMs into one. Since for each zone, there are two possible locations, the total possible ESM locations are thirteen with twelve of them inside six zones and one in the main bus.

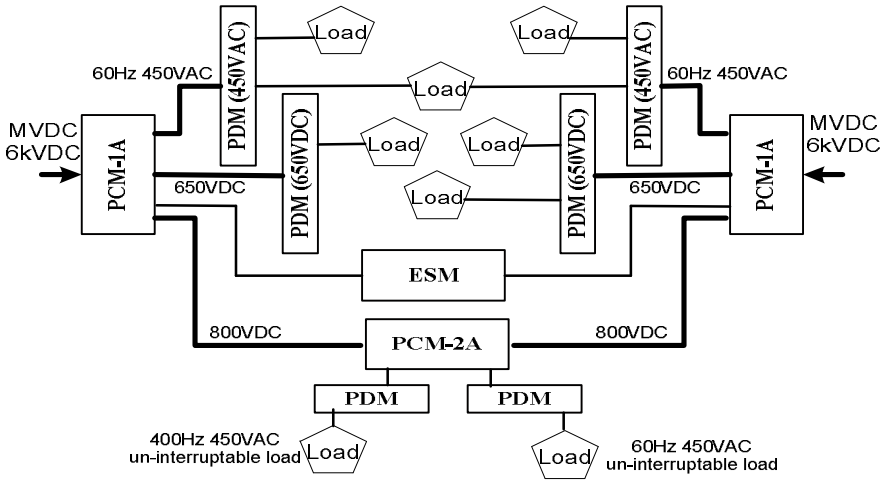

Fig. 5. Option 2 for ESM location strategy.

Other possibilities of ESM placement are to interface with the 650V dc or 60Hz 450V ac modules in PCM-1A. However, in this paper, these two possibilities are not considered because they can neither supplying power to critical loads nor PMM and generator startup.

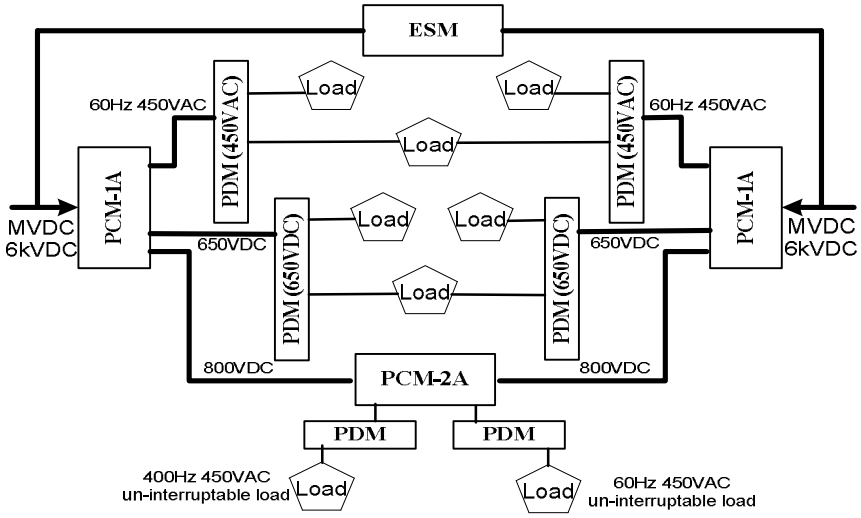

Fig. 6. Option 3 for ESM location strategy.

III. SYSTEM MODELING

The location study of ESS is to evaluate distribution solutions and calculate an optimal one. According to loads list in Appendix I, it is reasonable to define 28 load nodes based on power type and QOS categories, which are shown in Table 3.

In order to evaluate ESMs design, a fitness function is needed. The primary aim of the design of a shipboard power system has traditionally been survivability and QOS consideration [19]. QOS is a metric to evaluate the continuity of service provided by the power system under normal operation. Survivability relates to the ability of continuity of service provided by the power system under damaged condition. Furthermore, cost is a key factor in ship power system design. In this study, three factors are considered in order to evaluate the ESS location and size design: QOS, survivability and cost.

A. QOS

QOS has been defined as a metric of the continuity of the electrical power supply under normal operation, which is measured in terms of a mean time between service interruption (MTBSI) [19, 25]. In [19], a basic method for calculating QOS is proposed. In [20], a detail approach to calculate QOS is presented. In this paper, the approach in [20] is employed to calculate QOS for a certain ESM design. For a time instant, if all loads can be supplied with rated power, it means it can fulfill the current mission. Otherwise, it has a QOS failure.

Initialize a six-month ship mission profile. Mission profile includes time allocation for each operating condition and PMM loads. A typical Navy ship deployment has a duration of six months [20]. Within this deployment, two-thirds of underway time is spent in the cruise conditions, divided equally between summer cruise (SC) and winter cruise (WC), while summer battle (SB) and winter battle (WB) conditions account for one-third of underway time [20]. Time fraction for anchor (AN) and emergency (EM) conditions are 10% and 2% respectively. The time step for mission profile is set to be 5 minutes. Therefore, there are 4380 hours (52560 time instants) for a six-month mission profile. The flowchart for generating the mission profile is shown in Fig.7. The detailed implementation can be found in the literature [20].

Table 3. Load Nodes

Node	Zone	Power Type	QOS Cat
1	1	60Hz AC	UI
2	1	60Hz AC	STI
3	1	60Hz AC	LTI
4	1	650VDC	LTI
5	2	400Hz AC	UI
6	2	60Hz AC	UI
7	2	60Hz AC	STI
8	2	60Hz AC	LTI
9	2	650VDC	LTI
10	3	60Hz AC	UI
11	3	60Hz AC	STI
12	3	60Hz AC	LTI
13	3	650VDC	STI
14	3	650VDC	LTI
15	4	60Hz AC	UI
16	4	60Hz AC	STI
17	4	60Hz AC	LTI
18	4	650VDC	STI
19	4	650VDC	LTI
20	5	400Hz AC	UI
21	5	60Hz AC	UI
22	5	60Hz AC	STI
23	5	60Hz AC	LTI
24	5	650VDC	LTI
25	6	60Hz AC	UI
26	6	60Hz AC	STI
27	6	60Hz AC	LTI
28	6	60Hz AC	LTI
29		PMM	Exempt

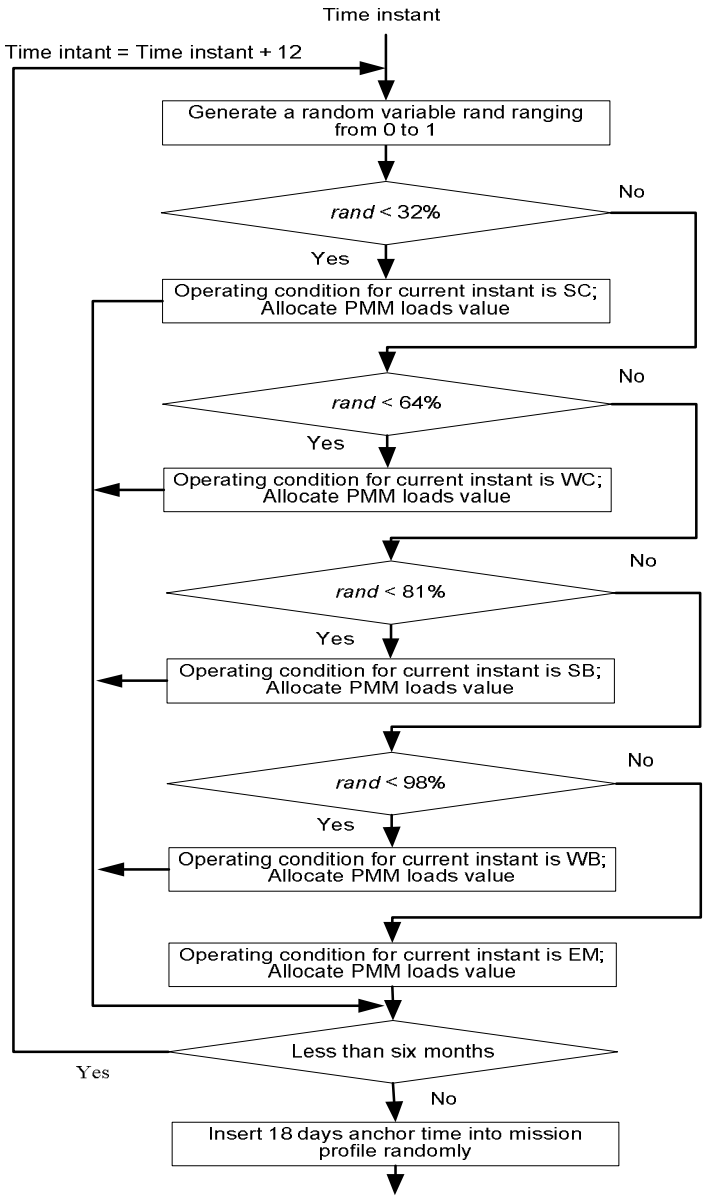

Fig. 7. Flowchart for generating ship mission profile.

Generate device availability for each time increment. The devices consist of four generators, 99 SSIMs/SSCMs, 12 PCM-4A and 36 PDMs in six zones, with a total number 147. Each type of devices has its mean time between failures (MTBF) and mean time to repair (MTTR) values, which are listed in the literature [20]. By assuming constant failure rate (λ) for all devices, the probability density function and cumulative density function for the time to failure is given by (1) and (2) respectively [20].

$$f(t) = \lambda e^{-\lambda t} \tag{1}$$

$$F(t) = 1 - e^{-\lambda t} \tag{2}$$

The probability that the item has not failed by time *t* and MTBF can be obtained using (3) and (4) respectively.

$$R(t) = 1 - F(t) = e^{-\lambda t} \tag{3}$$

$$MTBF = \int_0^\infty R(t)dt = \frac{1}{\lambda} \tag{4}$$

Therefore, the time t_{NF} that the item has not failed can be calculated using (5).

$$t_{NF} = -\frac{\log(R(t))}{\lambda} = -\log(R(t)) \times MTBF \tag{5}$$

The detailed implementation process can be found in [20].

Generate generator, ESM and load profiles. The generator determines available power generation for each time increment. The generators dispatch for different operating modes is shown in Table 4. The MTTR for generators is set to be 5 hours while the time to bring a standby machine online is set to be 5 minutes [20].

Table 4. Generators Dispatch for Different Operating Modes

	MTG1	MTG2	ATG1	ATG2
SC	online	standby	standby	standby
WC	online	standby	standby	standby
SB	online	online	standby	standby
WB	online	online	standby	standby
AN	standby	standby	online	online
EM	standby	standby	online	standby

The ESM profile consists of two factors: stored power capacity for each time increment and maximum power capacity. As is described in the previous section, there are thirteen ESM locations. If the maximum power capacity for one location is zero, it means there is no ESM in that location.

The load profile determines available load capacity for power nodes for each time increment. According to Appendix I, for different operating modes, the operational load factors (OF) show the loads online time fraction. A random number ranging from 0 to 1 is generated and compared with OF to determine whether this load is on or off for each time increment. Therefore, the load capacity profile for different power nodes is obtained.

Obtain QOS failure information. Different from the approach in [20], a more detailed evaluation process is employed with analysis for each time instant. This approach makes ESM analysis and energy dispatch available. However, the computation complexity is much larger than the approach in [20]. The QOS failure is defined based on QOS categories. For UI loads, QOS failure is defined as interrupt for 2 seconds. For STI loads, QOS failure means interrupt ranging from 2seonds to 5 minutes, while for LTI loads, QOS failure means interrupt ranging from 5 to 10 minutes. Therefore, if any US or STI loads cannot be powered for one time increment, there is a QOS failure. Likewise, there is a QOS failure while LTI loads are not powered for two continuous time increment. The QOS failure information includes two parts: time instant and node number that QOS failure occurs. The detailed QOS failure process is shown in Fig. 8.

Evaluate ESM location and size. The QOS failure number is taken into consideration to evaluate ESM location and size. For each combination of ESM location and size, six-month case studies are run for *Max_Iter* iterations to get the average QOS failure information. A large *Max_Iter* decreases the random effect introduced by random generated mission profile. The average QOS failure number is used to evaluate the performance of ESM location and size. The detailed process is shown in Fig. 9.

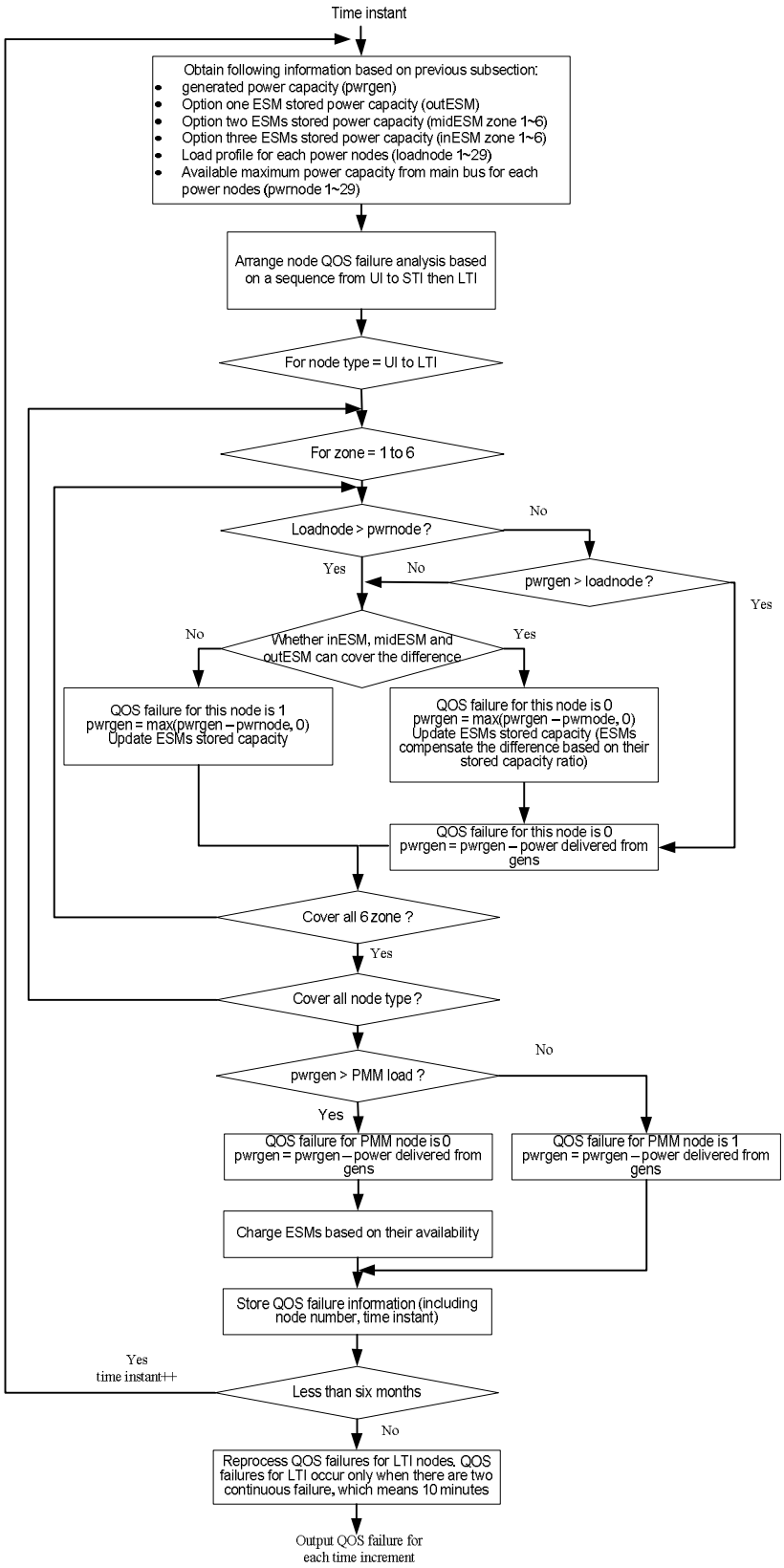

Fig. 8. Flowchart for obtaining QOS failure information.

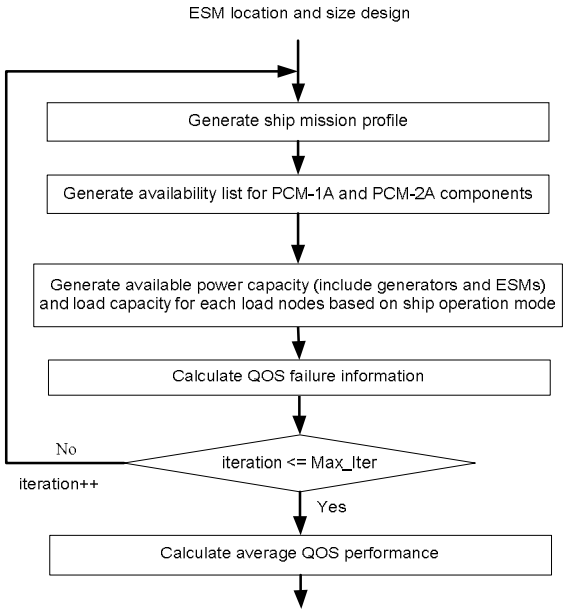

Fig. 9. Flowchart for ESM location and size evaluation.

B. Survivability

Survivability is defined as a metric of the continuity of the electrical power supply for critical loads under attack. This continuity can be defined as 10 minutes time frame to improve survivability [5]. Different form QOS, device failures for survivability study are outcome of attack threat. Therefore, the first step to evaluate ESM location and size is to build a potential threat outcome list. In this paper, four threat outcomes are considered in one zone, which is shown in Fig. 10. The PDM, 60Hz STI and LTI buses and 650VDC buses are not considered because the survivability study mainly focuses on critical loads. Furthermore, since no ESMs can supply power to loads if the corresponding PDMs are out of commission, PDMs are not considered for survivability studies.

For each zone, it is assumed that at most two faults can occur simultaneously, which means 10 combinations, which are shown in Table 5. Therein, a 1 entry means that there is no fault while 0 indicates a fault. One threat can influence two adjacent zones at most [30]. Therefore, the survivability study is divided into five different cases based on fault locations: zones 1 and 2; zones 2 and 3; zones 3 and 4; zones 4 and 5; zones 5 and 6. It is assumed that for each zone, at most two faults can occur simultaneously. Therefore,

there are 100 fault combinations for one case study. Furthermore, generator faults are also considered. As is shown in Fig.1, ATG1, ATG2, MTG1 and MTG2 are connected to zone 1, 6, 3 and 4 respectively. Therefore, it is reasonable to assume that threat outcomes in these zones could bring the corresponding generators offline. The online generators capacity for different zone faults cases for ten minute time frames is shown in Table 6, with an assumption that the time to bring a standby machine online is set to be 5 minutes [20].

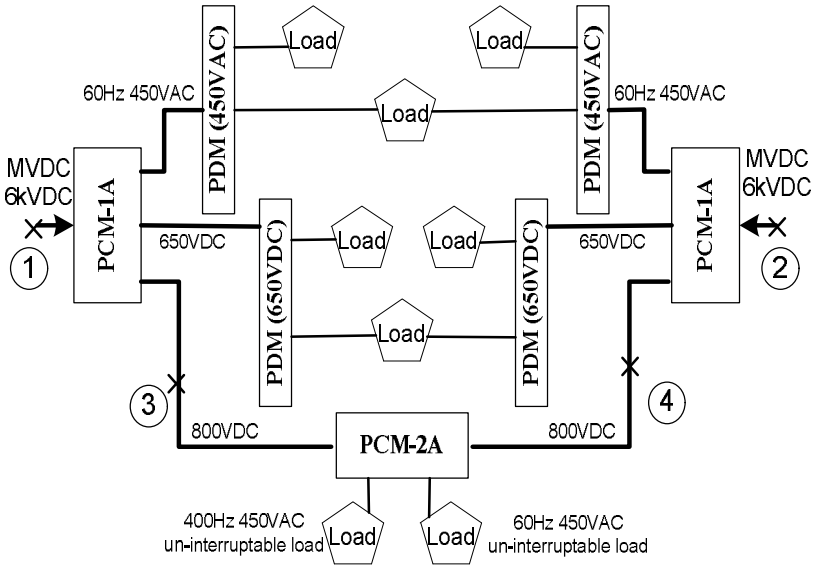

Fig. 10. Fault location for survivability study.

Table 5. Faults Cases

	Fault 1	Fault 2	Fault 3	Fault 4
Case 1	1	1	1	0
Case 2	1	1	0	1
Case 3	1	0	1	1
Case 4	0	1	1	1
Case 5	1	1	0	0
Case 6	1	0	1	0
Case 7	0	1	1	0
Case 8	0	0	1	1
Case 9	0	1	0	1
Case 10	1	0	0	1

Table 6. Online Generators Capacity for Different Zone Faults Cases

	Online generators capacity (0~5 minutes)	Online generators capacity (6~10 minutes)
Zone 1&2	72000kW	72000 kW
Zone 2&3	72000 kW	72000 kW
	36000 kW	43960 kW
Zone 3&4	72000 kW	72000 kW
	36000 kW	43960 kW
	0	7960kW
Zone 4&5	72000 kW	72000 kW
	36000 kW	43960 kW
Zone 5&6	72000 kW	72000 kW

Two operation modes are studied for survivability. The first is the battle condition mode. In this mode, the survivability is measured based on supplying power for all battle condition loads. The generator and load profiles are shown in Table 5 and Appendix I in [20] respectively. Another is the emergency mode which is measured by supplying power for all UI loads. Since at least two generators can survive and the total UI loads capacity is much lower than ATG capacity, it is reasonable to assume that generated power can always meet the loads demand.

Since the time frame for survivability study is ten minutes, it is divided into two time instants with each one being 5 minutes. Furthermore, PMM loads are set to be 2MW, which can provide a ship speed of 12 knots for 10 minutes [5].

Based on generation capacity, load profile and device availability, the total survivability failure number can be calculated using a similar process with Fig. 8. One difference is that the time increments are 2 for the survivability study. Furthermore, for survivability, the PMM is regarded as UI load while in QOS, PMM is regarded as LTI. The detailed survivability failure study for evaluating ESM location and size is shown in Fig. 11.

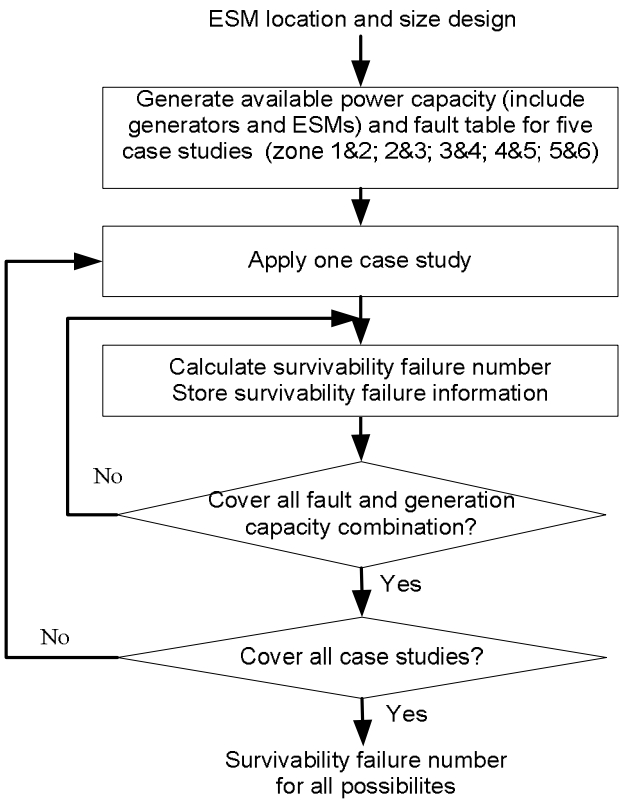

Fig. 11. Flowchart for survivability failure study for evaluating ESM location and size.

C. Cost

The cost for ESMs can be divided into two parts. One part is energy storage devices and corresponding bi-directional power conversion system. Another is auxiliary devices such as cooling and protection devices. Both of them are directly related with ESM quantity. Therefore, in this paper, the total number of ESMs is used to represent ESM cost.

IV. MOPSO

MOPSO is a swarm intelligence technique (a search method based on nature inspired systems), which is an efficient method for solving multiple large scale nonlinear optimization problems [26-28]. For each ESM location and size design, three factors are needed to be minimized: QOS failure number, survivability failure number and cost.

Therefore, the ESM design turns into three objectives optimization problems. The design steps for MOPSO are shown below.

1) Initialize particle positions. Randomly generate *N* particles. Each particle consists of 13 columns with each column represents ESM quantity for one location. The range for in-zone ESMs quantity is from 0 to 10, which means from 0 to 1250kW for 10 minutes. The range for main bus ESM quantity is from 0 to 500, which is 0 to 62500kW for 10 minutes. The population *N* is set to be 100 [26].

2) Initialize particle velocities. Make velocities for each particle to be 0.

3) Evaluate all particles. Apply particles for QOS, survivability and cost studies and get the corresponding fitness.

4) Generate repository and hypercubes. Store nondominated particles into the repository (*REP*). The size of *REP* is set to be 100 [26]. Divide the range of *REP* into *D*-1 divisions. Then extend half division for each side to form the hypercubes space. Location *REP* using hypercubes as a coordinate system. *D* is set to be 30 [26].

5) Initialize local best particles (Pbest). Make *Pbest* equal to initialized particles.

6) Enter the main loop. The maximum number of iterations is set to be 100 in this paper.

a) Update particle velocities and position using (6) and (7). All particle positions are constrained within their corresponding initialization range.

$$\begin{aligned} VEL(i) &= w \times VEL(i) \\ &+ r_1 \times rand \times (Pbest(i) - POP(i)) \\ &+ r_2 \times rand \times (REP(h) - POP(i)) \end{aligned} \tag{6}$$

$$POP(i) = POP(i) + VEL(i) \tag{7}$$

where *w* is inertia weight which is set to be 0.4;

r_1 and r_2 are set to be 2;

rand is random number in the range from 0 to 1;

i is the index for particles;

VEL is the particle velocity;

POP is the particle position;

h is an index which can guide particles to less populated area.

The selection of *h* is described in [26].

b) Evaluate each particles and get their corresponding fitness.

c) Update *REP* and hypercubes.

d) Update *Pbest*.

After the tuning process, *REP* stores the Pareto fronts for QOS, survivability and cost. The detailed process is shown in Fig. 12.

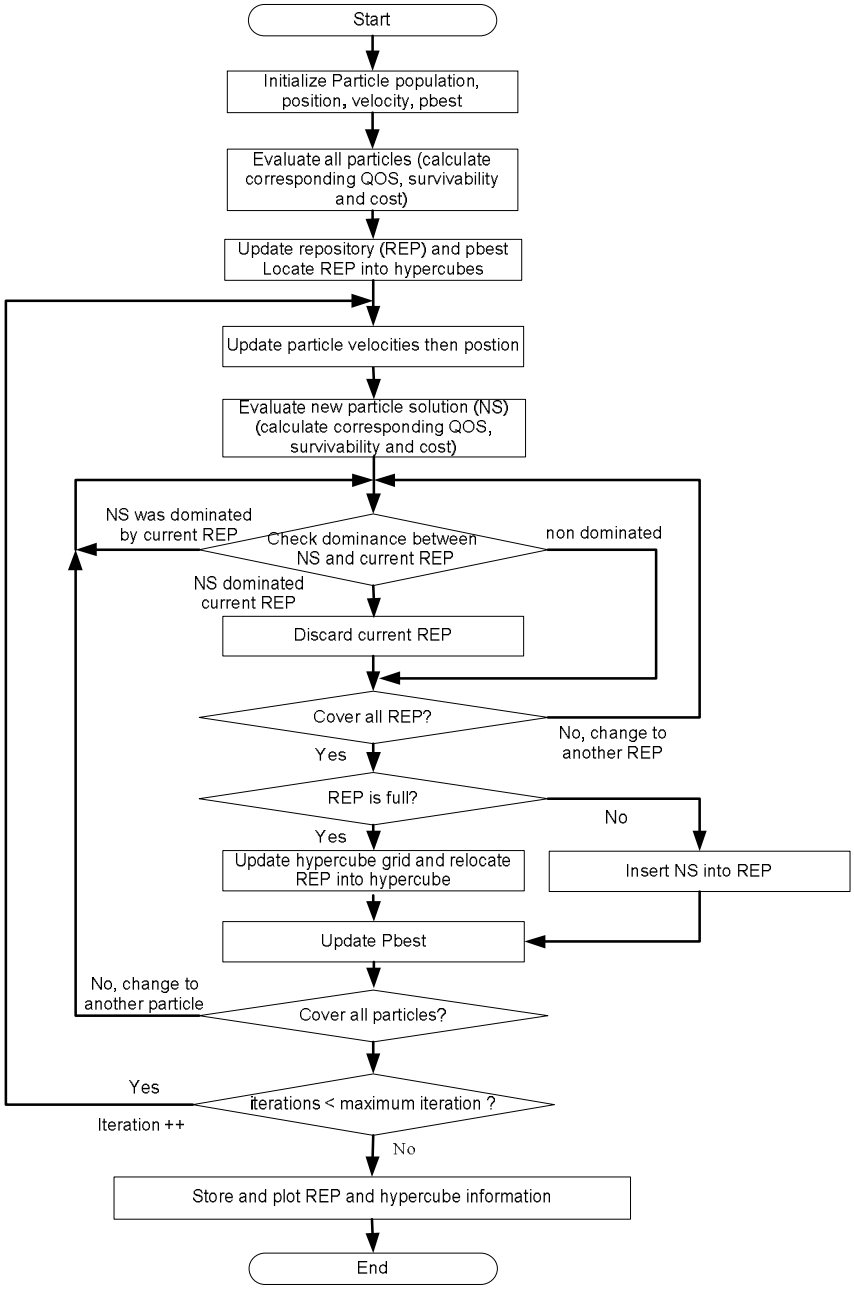

Fig. 12. Flowchart for MOPSO.

V. SIMULATION RESULTS

The MVDC ship power sysetm without ESMs is first studied to obtain the QOS and survivability characteristics. Then the study with ESMs is carried out and compared with the one without ESMs. Simulation is carried out using Matlab.

A. MVDC without ESMs

1) QOS. QOS characteristics for the non-ESM case are divided into two parts: all nodes study and non-PMM nodes study. The maximum iteration (*Max_Iter*) is set to be 100 to get the average QOS performance. The QOS failure percentage analysis for all nodes study and non-PMM nodes study are shown in Fig. 13 and 15 respectively. The detailed failure information is shown in Table 7. As is shown in Fig.13, the total PMM failure time instants are 8193, which is 51.81% of total QOS failures. Therefore, the average PMM failure time instants are 81.93, which mean average 6.8275 hours for one six-month mission profile. PMM QOS failure mainly results from generator malfunctions. In Fig. 14, it is clearly shown that UI power nodes have higher QOS failure percentage than other non-PMM nodes. This is because 60Hz UI loads for each zone connect to one PDM. If the PDM has QOS failure, all 60Hz UI loads have no power. Also, the MTTR for PDM is 30 minutes. ESMs cannot improve QOS for this case. In addition to UI nodes, STI and LTI nodes have relatively less QOS failure because of two power sources. ESMs can contribute for this case because the generator malfunction is the main failure source. Furthermore, it is clearly shown that LTI nodes have lowest failures because two continuous time increment QOS failure result in one LTI failure however the time to bring a standby generator online is 5 minutes (one time increment). And ESMs can contribute for this case as well.

2) Survivability. Survivability characteristics for thenon-ESMs case are divided into two cases based on operation mode: battle mode case and critical loads case. For the battle mode case, survivability is measured by supplying uninterrupted power to all loads in battle mode for 10 minutes. The generated power capacity is shown in Table 6. For the critical load case, survivability is measured by supplying uninterrupted power to all UI loads for 10 minutes. The survivability failure study without generator failure is shown in Table 8. For nodes with 80 survivability failures, they result from fault cases 5, 7, 8 and 10. For nodes with 20 survivability failures, they result from fault case 8. For nodes with

200 survivability failures, they have failure for any fault cases. It is because that the SSIM/SSCM design follows *N*+1 redundancy strategy rather than 100% margined UI loads strategy. Furthermore, the capacity of UI loads for those nodes is larger than the capacity of half *N*+1SSCMs. Therefore, they have failures for any fault cases. PMM survivability failure analysis with generator failures is shown in Table 9. Since battle mode for survivability study is more practical, ESM study only consider battle mode for survivability study.

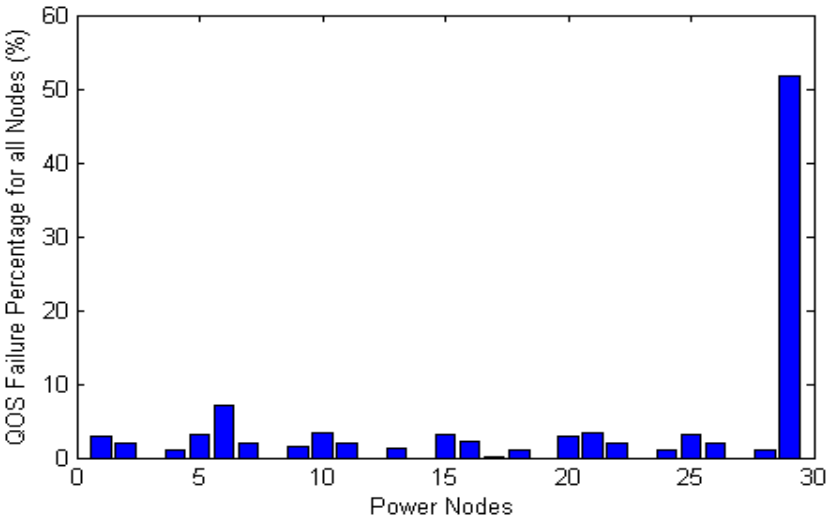

Fig. 13. QOS failure percentage analysis for all nodes.

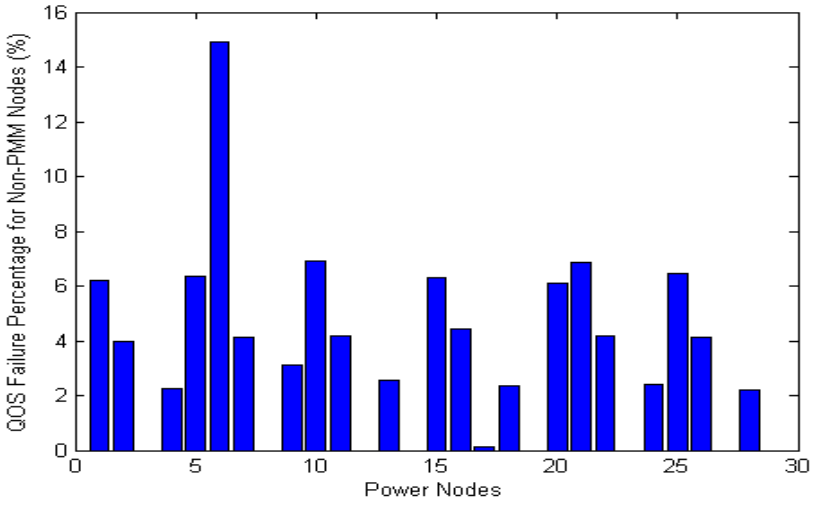

Fig. 14. QOS failure percentage analysis with PMM node excluded.

Table 7. QOS Failure Analysis For 100 Runs

Node	Total QOS Failure	QOS failure percentage for all nodes (%)	QOS failure percentage for non-PMM nodes (%)
1	471	2.9782	6.1795
2	302	1.9096	3.9622
3	0	0	0
4	171	1.0813	2.2435
5	484	3.0604	6.35
6	1138	7.1957	14.9305
7	313	1.9791	4.1065
8	0	0	0
9	236	1.4923	3.0963
10	527	3.3323	6.9142
11	317	2.0044	4.159
12	0	0	0
13	193	1.2204	2.5321
14	0	0	0
15	482	3.0477	6.3238
16	339	2.1435	4.4477
17	9	0.0569	0.1181
18	178	1.1255	2.3353
19	0	0	0
20	466	2.9466	6.1139
21	522	3.3007	6.8486
22	317	2.0044	4.159
23	0	0	0
24	182	1.1508	2.3878
25	491	3.1046	6.4419
26	316	1.9981	4.1459
27	0	0	0
28	168	1.0623	2.2041
29	8193	51.8052	

Table 8. Survivability Failure Analysis without Generator Failure

Case	Node	Survivability Failure for critical loads mode	Survivability Failure for battle mode
Zone 1 & 2	1	80	80
	2	0	20
	3	0	20
	4	0	20
	5	80	80
	6	80	80
	7	0	20
	8	0	20
	9	0	20
	29	0	0
Zone 2 & 3	5	80	80
	6	80	80
	7	0	20
	8	0	20
	9	0	20
	10	80	80
	11	0	20
	12	0	20
	13	0	20
	14	0	20
	29	0	0
Zone 3 & 4	10	80	80
	11	0	20
	12	0	20
	13	0	20
	14	0	20
	15	140	140
	16	0	80
	17	0	80
	18	0	20
	19	0	20
	29	0	0

Table 8. (Continued)

Zone 4 & 5	15	140	140
	16	0	80
	17	0	80
	18	0	20
	19	0	20
	20	80	80
	21	200	200
	22	0	20
	23	0	20
	24	0	20
	29	0	0
Zone 5 & 6	20	80	80
	21	200	200
	22	0	20
	23	0	20
	24	0	20
	25	200	200
	26	0	20
	27	0	20
	28	0	20
	29	0	0

Table 9. PMM Survivability Failure Analysis with Online Generators Capacity for Different Zone Faults Cases Without ESMs

	Generators capacity for two time increments	PMM Survivability Failure		
		Standard Bell (6055 kW)	Full Bell (13840 kW)	Flank Bell (67773 kW)
Zone 2&3	36000 kW 43960 kW	0	0	200
Zone 3&4	36000 kW 43960 kW	0	0	200
	0 7960 kW	200	200	200
Zone 4&5	36000 kW 43960 kW	0	0	200

B. MVDC with ESMs

MOPSO is used to search for Pareto fronts of ESM location and sizing design. The detailed MOPSO settings are shown in Table 10. To limit ESM cost, total ESM quantity is constrained within 500. To speed up the simulation, the parameter *Max_Iter* for QOS is set to 5. The Pareto fronts for cost and QOS failure is shown in Fig. 15. Some points are not around the Pareto fronts because of low *Max_Iter* value for QOS. The Pareto fronts for cost and survivability failure is shown in Fig. 16. It is clearly shown that ESM improve both QOS and survivability greatly. As is shown in Fig. 16, ESM decreases survivability failure which cause by *N*+1SSCMs design. Therefore, it is clearly shown that ESM has potential to reduce SSCM number, which means reduce cost, without sacrificing survivability. The three-dimension Pareto fronts for cost, survivability failure and QOS failure is shown in Fig. 17.

Table 10. MOPSO Settings

Population	100	Division (*Div*)	30
REP size	100	c_1, c_2	2
Iterations	50	w	0.4
Fitness number (NF)	3	Particle Dimension	13
Initialization Range for in-zone ESM quantity	From 0 to 20 (0 to 5MW)	Initialization Range for main bus ESM quantity	From 0 to 500 (0 to 125MW)

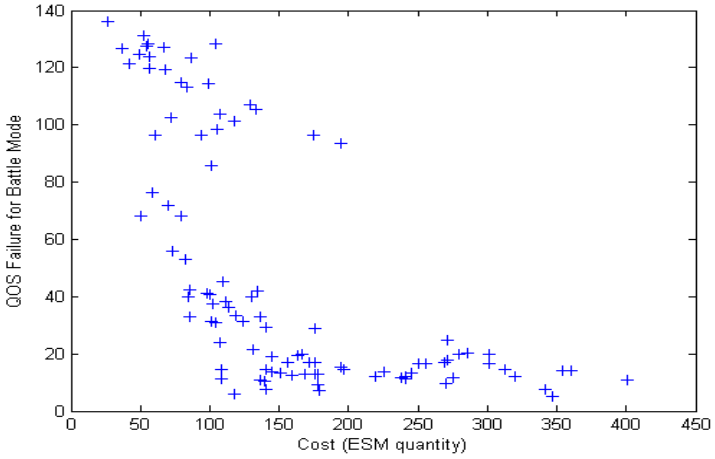

Fig. 15. Pareto fronts for cost and QOS failure.

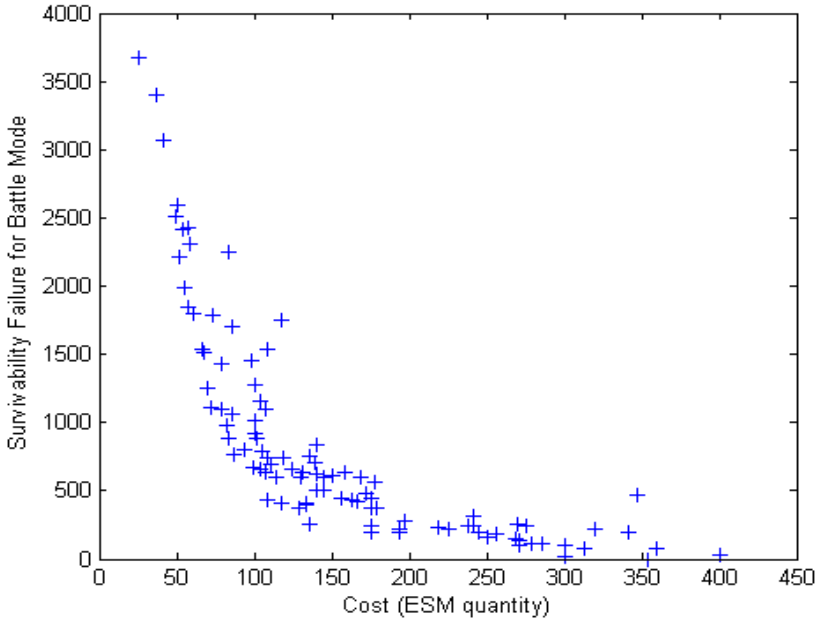

Fig. 16. Pareto fronts for cost and survivability failure.

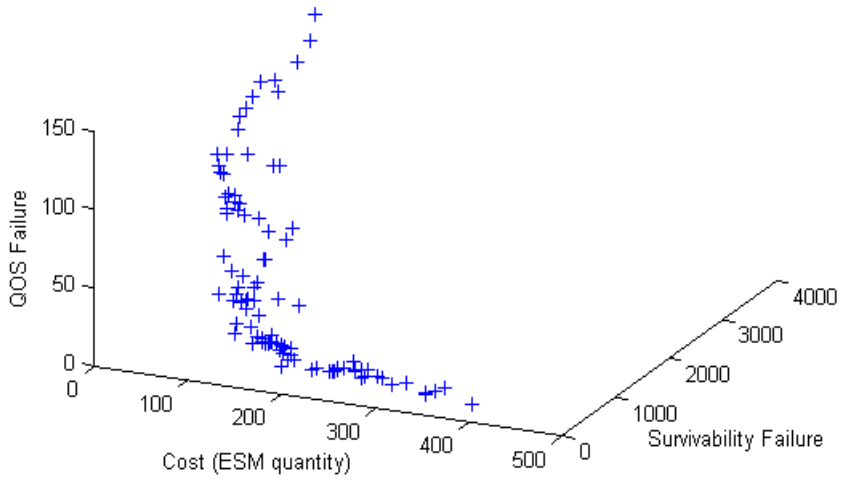

Fig. 17. Three-dimension Pareto fronts for cost, survivability failure and QOS failure.

MOPSO is used to search for Pareto fronts of ESM location and sizing design. A solution with lowest total failure is chosen, which is (7, 20, 20, 18, 20, 20, 20, 20, 4, 20, 20, 9, 156). The QOS failure analysis is reproduced first. The average QOS failure is 14.2. Compared with 158.15 average QOS failure without ESM, the new solution reduced QOS failure dramatically. In addition to QOS study, survivability failure analysis without generator failure is reproduced. The survivability failure for all cases is 0. The PMM survivability failure analysis with generator failure is reproduced with ESMs, which is shown in Table 11. It is clearly shown that ship can maintain Full Bell for 10 minutes even when two MTG are offline. Therefore, the proposed solution not only improves QOS, but also maintains ship under battle mode for 10 minutes even for the worst case.

Table 11. PMM Survivability Failure Analysis with Online Generators Capacity for Different Zone Faults Cases With ESMs

	Generators capacity for two time increments	PMM Survivability Failure		
		Standard Bell (6055 kW)	Full Bell (13840 kW)	Flank Bell (67773 kW)
Zone 2&3	36000 kW 43960 kW	0	0	36
Zone 3&4	36000 kW 43960 kW	0	0	6
	0 7960 kW	0	0	200
Zone 4&5	36000 kW 43960 kW	0	0	6

Since there are totally 100 solutions for ESM location and sizing design, it assists the ship designer to adopt certain designs based on their constrains (mostly ESM quantity, because of cost and ship space limitation). Furthermore, because of flexibility of MOPSO, constrains for more practical application can be easily implanted, such as zonal space.

VI. CONCLUSION

An approach to evaluate energy storage module location and sizing is proposed with quality of service, survivability, and cost as metrics. Multi-objective particle swarm optimization is used to optimize these metrics and provide Pareto fronts for energy storage module location and sizing. The simulation results show that an optimized energy storage module location and sizing design improve quality of service and survivability greatly with relatively low cost. Furthermore, it has the potential to decrease ship service inverter converter modules without scarifying quality of service and survivability.

VII. REFERENCE

[1]. G.T Little, S.S. Young and J. M Newell, "The electric warship VII – the reality," *IMAREST Evening Paper,* December 2001.

[2]. A. Monti, S. D'Arco, L. Gao and R. A. Dougal, "Energy storage management as key issue in control of power systems in future all electric ships," *International Symposium on Power Electronics, Electrical Drives, Automation and Motion*, pp.580-585, 2008.

[3]. A. Ouroua, J. Beno and R. Hebner, "Analysis of Fault Events in MVDC Architecture," *Electric Ship Technologies Symposium,* pp.380-387, 2009.

[4]. S. R. Rudraraju, A. K. Srivastava, S. C. Srivastava and N. N. Schulz, "Small Signal Stability Analysis of A Shipboard MVDC Power System," *Electric Ship Technologies Symposium,* pp.135-141, 2009.

[5]. Holsonback, C., T. Webb, T. Kiehne and C. C. Seepersad, "System-Level Modeling and Optimal Design of an All-Electric Ship Energy Storage Module," *Electric Machines Technology Symposium,* Philadelphia, PA. May, 2006.

[6]. W. Du, H.F. Wang, R. Duun, "Power System Oscillation stability and control by FACTS and ESS - A survey," International conference on Sustainable Power Generation and Supply, pp.1-13, 2009.

[7]. F. C. Beach and I.R. McNab, "Present and Future Naval Applications for Pulsed Power," *IEEE Pulsed Power,* pp.1-7, 2005.

[8]. J.V. Amy, "Considerations in the Design of Naval Electric Power Systems," *IEEE Proceedings of Power Engineering Society Summer Meeting,* pp.331-335, 2002.

[9]. N. Doerry, "Next Generation Integrated Power Systems (NGIPS) for the Future Fleet, *Electric Ship Technologies Symposium*, 2009.

[10]. National academy press. Technology for the United States Navy and Marine Corps 2000-2035 Becoming a 21st-Century Force: Volume 2: Technology, Chapter 8, 1997.

[11]. S. Young, J. Newell and G. Little, "Beyond Electric Ship," *Naval Engineers Journal*, vol.113, no.4, pp.79-92, 2001.

[12]. N. Doerry, "Institutionalizing the Electric Warship," *Naval Engineers Journal*, vol.118, no.4, pp.57-64, 2008.

[13]. A Monti, S.D. Arco, L.Gao and R.A. Dougal, "Energy storage management as key issue in control of power systems in future All Electric Ships," *International Symposium on Power Electronics, Electrical Drives, Automation and Motion*, pp.580-585, 2008.

[14]. W. Wu, D. Wang, A. Arapostathis and K. Davey, "Optimal Power Generation Scheduling of a Shipboard Power System," *Electric Ship Technologies Symposium*, pp.519-522, 2007.

[15]. L Liu, H. Li and J.M. Kim, "An Ultracapacitor-based Energy Storage System Design for High Power Motor Drive with Dynamic Real Power Compensation and harmonic Cancellation," *IEEE Energy Conversion Congress and Exposition (ECCE'01)*, pp.1745-1752, 2009.

[16]. L Liu, Z W and H. Li, "A Single-stage Grid-connected Inverter with Wide Range Reactive Power Compensation using Energy Storage System (ESS)," *IEEE Applied Power Electronics Conference and Exposition, (APEC'10)*, Feb, 2010.

[17]. G.T. Little, P.A. Erskine and P. Norton, "Demonstrating the Electric Ship," *Naval Engineers Journal*, vol.115, no.4,pp.91-105, Oct 2008.

[18]. N. Doerry, "In-Zone Power Distribution for the Next Generation Integrated Power System," *ASNE*, pp.1-15, December 2008.

[19]. N. Doerry, "Designing Electrical Power Systems for Survivability and Quality of Service," *Naval Engineers Journal*, vol.119, no.2,pp.25-34, Oct 2007.

[20]. B.F. Hawbaker, "Analyzing the Effect of Componemnt Reliability on Naval Integrated Power System Quality of Service," *dissertation at MIT*, June 2008.

[21]. Z. Ding, S.K. Srivastava, D.A. Cartes and S. Suryanarayanan, "Dynamic Simulation-Based Analysis of a New Load Shedding Scheme for a Notional Destroyer-Class Shipboard Power System," *IEEE Transactions on Industry Applications*, vol. 45, No.3, pp. 1166-1174, 2009.

[22]. A.J. Brown and J. Salcedo, "Multiple Objective Genetic Optimization in Naval Ship Design," *Naval Engineers Journal*, vol.115, no.4, pp.49-61, 2003.

[23]. T. Mierzwicki, A.J. Brown, "Risk Metric for Multi-Objective Design of Naval Ships," *Naval Engineers Journal*, vol.116, no.2, pp.55-71, 2004.

[24]. S.N. Neti, "Ship Design Optimization Using ASSET," MS Thesis, Department of Aerospace and Ocean Engineering, Virginia Tech, February 10, 2005.

[25]. N. Doerry and D.H. Clayton, "shipboard electrical power quality of service," *IEEE Electric Ship Technologies Symposium*, pp.274-279, 2005.

[26]. C.A.C. Coello, G.T. Pulido and M.S. Lechuga, "Handling Multiple Objectives with Particle Swarm Optimization," *IEEE Transactions on Evolutionary Computation*, vol.8, no.3, pp.256-279, 2004.

[27]. L.D.S. Coelho, L.Z. Barbosa and L. Lebensztajn, "Multiobjective Particle Swarm Approach ofr the design of a Brushless DC whell Motor," *IEEE Transactions on Magnetics*, vol.46, no.8, pp.2994-2997, 2010.

[28]. J.S. Heo, K.Y. Lee and R. Garduno-Ramirez, "Multiobjective Control of Power Plants using Particle Swarm Optimization Techniques," *IEEE Transactions on Energy Conversion*, vol.21, no.2, pp.552-561, 2006.

[29]. http://www.dtic.mil/cgi-bin/GetTRDoc?AD=ADA519753&Location=U2&doc=GetTRDoc.pdf, NGIPS Technology Development Roadmap, August, 2010.

[30]. N.H. Doerry and H. Fireman, "Designing All Electric Ships," *Proceedings of the 9th International marine Design Conference*, pp.475-497, May, 2006.

2. CONCLUSION

To improve the power quality of electric ship power system, optimal excitation systems, and optimal location and sizing of energy storage modules (ESMs) are studied. For excitation system, two three computational intelligence based algorithms are used to implement optimal controllers: CSA, PSO and SPPSO. The proposed optimal controllers have features such as optimal oriented and no machine parameters needed. Based on these, an AIS based adaptive excitation controller is proposed with features such as adaptive to disturbance and multi-machine coordinate control. Both simulation and hardware results show that the proposed controllers can improve power quality after high power energy loads are experienced.

In addition, an approach to evaluate ESM location and sizing is proposed using three metrics: quality of service, survivability and cost. Multiple objective particle swarm optimization (MOPSO) is used to optimize these metrics and provide Pareto fronts for optimal ESM location and sizing. The simulation results show that an optimized ESM location and sizing design improve QOS and survivability greatly with relatively low cost.

2.1. SUMMARY OF CONTRIBUTIONS

This subsection summarizes the main contributions of the four journal papers that form this dissertation work.

In paper 1, an online designed optimal excitation controller using a clonal selection algorithm (CSA) has been presented. This controller has advantages including optimal oriented, no generator parameters needed and minimal human involvement. Comparing CSA with PSO, both simulation and hardware results show that CSA-based controller can restore and stabilize the terminal voltage effectively and quickly with little disturbance introduced after high power pulsed loads are experienced.

In paper 2, an online optimal excitation controller using ‘optimal’ SPPSO algorithm has been proposed and demonstrated on two platforms of a Navy’s electric ship power system, namely, a Matlab/Simulink simulation and on an laboratory scaled down power system. The SPPSO algorithm based controller development has numerous

advantages for time critical tuning including optimal oriented, no generator parameters needed and no human involved. The number of particles to participate in the regeneration process and the frequency at which they do have been determined to provide the most effective SPPSO algorithm for online controller tuning. Matlab simulation results show that SPPSO has consistent convergence around the average value although PSO has a better average value. SPPSO based design can greatly reduce search time which means less number of fitness evaluations to find good controller parameters. This translates to less strain on the machine rotor and extended life. Both simulation and hardware results show that parameters obtained from the 'optimal' SPPSO algorithm can restore and stabilize the terminal voltage effectively and very quickly after high-power pulsed loads are experienced. Therefore, the 'optimal' SPPSO has potential for time critical controller tuning and reconfiguration.

In paper 3, an artificial immune system based excitation controller has been proposed and implemented on innovative M67 DSP and RTDS hardware platform to coordinately control the multi-machine power system for the Navy's Future Electric ship. This controller has advantages including optimal oriented with innate immunity, no generator parameters needed and no human involved, and adaptive immunity. Compared with PSO based optimal controller, the hardware simulation results show that AIS-based controller can adaptively restore and stabilize the terminal voltage effectively and very quickly after high power pulse loads are experienced.

Finally, in paper 4, an approach to evaluate optimal ESM location and size is presented. Three important factors considered in the evaluation are: QOS, survivability and cost. MOPSO is used to optimize these metrics and provide Pareto fronts for ESM location and sizing. The results show that an optimized ESM location and sizing design improve QOS and survivability greatly with relatively low cost. Furthermore, it has the potential to decrease SSIM/SSCM without scarifying QOS and survivability.

2.2. FUTURE WORK

For development of excitation controllers for generators on an electric ship, the future research will focus on coordinated control with energy storage modules and other sources of generation. An optimal coordinated control and management of excitation

systems and ESMs on an electric ship cannot only improve power quality, but also improve system efficiency so that cost of operations (such as fuel cost) can be minimized.

For ESM, the future research will try to find out a more practical approach to evaluate survivability based on statistical data. Furthermore, optimal SSIM/SSCM design with ESMs will be studied to improve QOS, survivability and minimize cost.

VITA

Chuan Yan, was born in Handan, China, on January 22, 1982. He received his B.S. degree in Electrical Engineering from Lanzhou University of Technology, China, in 2005. He received his M.S degree in Electrical Engineering from Chongqing University, China, in 2008. He began his research on electrical machinery and Navy electric ship in the Real-Time Power and Intelligent Systems Laboratory, Electrical and Computer Engineering Department of the Missouri University of Science and Technology (formerly known as the University of Missouri-Rolla) in 2007. He earned his Ph.D. degree in Electrical and Computer Engineering Department at Missouri University of Science and Technology in December 2010.